

SANDIA LETTER REPORT

Revision 2 Completed: November 2006

Mitigation of Spent Fuel Pool Loss-of-Coolant Inventory Accidents And Extension of Reference Plant Analyses to Other Spent Fuel Pools

K. C. Wagner
R. O. Gauntt

Prepared by
Sandia National Laboratories
Albuquerque, New Mexico 87185 and Livermore, California 94550

Sandia is a multiprogram laboratory operated by Sandia Corporation,
a Lockheed Martin Company, for the United States Department of Energy's
National Nuclear Security Administration under Contract DE-AC04-94AL85000.



Sandia National Laboratories

~~OFFICIAL USE ONLY - SECURITY RELATED INFORMATION~~

Issued by Sandia National Laboratories, operated for the United States Department of Energy by Sandia Corporation.

NOTICE: This report was prepared as an account of work sponsored by an agency of the United States Government. Neither the United States Government, nor any agency thereof, nor any of their employees, nor any of their contractors, subcontractors, or their employees, make any warranty, express or implied, or assume any legal liability or responsibility for the accuracy, completeness, or usefulness of any information, apparatus, product, or process disclosed, or represent that its use would not infringe privately owned rights. Reference herein to any specific commercial product, process, or service by trade name, trademark, manufacturer, or otherwise, does not necessarily constitute or imply its endorsement, recommendation, or favoring by the United States Government, any agency thereof, or any of their contractors or subcontractors. The views and opinions expressed herein do not necessarily state or reflect those of the United States Government, any agency thereof, or any of their contractors.



~~OFFICIAL USE ONLY - SECURITY RELATED INFORMATION~~

SANDIA Letter Report
Revision 2, November 2006

Mitigation of Spent Fuel Pool Loss-of-Coolant Inventory Accidents And Extension of Reference Plant Analyses to Other Spent Fuel Pools

K. C. Wagner
R. O. Gauntt

Analysis and Modeling Division
Sandia National Laboratories
P.O. Box 5800
Albuquerque, New Mexico 87185-MS-0748

Abstract

This report summarizes the findings from loss-of-coolant inventory analyses for pressurized water reactor (PWR) and boiling water reactor (BWR) spent fuel pools (SFPs). The important strategies for mitigating the consequences are discussed. The data used to perform these calculations were developed from an operating BWR and an operating PWR. The extensions of the findings to other SFPs are discussed. The analyses were performed using the MELCOR severe accident analysis code and the FLUENT and FLOW-3D computational fluid dynamics codes.

EXECUTIVE SUMMARY

In 2001, United State Nuclear Regulatory Commission (NRC) staff performed an evaluation of the potential accident risk in a spent fuel pool (SFP) at decommissioning plants in the United States [NUREG-1738]. The study was prepared to provide a technical basis for decommissioning rulemaking for permanently shutdown nuclear power plants. The study described a modeling approach of a typical decommissioning plant with design assumptions and industry commitments; the thermal-hydraulic analyses performed to evaluate spent fuel stored in the spent fuel pool at decommissioning plants; the risk assessment of spent fuel pool accidents; the consequence calculations; and the implications for decommissioning regulatory requirements. It was known that some of the assumptions in the accident progression in NUREG-1738 were conservative, especially the estimation of the fuel damage. Subsequently, the NRC desired to expand the study to include accidents in the spent fuel pools of operating power plants. Consequently, the NRC has continued spent fuel pool accident research by applying best-estimate computer codes to predict the severe accident progression following various postulated accident initiators.

Two reports were prepared that described the response of a boiling water reactor (BWR) spent fuel pool to accident conditions (i.e., [Wagner, 2003] and [Wagner, 2004]). The National Academy of Sciences (NAS) reviewed the reports and offered recommendations to improve the fidelity of the work [Lanzerotti, 2006]. Since that time, NRC has continued conducting research to improve their understanding of SFP accidents including pressurized water reactor (PWR) spent fuel pools. Since the original calculations were performed, several new enhancements have been added to the MELCOR computer code that improved the simulation of the SFP configuration [Gauntt]. In addition, new data and assembly drawings have been obtained as part of the Sandia National Laboratories (SNL) SFP experimental testing program that improved the accuracy of the physical and hydraulic representation. New studies have been completed which updated the analyses of the BWR SFP (i.e., [Wagner, 2005a] and [Wagner, 2006b]). Other studies were performed to analyze PWR SFP response to loss-of-coolant inventory conditions ([Khalil, 2005], [Wagner, 2005a], and [Wagner, 2006c]). Finally, a study was performed to analyze emergency spray effectiveness in a BWR SFP [Wagner, 2006a]. The purpose of the present report is to summarize strategies for mitigation of loss-of-coolant inventory accidents and discuss their application to other plants.

The data used to perform the SFP calculations were developed from an operating BWR and an operating PWR. The reference plants are typical of many with fuel in the SFP from several decades old to the most recent offload. The reference plants discharge one-third to one-half of the reactor fuel each outage. Both plants have begun a dry or on-site fuel storage program

Ex. 2

(b)(2) High

The BWR plant removes an equivalent amount of various aged fuel between outages for storage in dry casks, thereby maintaining a relatively constant number of assemblies in the SFP. Both plant's SFPs are relatively full but have sufficient storage for an emergency offload of all the fuel from the reactor. A schematic of the reference PWR and BWR spent fuel pool buildings are shown in Figure ES-1 and ES-2, respectively.

(b)(2)High

Ex.
2

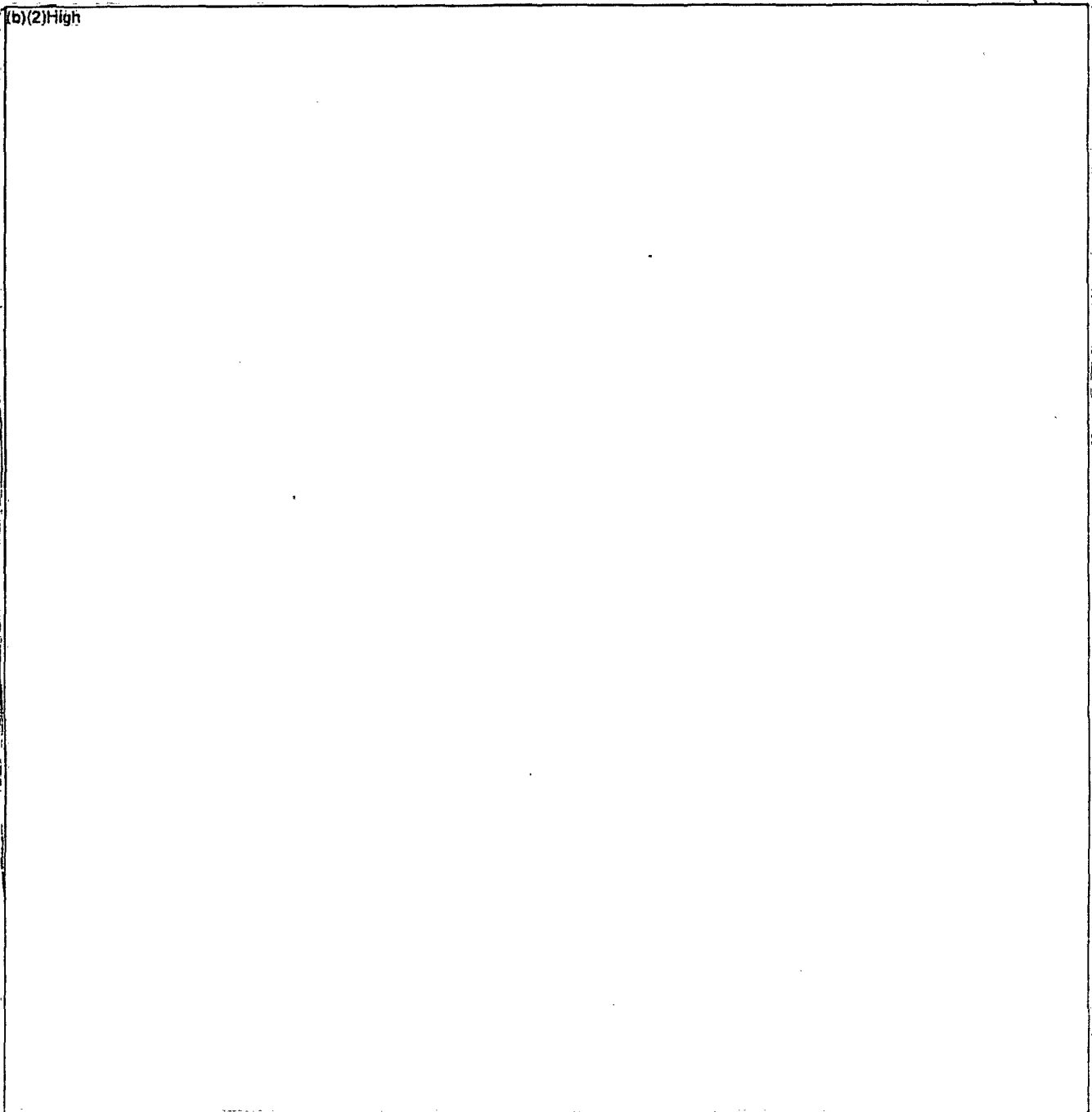


Figure ES-1. Schematic of Reference PWR Fuel Storage Building showing the Spent Fuel Pool.

(b)(2)High

Ex.
2

The purpose of the previous studies was to evaluate the response of a SFP to a loss-of-coolant inventory accident. The accidents are initiated with a leak in the SFP. Once the water level has reached (b)(2)High there would be inadequate cooling. The studies analyzed a

Ex. 2

variety of scenario variations and phenomenological uncertainties to identify the most important factors affecting the progression. Based on the insights from the studies, the following topics were identified that can help to mitigate loss-of-coolant inventory accidents,

- Make-up water and leak repair
- Well organized (i.e., dispersed) fuel configurations
- Emergency sprays
- Building ventilation
- Pool configuration
- Miscellaneous other factors

The key findings for each topic are discussed below based on insights from a wide range of separate effect and integral calculations for both BWR and PWR SFPs. The separate effects calculations were an examination of one to a few assemblies with specified boundary conditions, which gave the best control to simulate localized phenomena. The integral calculations simulated the entire SFP and surrounding building, which gave insights into global phenomena. Values are cited in the report for both BWR and PWR SFPs, and for integral calculations and separate effects calculations, depending on which analyses are most relevant for the given point being made. However, the trends were qualitatively similar for the reference PWR and the reference BWR. Specific timings and other quantitative values should be viewed as approximate, as variation in pool design, fuel design, building design, computational model implementation and modeling uncertainty necessarily have some impact on the results. The sensitivity of the results to these physical and modeling variations are extensively studied in the previous reports cited herein.

Make-up water and leak repair

The most obvious solution to a loss-of-coolant inventory accident consists of leak repair and make-up water. The NRC, along with industry, has identified potential water sources to the SFP. Various size leaks were simulated, which permitted calculation of the level response and water requirements. While not directly addressed in this study, there are obvious benefits from emergency leak repair. If the leak can be repaired prior to the water level dropping (b)(2)High

Ex. 2

(b)(2)High a modest make-up flow (b)(2)High is required to remove decay heat from the reference BWR or PWR at 30 days following shutdown.

Ex. 2

If there was a leak that completely drains the SFP, then adding make-up water could cover the bottom of the rack and preclude natural circulation flow. Depending upon several factors (e.g., fuel age, storage configuration, presence of a flow downcomer, adequate ventilation, etc.), the fuel could be coolable with air ventilation. Once the air convection is stopped with the make-up flow, the heat removal decreases and the fuel will heat more quickly. Hence, with heat removal due to air convection, the make-up flow must fill the pool above the (b)(2)High before the fuel heats to ignition conditions, which may require a very high capacity flow system. As will be discussed later, a uniform spray flow that provides top-down cooling could provide sufficient cooling at a much lower flowrate.

Ex. 2

Well organized (i.e., dispersed) fuel configurations

A significant effort in the SFP studies was spent identifying and quantifying the response of different fuel configurations. An arrangement that placed all the most recently discharged fuel assemblies in a contiguous pattern was the least effective pattern to store the fuel. Radial heat transfer from assemblies with high decay heat powers to low-powered or empty cells can significantly improve the assembly's coolability or timing to ignition. For example, Table ES-1 shows the gains from a uniform pattern of recently discharged assemblies to other better configured arrangements in a complete loss-of-coolant accident. If the most recently discharged, highest-powered assemblies are surrounded by assemblies at or below the median SFP assembly decay power, then there are substantial gains in the minimum amount of aging for coolability for a checkerboard or 1x4 pattern. Similarly, if the highest-powered assemblies are surrounded with empty cells, the improvements are also significant. In summary, spent fuel assemblies from the most recent offload stored in a non-dispersed pattern (e.g., a uniform region of high-powered assemblies) are not coolable for (b)(2)High versus being coolable after just (b)(2)High aging in a 1x4 configuration (see Figure ES-3) in a complete loss-of-coolant accident.

Ex. 2

Comparative partial loss-of-coolant calculations were also performed for dispersed and non-dispersed configurations. The dispersed configurations provided additional time for mitigative actions before the release of fission products versus a non-dispersed configuration. For example, BWR whole pool calculations with (b)(2)High

Ex. 2

Ex. 2

(b)(2)High showed an decrease from (b)(2)High from the start of fission product releases for the actual (i.e., a fairly well dispersed configuration) to (b)(2)High for poorly dispersed configuration.

Ex. 2

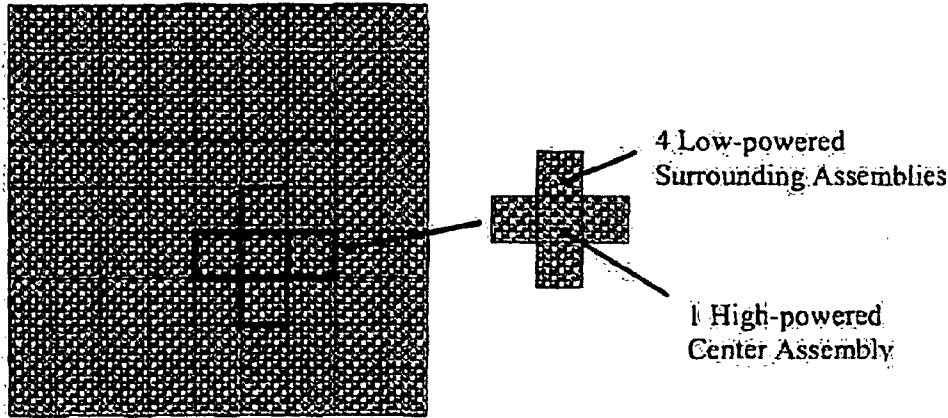
Table ES-1. Summary of BWR and PWR Coolability Aging Estimates for Assemblies in Air.

(b)(2)High

Ex. 2

Notes:

- A. The calculations assumed a complete and rapid loss-of-coolant inventory from the SFP. There are many other assumptions in these calculations that are carefully outlined in the main report and previous studies but they illustrate the relative gains achievable for well-configured pools.
- B. The BWR results with adjacent empty cells are based on a slightly older modeling approach but are believed to be representative.



1x4 Repeating Pattern

1x4 Separate Effects Model

Figure ES-3 Example of a Repeating Pattern for 1x4 Assembly Configurations.

Emergency sprays

Emergency spray calculations were performed to examine the effectiveness of spray cooling in the reference BWR SFP for loss-of-coolant inventory accidents. Based on input from the NRC,

Ex. 2 (b)(2)High was assumed for spray initiation and a spray flow rate of (b)(2)High was employed for the majority of calculations. (b)(2)High

Ex. 2 (b)(2)High.

A summary of predicted fuel coolability is provided in Table ES-2 for a (b)(2)High

Ex. 2 (b)(2)High following shutdown. For a configuration in which the recently offloaded fuel has been

Ex. 2 dispersed (i.e., a 1x4 or checkerboard pattern), a spray flow rate of (b)(2)High provided adequate

Ex. 2 cooling a (b)(2)High following shutdown. Under the same conditions, fuel which has not been dispersed (i.e., uniform fuel loading) is not coolable but becomes coolable at approximately

Ex. 2 (b)(2)High following shutdown. (b)(2)High would be

Ex. 2 necessary to cool a uniform configuration at (b)(2)High following shutdown.

Table ES-2 Summary of BWR Coolability Aging Estimates for Assemblies in Air with Spray Mitigation.^A

Ex. 2

(b)(2)High

The results presented above are for the reference BWR SFP. The results are expected to be representative of pressurized-water reactor (PWR) SFPs as well, based on simple scaling arguments. For extension to other SFPs, the spray flow rate must be scaled to provide the same flow per assembly as the reference calculations.

The emergency spray calculations identified some combinations of leakage rates and spray flowrates that would maintain a pool level above the bottom of the pool racks. When the inlet of the pool racks is plugged with water, the phenomena and thermal response for cases with the inlet plugged by the water level are different than the response when there is air flow in the assembly. Most importantly, the blocked inlet configuration substantially decreases the assembly heat removal. However, the spray calculations with a plugged inlet showed a much less significant impact after the spray initiation. The spray flow source provided an active heat removal mechanism that reduced the necessity of convective air flow.

Building ventilation

In complete loss-of-coolant inventory scenarios, air circulation patterns develop that circulate air into the SFP and through the spent fuel assemblies. If the building heat removal is inadequate, then the room will heat as well as the air circulating through the spent fuel pool racks. At steady conditions, the decay heat power of the SFP must be removed by the ventilation system and/or building leakage. In the reference plant SFPs, the total pool decay heat ranges from ~3 MW at 20 days to <1 MW at one year. In the absence or in addition to a forced ventilation system, the ideal ventilation configuration would supply cool air at the bottom of the room with the SFP and exhaust air from above the SFP. (b)(2)High

Ex. 2 (b)(2)High

(b)(2)High In both the reference plants, nominal leakage and heat loss through the walls and ceiling provided a

Ex. 2

significant amount of heat removal. (b)(2)High re:
(b)(2)High

In partial loss-of-coolant inventory conditions where there is no air flow through the assemblies, the role of ventilation is not a significant factor for coolability. The assembly heat removal occurs by boiling below water level and steam cooling above. Sustained coolability is much more difficult to achieve in partial loss-of-coolant inventory accidents without make-up water or sprays. (b)(2)High

Ex. 2

(b)(2)High
(b)(2)High It might seem intuitive to inhibit ventilation for a partial loss-of-coolant inventory accident to retain any released fission products. However, the by-product of steam oxidation with zirconium-based alloy cladding and stainless steel racks in the SFP is hydrogen. (b)(2)High

Ex. 2

(b)(2)High
(b)(2)High The potential benefit of increased fission product retention with reduced ventilation only applies to an accident which is mitigated prior to a hydrogen burn. In contrast, intentionally enhanced leakage could preclude hydrogen burns, permit re-isolation at a later time, and generically benefits the complete loss-of-coolant configuration, if the water level in the pool is unknown.

Pool configuration

Supporting computational fluid dynamic (CFD) calculations were performed to study the air flow patterns in the reference BWR and PWR spent fuel storage buildings during a complete loss-of-coolant inventory accident. The CFD calculations showed the importance of an open 'downcomer' region to permit air flow to under the racks. In the reference plants, there was a large open region in the SFP for a dry storage cask. In a complete loss-of-coolant inventory accident, the air preferentially flowed into the cask region, under the racks, and upward through the assemblies. The large, open cask space region in one corner of the SFP allowed the downward flow of cool air to reach the bottom of the racks with minimal thermal mixing with the hot plume leaving the assemblies. Parametric calculations were performed, which showed substantially decreasing or eliminating an open downcomer region as an inlet path to under the racks inhibited the natural circulation flow through the racks. In particular, if the open cross-sectional area of the SFP was (b)(2)High

Ex. 2

there was no impact of the average fuel temperature in the racks.

Both the reference plants had a large cask region and concentrations of empty cells, which permitted a robust, natural circulation flow pattern with minimal thermal mixing with the exiting hot plume. (b)(2)High

Ex. 2

(b)(2)High

Ex. 2

Ex. 2

The nominal open flow area in the reference BWR SFP was (b)(2)High of the cross-sectional area due to large gaps on the sides of the pool and many empty cells. The CFD sensitivity calculation with (b)(2)High of the flow area open did not show any impact on the average rack temperature for the conditions simulated. Further reductions in the flow area resulted in an increase in the rack temperature. The results and assumptions associated with these conclusions are further discussed in the report.

(b)(2)High

Ex. 2

Finally, the reference PWR SFP had several racks with open flux traps adjacent to each rack cell for criticality control (see Figure ES-4). The benefit of the open flux traps contributing to down flow was not quantified. Since the flux traps are dispersed throughout the rack cells, they would not provide a contiguous flow path near the SFP wall. Consequently, their benefit is expected to be less beneficial than the aforementioned configuration. Nevertheless, the assemblies adjacent to open flux channels were quantified to enhance the coolability of the reference PWR assemblies relative to a uniform configuration but not as advantageous as a checkerboard configuration.

Miscellaneous other factors

The following factors can help enhance the assembly coolability.

- Most rack designs allow assemblies to be placed over rack feet. The rack foot is hollow and has holes on the sides to permit flow. Particularly in the reference PWR rack design, the additional resistance through the flow holes increased the aging time for coolability. Since the BWR assemblies are already restricted at the assembly nose-piece, the impact was not as substantial.
- The PWR reference SFP had 3 racks with an open flux channel design to store low or un-irradiated fuel. The flux channel enhanced heat removal by providing an empty flow channel for additional convective heat removal (see Figure ES-4).

(b)(2)High

(b)(2)High

Ex. 2

- Neither of the reference plant rack designs had drain holes in the sides of the rack cells. However, the SNL SFP experimental program rack design had two 1" drain holes near the bottom of the racks. The drain holes enhanced flow into the annulus between the BWR canister and the rack wall, which enhanced the assembly cooling.
- The CFD analyses showed a high speed air flow adjacent to the cask region as air flowed under the racks. Since the air flow is tangential to the rack inlet holes, it creates a low pressure region or Bernoulli Effect, which retards air flow into the racks. Consequently, an empty rack cell buffer zone adjacent to the cask region or multiple open regions for flow under the racks will minimize the adverse effects of high speed flows.
- The reference PWR plant stored assemblies with different control materials in the guide tube locations. If the control materials and the end plugs could be removed, the additional flow through the guide tubes was shown to be beneficial. Similarly, removing the BWR canister enhanced the coolability of the assemblies. It is recognized that these suggestions may not be practical.

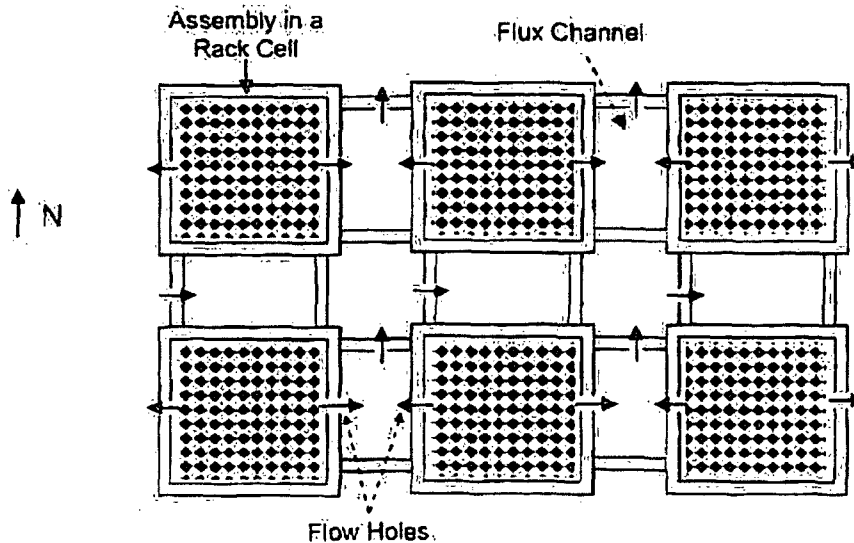


Figure ES-4 Illustration of the Reference PWR Plant Region I Racks with Flux Traps.

Finally, Table ES-3 summarizes the various mitigation options above. The impact of each mitigation option is qualitatively ranked. As noted in the comments, some options are only effective for complete loss-of-coolant inventory accidents where a natural convection air flow can be established. Depending on the available instrumentation and an ability to diagnose the accident, it may be difficult to know where the leak is located and whether the accident will progress like a complete or partial loss-of-coolant inventory accident. Nevertheless, the first three options are ranked as having very high to high impact on the assembly coolability, regardless of the accident type. Preparation and application of multiple mitigation options can provide a compounding beneficial effect. (b)(2)High

Ex. 2

(b)(2)High

(b)(2)High Selected measures are being incorporated in to the procedures of NRC licensee's as a part of the NRC and industry's SFP mitigative strategies study.

Table ES-3 Impact of Mitigation Options on Assembly Coolability.

(b)(2) High

Ex. 2

Ex. 2

TABLE OF CONTENTS

1. INTRODUCTION..... 1

2. BACKGROUND 3

2.1 Description of the Reference BWR Spent Fuel Pool 3

2.2 Description of the Reference PWR Spent Fuel Pool..... 6

2.3 SFP Accident Scenarios..... 11

 2.3.1 Complete Loss-of-Coolant Inventory Accident..... 11

 2.3.2 Partial Loss-of-Coolant Inventory Accident..... 13

3. MITIGATION OF SFP LOSS-OF-COOLANT INVENTORY ACCIDENTS 15

3.1 Make-up Water and Leak Repair 16

 3.1.1 Minimum Level Cooling..... 16

 3.1.2 Level Response Timing for Non-dispersed Fuel Configuration..... 22

 3.1.3 Calculations for Minimum Make-up Flow 34

 3.1.4 Calculations for Level Make-up Time..... 37

 3.1.5 Summary of Make-up Flow Requirements and Extension to Other Sites..... 41

3.2 Well-Organized Fuel Configurations..... 44

 3.2.1 Summary of Well-Configured Patterns in Complete Loss-of-Coolant Inventory
 Accidents..... 44

 3.2.2 Summary of Well-Configured Patterns in Partial Loss-of-Coolant Inventory
 Accidents..... 48

 3.2.3 Extension of Well-Configured Patterns to Other Sites..... 53

3.3 Emergency Sprays 56

 3.3.1 Hand Calculations for Minimum Spray Flow..... 56

 3.3.2 MELCOR Calculations for Minimum Spray Flow..... 59

 3.3.2.1 Basic Assumptions in the MELCOR Spray Analyses 59

 3.3.2.2 SFP Water Level Response with Sprays..... 59

 3.3.2.3 Separate Effects Spray Calculations 61

 3.3.3 Summary of Spray Flow Requirements and Extension to Other Sites..... 64

3.4 Building Ventilation..... 70

 3.4.1 Flow Patterns in the Reference PWR Fuel Storage Building 71

 3.4.2 Separate Effect Sensitivity Analysis of Inlet Temperature 74

 3.4.3 Impact of Ventilation on Integral Whole Pool Calculations..... 78

 3.4.4 Summary of Ventilation Findings and Extension to Other Sites..... 82

3.5 Pool Configuration..... 86

 3.5.1 Summary of Pool Configuration Findings and Extension to Other Sites 92

3.6 Miscellaneous Other Factors 94

4. SUMMARY OF MITIGATION OPTIONS..... 98

5. REFERENCES..... 100

List of Tables

	Table 1	BWR Spent Fuel Pool Data.....	4
	Table 2	BWR Fuel Assembly Data.....	5
	Table 3	BWR Spent Fuel Pool Rack Data.....	5
	Table 4	PWR Spent Fuel Pool Data.....	9
	Table 5	PWR Fuel Assembly Data.....	9
	Table 6	PWR Spent Fuel Pool Rack Data.....	10
	Table 7	Summary of the PCTs versus Collapsed Water Level.....	18
Ex. 2	Table 8	Summary of Timings to Elevations as a Function of Hole Size for a Non-Dispersed Configuration at (b)(2)High Since Shutdown.....	24
Ex. 2	Table 9	Summary of Timings to Elevations as a Function of Hole Size for a Non-Dispersed Configuration at (b)(2)High Since Shutdown.....	25
Ex. 2	Table 10	Summary of Timings to Restore the PWR SFP Level (b)(2)High.....	38
	Table 11	Summary of BWR and PWR Coolability Aging Estimates for Assemblies in Air.....	45
Ex. 2	Table 12	Summary of Reference BWR (b)(2)High Since Discharge Partial Loss-of-Coolant Inventory with the Leak Location (b)(2)High Active Level Results.....	52
Ex. 2	Table 13	Summary of the Steady-State Water Levels as a Function of Leakage Hole Size and Spray Flow Rate.....	60
	Table 14	Summary of Separate Effects Spray Calculation Results.....	62
	Table 15	Key Calculated Results Using FLUENT.....	72
	Table 16	Summary of Ventilation Sensitivity Study Specifications and Results.....	80
	Table 17	Summary of BWR CFD Cases with Variable SFP Open Flow Area Configurations.....	89
	Table 18	Impact of Mitigation Options on Assembly Coolability.....	99

List of Figures

	Figure 2-1	Reference BWR Spent Fuel Pool Rack Layout.....	4
	Figure 2-2	Typical Spent Fuel Pool Rack Cut-away Cross-Section Showing the Fuel Assembly.....	6
	Figure 2-3	Reference PWR Spent Fuel Pool Rack Layout.....	8
	Figure 2-4	SFP Region I and II Rack Cell Design and Dimensions.....	8
	Figure 2-5	Typical Region II Spent Fuel Pool Rack Cut-away Cross-section Showing the Fuel Assembly.....	11
Ex. 2	Figure 3-1	Comparison of the PCT versus a Function of the Collapsed Liquid Level Outside of the Assembly (b)(2)High Aging Time Since the Assembly was Discharged.....	18
Ex. 2	Figure 3-2	Comparison of the PCT versus a Function of the Collapsed Liquid Level Outside of the Assembly (b)(2)High Aging Time Since the Assembly was Discharged.....	19
Ex. 2	Figure 3-3	Comparison of the PCT versus a Function of the Collapsed Liquid Level Outside of the Assembly (b)(2)High Aging Time Since the Assembly was Discharged.....	19

Ex. 2 Figure 3-4 Comparison of the PCT versus a Function of the Decay Power of the Assembly (b)(2)High Collapsed Water Level..... 20

Ex. 2 Figure 3-5 Comparison of the PCT versus a Function of the Decay Power of the Assembly (b)(2)High Collapsed Water Level..... 20

Ex. 2 Figure 3-6 Comparison of the PCT versus a Function of the Decay Power of the Assembly (b)(2)High Collapsed Water Level..... 21

Ex. 2 Figure 3-7 Comparison of Pool Drain Rates (b)(2)High as a Function of Leak Location (b)(2)High..... 26

Ex. 2 Figure 3-8 Comparison of Peak Cladding Temperatures (b)(2)High as a Function of Leak Location (b)(2)High..... 26

Ex. 2 Figure 3-9 Comparison of Pool Drain Rates (b)(2)High as a Function of Leak Location (b)(2)High..... 27

Ex. 2 Figure 3-10 Comparison of Peak Cladding Temperatures (b)(2)High as a Function of Leak Location (b)(2)High..... 27

Ex. 2 Figure 3-11 Comparison of Pool Drain Rates (b)(2)High as a Function of Leak Location (b)(2)High..... 28

Ex. 2 Figure 3-12 Comparison of Peak Cladding Temperatures (b)(2)High as a Function of Leak Location (b)(2)High..... 28

Ex. 2 Figure 3-13 Pool Drain Rates for Loss-of-Heat Removal Accident (i.e., No Leakage Hole) (b)(2)High..... 29

Ex. 2 Figure 3-14 Peak Cladding Temperature for Loss-of-Heat Removal Accident (i.e., No Leakage Hole) (b)(2)High..... 29

Ex. 2 Figure 3-15 Comparison of Pool Drain Rates (b)(2)High as a Function of Leak Location (b)(2)High..... 30

Ex. 2 Figure 3-16 Comparison of Peak Cladding Temperatures (b)(2)High as a Function of Leak Location (b)(2)High..... 30

Ex. 2 Figure 3-17 Comparison of Pool Drain Rates (b)(2)High as a Function of Leak Location (b)(2)High..... 31

Ex. 2 Figure 3-18 Comparison of Peak Cladding Temperatures (b)(2)High as a Function of Leak Location (b)(2)High..... 31

Ex. 2 Figure 3-19 Comparison of Pool Drain Rates (b)(2)High as a Function of Leak Location (b)(2)High..... 32

Ex. 2 Figure 3-20 Comparison of Peak Cladding Temperatures (b)(2)High as a Function of Leak Location (b)(2)High..... 32

Ex. 2 Figure 3-21 Pool Drain Rates for Loss-of-Heat Removal Accident (i.e., No Leakage Hole) (b)(2)High..... 33

Ex. 2 Figure 3-22 Peak Cladding Temperature for Loss-of-Heat Removal Accident (i.e., No Leakage Hole) (b)(2)High..... 33

Figure 3-23 Total Pool Decay Heat Power in the Reference BWR SFP..... 35

Figure 3-24 Total Pool Decay Heat Power in the Reference PWR SFP..... 35

Figure 3-25 Make-up Flowrate for the Reference BWR SFP..... 36

Figure 3-26 Make-up Flowrate for the Reference PWR SFP..... 36

Ex. 2 Figure 3-27 Level Response as a Function of Make-up Flow (b)(2)High following Reactor Shutdown in the Reference PWR SFP..... 39

Ex. 2 Figure 3-28 Level Response as a Function of Make-up Flow (b)(2)High following Reactor Shutdown in the Reference PWR SFP..... 40

Figure 3-29	Comparison of Leakage Rates versus Water Level Height as a Function of Leak Size.....	42
Figure 3-30	Comparison of the Reference BWR SFP Assembly Decay Heat Rates as a Function of Time and Sorted by Decay Power.....	43
Figure 3-31	Comparison of the Reference PWR SFP Assembly Decay Heat Rates as a Function of Time and Sorted by Decay Power.....	43
Figure 3-32	Fuel Configurations Considered in the MELCOR Separate Effects Models.....	47
Figure 3-33	Reference BWR Spent Fuel Decay Heat Level at 1 Month after Discharge to the SFP (circa 2002).....	49
Figure 3-34	Comparison of the Peak Cladding Temperature for a Partial Loss-of-Coolant Accident in the Reference BWR SFP for Partially Dispersed and Non-Dispersed Fuel Configurations.....	50
Figure 3-35	Comparison of the Peak Cladding Temperature for a Partial Loss-of-Coolant Accident in the Reference PWR SFP for Dispersed and Non-Dispersed Fuel Configurations.....	51
Figure 3-36	Example of the Reference BWR SFP in a Well-Configured Arrangement using Repeating 1x4 Patterns.....	54
Figure 3-37	Example of the Reference PWR SFP in a Well-Configured Arrangement using Repeating 1x4 Patterns.....	55
Figure 3-38	Hand Calculations to Estimate Spray Heat Removal Requirements for the Reference BWR SFP.....	58
Figure 3-39	Hand Calculations to Estimate Spray Heat Removal Requirements for the Reference PWR SFP.....	58
Figure 3-40	Level Response ^{(b)(2)High}	60
Ex. 2	^{(b)(2)High}	60
Figure 3-41	Comparison of the Leak Rate and Spray Flowrate Response ^{(b)(2)High}	61
Ex. 2	^{(b)(2)High}	61
Figure 3-42	Comparison of the Peak Cladding Temperatures for the Uniform Configuration with Various Aging Periods and a Whole Pool Spray Flow <input type="checkbox"/> ^{(b)(2)High}	63
Ex. 2	^{(b)(2)High}	63
Figure 3-43	Comparison of the Peak Cladding Temperatures for the Uniform Configuration with Various Aging Periods and a Whole Pool Spray Flow <input type="checkbox"/> ^{(b)(2)High}	63
Ex. 2	^{(b)(2)High}	63
Figure 3-44	Comparison of the Peak Cladding Temperatures for the Uniform Configuration with Various Aging Periods and a Whole Pool Spray Flow <input type="checkbox"/> ^{(b)(2)High}	64
Ex. 2	^{(b)(2)High}	64
Figure 3-45	Base and Modified Hand Calculations to Estimate Spray Heat Removal Requirements for the Reference BWR SFP.....	65
Figure 3-46	Base and Modified Hand Calculations to Estimate Spray Heat Removal Requirements for the Reference BWR SFP (Uniform Configuration).....	68
Figure 3-47	Minimum BWR and PWR Spray Flux (Uniform Configuration).....	69
Figure 3-48	Flow Patterns into the SFP From FLUENT Calculations With Open Roll Door.....	73

Ex. 2

Figure 3-49 Comparison of the PCT versus the Assembly Inlet Temperature Aging Time Since the Assembly was Discharged for the Uniform Configuration. (b)(2)High 76

Figure 3-50 Comparison of the PCT versus the Aging Time at an Assembly Inlet Temperature of 350 K. 76

Figure 3-51 Comparison of the PCT versus the Aging Time at an Assembly Inlet Temperature of 400 K for the Uniform Configuration. 77

Figure 3-52 Comparison of the Convective Heat Removal Rates at 300 K versus 350 K Inlet Temperatures as a Function of Exit Temperature. 77

Figure 3-53 Comparison of the PCT versus the Aging Time at an Assembly Inlet Temperature of 350 K in a 1x4 Configuration. 78

Ex. 2 Figure 3-54 Comparison of the SFP Building Ventilation Flows (b)(2)High 81

Ex. 2 Figure 3-55 Comparison of the Gas Temperatures Flowing into the SFP (b)(2)High 81

Ex. 2 Figure 3-56 Comparison of the Peak Cladding Temperature Responses (b)(2)High 82

Figure 3-57 Hand Calculation of Ventilation Requirements for the Reference PWR SEP (SI Units). 85

Figure 3-58 Hand Calculation of Ventilation Requirements for the Reference PWR SEP (British Units). 85

Figure 3-59 Schematic of the Reference BWR Reactor Building Showing the CFD Model Mesh. 87

Figure 3-60 CFD Model Cross-Section of the SFP Racks for the Reference BWR SFP. . 90

Figure 3-61 Peak Assembly Gas Temperatures for the Various Shaped Open Area Configurations. 91

Figure 3-62 Peak Assembly Gas Temperatures for the Shaped Cask Area Configurations. 91

Figure 3-63 Illustration of the Reference PWR Plant Region I Racks with Flux Traps. . 96

Figure 3-64 Gas Velocity Vectors Below the Racks in a Fluent CFD Calculation of a Complete Loss-of-Coolant Inventory Accident. 96

Figure 3-65 Comparison of the PCT versus the Range of Assembly Configurations in the Reference PWR SFP. 97

Mitigation of Spent Fuel Pool Loss-of-Coolant Inventory Accidents And Extension of Reference Plant Analyses to Other Spent Fuel Pools

1. INTRODUCTION

In 2001, United State Nuclear Regulatory Commission (NRC) staff performed an evaluation of the potential accident risk in a spent fuel pool (SFP) at decommissioning plants in the United States [NUREG-1738]. The study was prepared to provide a technical basis for decommissioning rulemaking for permanently shutdown nuclear power plants. The study described a modeling approach of a typical decommissioning plant with design assumptions and industry commitments; the thermal-hydraulic analyses performed to evaluate spent fuel stored in the spent fuel pool at decommissioning plants; the risk assessment of spent fuel pool accidents; the consequence calculations; and the implications for decommissioning regulatory requirements. It was known that some of the assumptions in the accident progression in NUREG-1738 were conservative, especially the estimation of the fuel damage. Subsequently, the NRC desired to expand the study to include accidents in the spent fuel pools of operating power plants. Consequently, the NRC has continued spent fuel pool accident research by applying best-estimate computer codes to predict the severe accident progression following various postulated accident initiators.

Two reports were prepared that described the response of a boiling water reactor (BWR) spent fuel pool to accident conditions (i.e., [Wagner, 2003] and [Wagner, 2004]). The National Academy of Sciences (NAS) reviewed the reports and offered recommendations to improve the fidelity of the work [Lanzerotti, 2006]. Since that time, NRC has continued conducting research to improve their understanding of SFP accidents including pressurized water reactor (PWR) spent fuel pools. Since the original calculations were performed, several new enhancements have been added to the MELCOR computer code that improved the simulation of the SFP configuration. In addition, new data and assembly drawings have been obtained as part of the Sandia National Laboratories (SNL) SFP experimental testing program that improved the accuracy of the physical and hydraulic representation. New studies have been completed which updated the analyses of the BWR SFP (i.e., [Wagner, 2005a] and [Wagner, 2006b]). Other studies were performed to analyze PWR SFP response to loss-of-coolant inventory conditions ([Khalil, 2005], [Wagner, 2005b], and [Wagner, 2006c]). Finally, a study was performed to analyze emergency spray effectiveness in a BWR SFP [Wagner, 2006a]. The purpose of the present report is to summarize strategies for mitigation of loss-of-coolant inventory accidents and discuss their application to other plants.

The data used to perform the SFP calculations were developed from an operating BWR and an operating PWR. The reference plants are typical of many with fuel in the SFP from several decades old to the most recent offload. The reference plants discharge one-third to one-half of

the reactor fuel each outage. Both plants have begun a dry or on-site fuel storage program

Ex. 2

(b)(2)High

The BWR plant removes an equivalent amount of various aged fuel between outages for storage in dry casks, thereby maintaining a relatively constant number of assemblies in the SFP. Both plant's SFPs are relatively full but have sufficient storage for an emergency offload of all the fuel from the reactor.

The purpose of the previous studies was to evaluate the response of a SFP to a loss-of-coolant inventory accident. First, Section 2 provides some background on the two reference plants spent fuel pool designs. Some general comments are also presented in Section 2 on the expected progression of a loss-of-coolant inventory accident. Based on insights from the various SFP analyses of the reference plants, Section 3 summarizes the key findings to enhance the coolability of the fuel assemblies, thereby mitigating the loss-of-coolant inventory accident consequences. The key findings are presented in separate subsections in Section 3. The applicability to other pool designs is discussed in the context of the various findings. The effectiveness of the mitigation options on assembly coolability is summarized in Section 4. The references are in Section 5.

2. BACKGROUND

The reference plants for the SFP analyses consist of a large operating PWR and BWR. Like most other nuclear plants, the reference plants have installed high-density racks to maximize the storage of fuel in the SFP. A description of the BWR and the PWR reference plant SFPs are given in Sections 2.1 and 2.2. The accidents considered in the present study consist of a loss-of-coolant inventory. A description of the accident progression is provided in Section 2.3.

2.1 Description of the Reference BWR Spent-Fuel Pool

The spent fuel pool, 40 feet wide by 35.3 feet long (cross-sectional area equals 1413 ft² or 131 m²) by 38 feet deep, is located on the refueling floor of the reactor building. The pool is constructed of reinforced concrete with a wall and floor lining of 1/4-inch thick stainless steel. The walls and the floor of the spent fuel pool are approximately 6-ft thick. In the northeast corner of the SFP is a cask area of 10-ft x 10-ft (see Figure 2-1). The general attributes of the spent fuel pool, the BWR fuel assemblies, and the spent fuel pool racks are described in Table 1, Table 2, and Table 3, respectively.

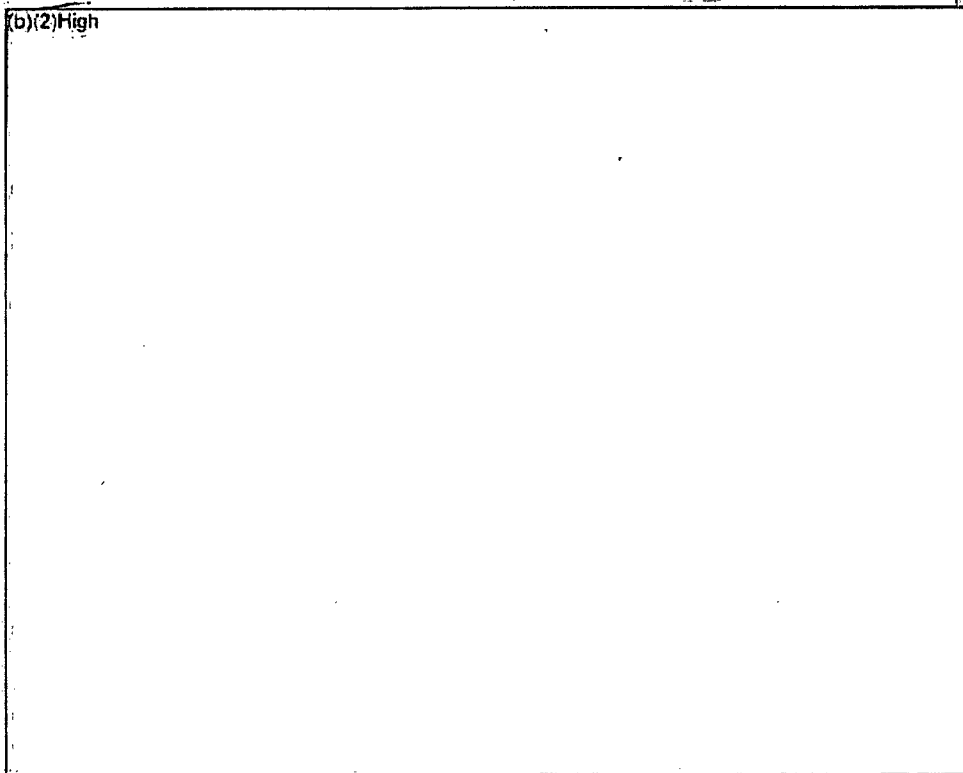
The high density SFP racks provide spent fuel storage at the bottom of the fuel pool. The fuel storage racks are normally covered with about 23 ft of water for radiation shielding. The SFP racks are freestanding, full length, top entry and are designed to maintain the spent fuel in a spaced geometry, which precludes the possibility of criticality under any condition.

Ex. 2 The high-density SFP racks are of the "poison" type utilizing a neutron absorbing material to maintain a subcritical fuel array. The racks are rectilinear in shape and are of nine different sizes. A total of storage locations are provided in the pool. The racks are constructed of stainless steel materials and each rack module is composed of cell assemblies, a base plate, and base support assemblies. Each cell is composed of (a) a full-length enclosure constructed of 0.075" thick stainless steel, (b) sections of Bisco Boraflex, which is a neutron absorbing material, and (c) wrapper plates constructed of 0.020" thick stainless steel. The inside square dimension of a cell enclosure is 6.07". The cell pitch is 6.28".

The base plate is a 0.5" thick stainless steel plate with 3.8" chamfered through holes centered at each storage location, which provides a seating surface for the fuel assemblies. These holes also provide passage for coolant flow.

Each rack module has base support assemblies (i.e., 'rack feet') located at the center of the corner cells within the module and at interior locations³ to distribute the pool floor loading (e.g., see Figure 2-2). Each base assembly is composed of a level block assembly, a leveling screw, and a support pad. The top of the leveling block assembly is welded to the bottom of the base plate. SFP fuel cells are located above each rack foot. Four 1" holes are drilled into the side of the support pad. The interior of the support pad is hollow and permits flow to the opening in the base plate.

³ There are several different rack sizes in the SFP. However, for a 19x10 size rack, there are 13 base support assemblies, 14 on the perimeter and 4 in the interior.



Ex. 2

Figure 2-1 Reference BWR Spent Fuel Pool Rack Layout.

Table 1 BWR Spent Fuel Pool Data.

SFP Pool Characteristics	Description or Dimensions
Dimensions	480" x 424" 10-ft x 10-ft square cask area in NW corner 39' high walls
Concrete thickness	~6 feet
SFP Volume	53,350 ft ³ (399,000 gal)
Number of storage locations	(b)(2)High

Ex. 2

Table 2 BWR Fuel Assembly Data.

Assembly Characteristics	Description or Dimensions
Fuel Type	Various, most recent are GE 9x9 design
Number of Fuel Rods	74
Fuel Pitch	0.566"
Fuel Rod Dimensions	0.44" OD 0.028" Cladding 146" Active Length
Maximum Initial Enrichment	4% U-235 by weight
Number of Water Rods	2
Water Rod Dimensions	0.98" OD Zircaloy
Canister dimensions	~5.276" ID ~0.065 thick ^A

A. The thickness is not uniform and the inner dimension varies slightly over the length of the canister.

Table 3 BWR Spent Fuel Pool Rack Data.

SFP Rack Characteristics	Description or Dimensions
Rack Height Above the Base Plate	169"
Baseplate Thickness	0.5"
Support Leg Height	7.25"
Poison Material	Boraflex
Cell Pitch	6.28
Cell Construction	0.075" (14 gage) 304 stainless steel walls with Bisco Boraflex B ₄ C particles clad in a non-metallic binder (0.081") with 0.020" stainless wrapper.

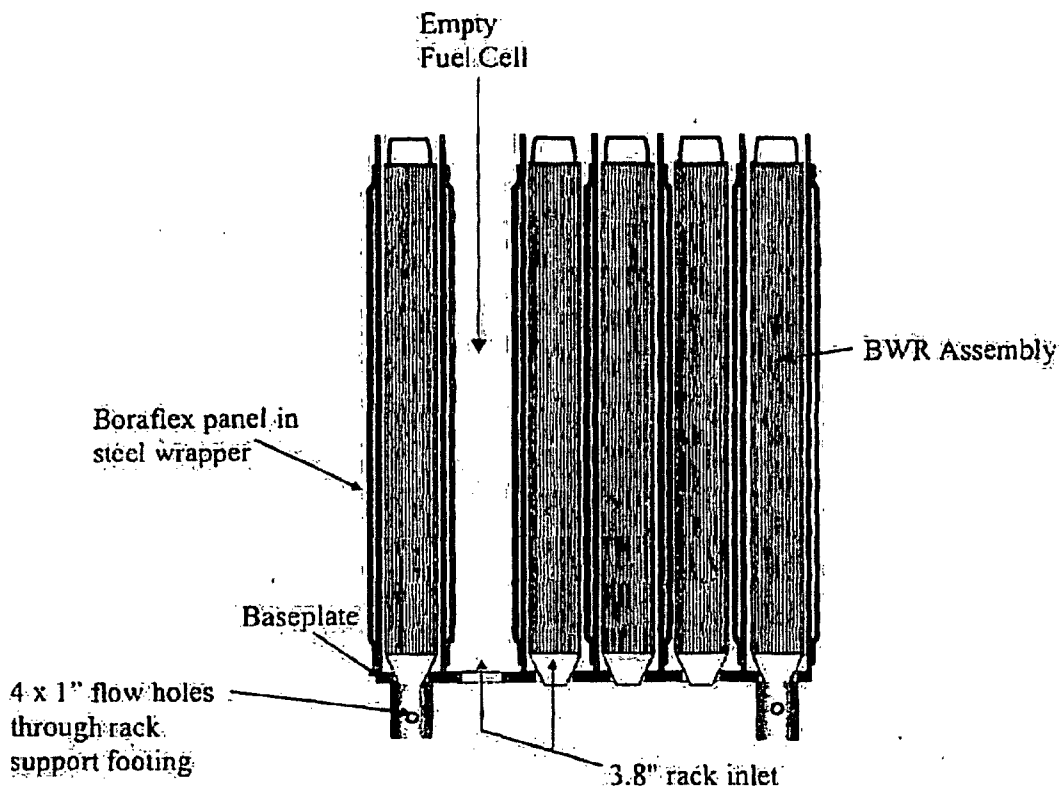


Figure 2-2. Typical Spent Fuel Pool Rack Cut-away Cross-Section Showing the Fuel Assembly.

2.2 Description of the Reference PWR Spent Fuel Pool

The spent fuel pool is approximately 36 feet by 33 feet (cross-sectional area equals 971 ft² or 90.2 m²) by 39 feet deep (see Figure 2-3). The SFP is located in the fuel storage building adjacent to the containment. The pool is constructed of reinforced concrete with a wall and floor lining of 1/4-inch thick stainless steel. The walls and the floor of the spent fuel pool range from 4' to 6' thick. In the southwest corner of the SFP is a cask area of 8.6' by 7.8' (see Figure 2-3). The general attributes of the spent fuel pool, the PWR fuel assemblies, and the spent fuel pool racks are described in Table 4, Table 5, and Table 6, respectively.

The high density SFP racks provide spent fuel storage at the bottom of the fuel pool. The fuel storage racks are normally covered with at least 23 ft of water for radiation shielding. The SFP racks are freestanding, full length, and top entry. The racks are arranged into two regions.

Ex. 2 (b)(2)High
(b)(2)High Their rack design includes a flux gap trap (i.e., a water channel as shown in Figure 2-4) between the rack

cells to provide additional protection against criticality. (b)(2)High

Ex. 2

(b)(2)High

(b)(2)High

There are also two

locations for the storage of failed fuel canisters. If Region II becomes full of irradiated fuel, Region I can also be used to store irradiated fuel. The total number of storage locations for both

Ex. 2

Regions I and II is [redacted] cells (i.e., including the two failed canister locations).

Both Region I and II racks utilize a neutron absorbing material (Boraflex) to maintain a subcritical fuel array. The racks are constructed of stainless steel materials. A rack module is composed of cell assemblies, a base plate, and base support assemblies. Each cell is composed of (a) a full-length enclosure constructed of 0.075" thick stainless steel, (b) sections of Boraflex, which is a neutron absorbing material, and (c) stainless steel wrapper plates. In addition, Region I racks have a water gap between cells for additional criticality protection. The Region I and II cell geometry and dimensions are summarized in Figure 2-4.

The base plate is 0.5" thick stainless steel with 6" diameter holes centered at each storage location, which provides a seating surface for the fuel assemblies. These holes also provide passage for coolant flow.

The rack module is supported by base assemblies (i.e., 'rack feet'), which are located at the center of the corner cells for support (e.g., see Figure 2-5). The base assembly is composed of a level block assembly, a leveling screw, and a support pad. The top of the leveling block assembly is welded to the bottom of the base plate. SFP fuel cells are located above each rack foot. Four 1" holes are drilled into the side of the support pad. The interior of the support pad is hollow and permits flow to the opening in the base plate.

(b)(2)High

Exp.
1

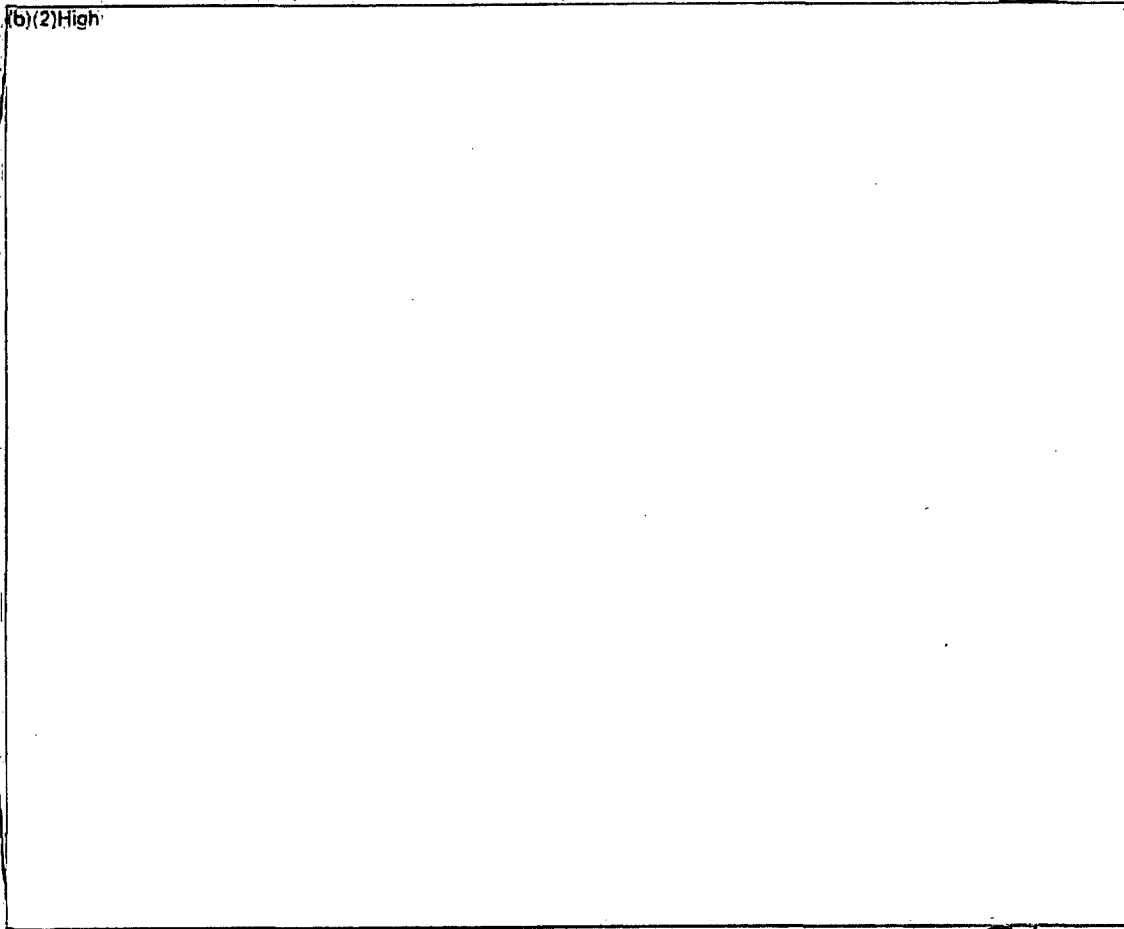


Figure 2-3 Reference PWR Spent Fuel Pool Rack Layout.

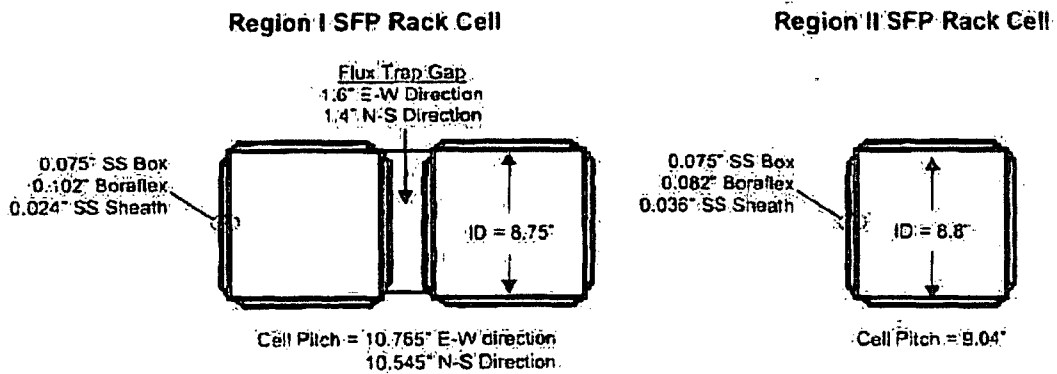


Figure 2-4 SFP Region I and II Rack Cell Design and Dimensions.

Table 4. PWR Spent Fuel Pool Data.

SFP Pool Characteristics	Description or Dimensions
Dimensions	See Figure 2-3
Concrete thickness	4-6 feet
Number of storage locations	(b)(2) High

Ex. 2

Table 5 PWR Fuel Assembly Data.

Assembly Characteristics	Description or Dimensions
Fuel Type	Various, all Westinghouse Most recent is VANTAGE+ design.
Lattice	15 x 15
Number of Fuel Rods	204
Number of Guide Tubes (GT)	20
Number of Instrument Thimbles (IT)	1
Control rod	Rod Control Cluster (RCC)
Burnable poison rod design type	Wet Annular Burnable Absorber (WABA)
Integral fuel burnable absorber rods	IFBA
Assembly pitch (in reactor)	21.5 cm (8.46")
Fuel Pitch	1.43 cm (0.563")
Fuel Rod Dimensions	0.422" OD 0.0243" Cladding thickness 144" Active Length
Clad Material	ZIRLO™
Rod Control Cluster (RCC)	Ag-In-Cd
Wet Annular Burnable Absorber (WABA) Rods	Al ₂ O ₃ -B ₄ C
Fuel Enrichment (wt% ²³⁵ U)	Various 2% - 5% (most recent discharge)
GT and IT outer diameter	1.354 cm (0.533")
GT and IT thickness	0.432 mm (0.017")
GT and IT material	ZIRLO™

Table 6 PWR Spent Fuel Pool Rack Data

SFP Rack Characteristics	Description or Dimensions
Rack Height Above the Base Plate	166"
Baseplate Thickness	0.5"
Support Leg Height	6"
Poison Material	Boraflex
Cell Inside Dimension	Region I 8.75" Region II 8.80"
Cell Pitch	Region I 10.765" E-W 10.545" N-S Region II 9.04"
Cell Construction	<p><u>Region I</u></p> <ul style="list-style-type: none"> • 0.075" (14 gage) 304 stainless steel walls • 0.102" x 7.5" x .144" Boraflex panels (powdered B₂C in a non-metallic polymer binder) • 0.024" stainless wrapper <p><u>Region II</u></p> <ul style="list-style-type: none"> • 0.075" (14 gage) 304 stainless steel walls • 0.082" x 7.5" x .150" Boraflex panels • 0.036" stainless wrapper

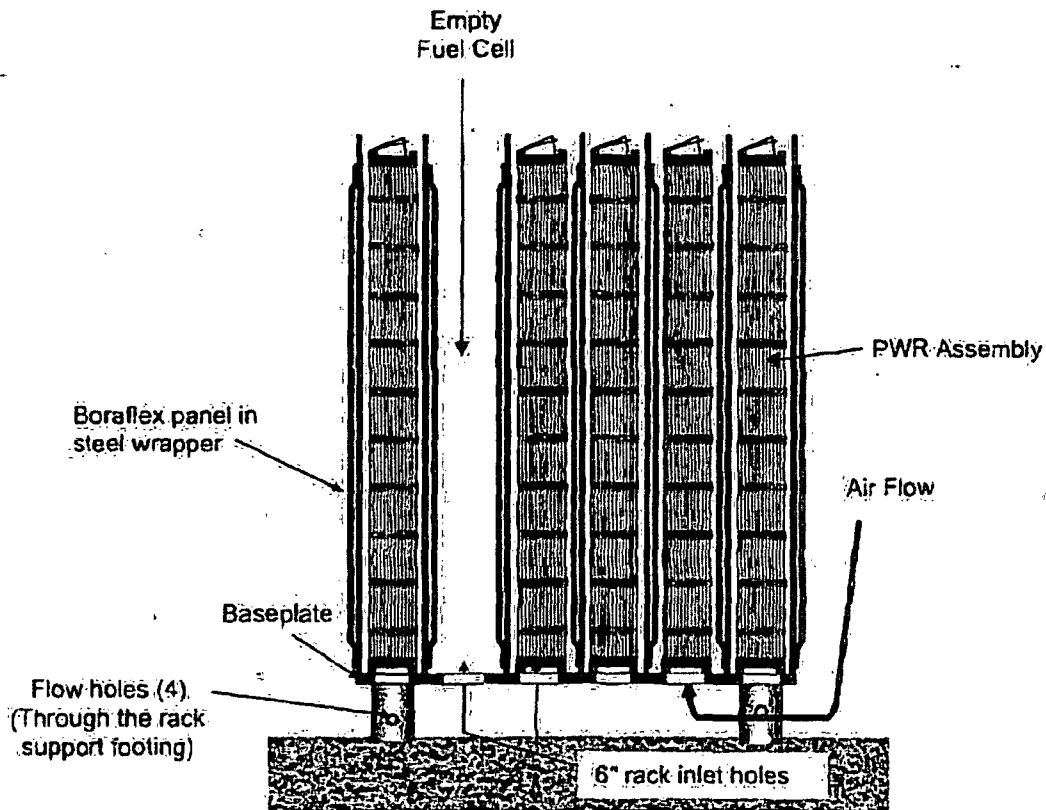


Figure 2-5 Typical Region II Spent Fuel Pool Rack Cut-away Cross-section Showing the Fuel Assembly.

2.3 SFP Accident Scenarios

From a natural circulation flow perspective, the SFP accidents are broken down into two categories; scenarios with water above the base plate of the racks and scenarios with a completely drained SFP. Each accident is described next.

2.3.1 Complete Loss-of-Coolant Inventory Accident

In the "air" flow case, the accident is initiated with a complete loss-of-coolant inventory accident (see Figure ES-1 and ES-2 for pre-accident building configuration and Figure 2-2 and Figure 2-5 for the BWR and PWR rack configurations, respectively). Due to the removal of the water, a heat-up of the fuel rods ensues. The fuel rods heat the air in the assemblies, which creates a natural circulation pattern. Complex flow patterns develop above and around the SFP racks and in the refueling room due to the interaction between the hot rising plume and descending cool air. After the hot plume exits the SFP, the plume will rise to the ceiling and spread radially within the hot gas layer at the top of the refueling room. The degree of heating in the fuel storage building and behavior of the hot gas layer depends on many factors including the rate of

ventilation (e.g., ventilation system operation, openings or leakage, and/or structural failures); the heat loss through the building walls and ceiling, and other accident thermal effects (e.g., fire).

The flow patterns of the gases under the racks are also complicated. The regions of down flow include the space between the rack and walls, some of the empty rack slots, and the cask region or other open areas. If a high speed flow region develops under the racks, then there can be a Bernoulli Effect. For example, if the air to the SFP cells is preferentially provided through the cask area, a high speed flow (i.e., 3 m/s) can develop under the rack cells adjacent to the cask area. The high speed flow reduces the upflow of gases into the affected assemblies, which leads to less heat removal and a faster heat-up (e.g., see [Wagner, 2000] or [Wagner, 2005b]).

If inadequate cooling is provided, then the fuel cladding will heat up and the zirconium-based alloy cladding will rapidly oxidize (i.e., burn) and to a lesser extent, nitride (i.e., combine with nitrogen if no oxygen or steam are available, which is not modeled in MELCOR). Since the oxidation and nitride processes are exothermic, the fuel rods could heat to melting conditions and structurally degrade. Meanwhile, the steel racks supporting the fuel assemblies will also heat due to convection and radiation from the fuel assemblies. The timing of the degradation of the specific fuel assemblies and racks are affected by the decay heat level (i.e., burn-up, power history, enrichment, and time since discharge), the assembly inlet temperature, convective and conductive heat removal rates, and the heat transfer rate from/to adjacent assemblies. Finally, and most importantly, the degradation of the fuel rods can lead to fission product releases.

An accurate analysis of the SFP response requires consideration of the aforementioned phenomena. As evidenced by the accident description, there is a large range of geometric length scales and modeling requirements. The length scales range from details of the individual assembly heat generation and flow patterns (e.g., also including multi-dimensional flow within an assembly, see [Ross, 2003]), intra-assembly heat transfer, large scale flow patterns above, below, and through the racks, and the building response (e.g., ventilation, heat loss, structural failures, etc.). The relevant physics and phenomena include heat transfer (convection, conduction, and radiation), fluid flow (small scale to large scale), chemical reactions (i.e., oxidation), severe accident fuel degradation behavior, and fission product release and transport.

In a related program, Sandia National Laboratories has conducted an experimental testing program for the NRC on the complete loss-of-coolant behavior. The program has generated data to validate and improve the MELCOR SFP models using prototypical BWR assembly components from Global Nuclear Fuels (GNF). The scope of the testing program included (1) a detailed hydrodynamic pressure drop characterization through the assembly, (2) characterization of the natural convective flows in the assembly, water rods, and annulus between the canister and the rack wall, (3) ignition of full-length Zircaloy assembly, (4) thermal radiation flux in a stagnant 1x4 configuration, and (5) ignition characteristics of 1x4 configuration with natural convection. At each phase of the program, MELCOR was used for pre-test planning and post-test assessment. The insights and findings from the experimental program were continuously fed into the SFP analysis to assess their impact. The MELCOR BWR calculation summary report [2006b] includes time-evolving findings from the experimental program.

2.3.2 Partial Loss-of-Coolant Inventory Accident

In the second type of accident, the SFP is partially drained (i.e., due to partial drain or boil-off) and does not include recirculation of hot gases through the bottom of racks. Consequently, the gas in the fuel assemblies above the pool level is relatively stagnant (i.e., except for steam flow from boiling). In this condition, steam cooling and/or a level swell from the boiling will keep the fuel rods cool unless the pool level drops too far. However, once the level drops below (b)(2)High

Ex. 2

(b)(2)High

the top of the fuel rods will heat-up and degrade.

If the top of the fuel is uncovered, then several new phenomena occur in a partial loss-of-coolant inventory accident. First, the convective flows are much smaller than a complete loss-of-coolant inventory accident. In the complete loss-of-coolant inventory accident, there was ample air flow as the assembly heated. However, in a partial loss-of-coolant inventory accident, the fluid in the assembly is relatively stagnant because the pool blocks the bottom of the racks. The primary source of cooling comes from steam flow due to boiling below the water level. Hence, there are competing effects of the lack of a strong convective flow versus the benefits of some steam cooling and axial conduction to the water. In summary, the scenarios with water include (a) two-phase boiling, (b) an assembly flow rate that is strongly affected by the amount of boiling below the water surface, and (c) gas inlet temperature that is limited to the boiling point of water (i.e., the air cases are not similarly constrained).

The oxidation of the zirconium-based alloy cladding is the second key difference expected in a partial loss-of-coolant inventory accident. In particular, the fluid next to the cladding will be steam rather than air. Steam also reacts exothermically with zirconium-based alloys but at a slower rate than with air. Furthermore, oxidation in steam air produces less chemical energy per mole of reacted Zircaloy than oxidation in air owing to the fact that there is disassociation energy invested in the case of breaking H_2O into H_2 and O_2 . The byproduct of the zirconium/steam reaction is hydrogen. The hydrogen will replace the steam and retard or stop the zirconium/steam reaction. Consequently, the reaction could become "steam starved" and controlled by the rate of steam production by boiling below the pool level, which is expected to be very low for aged spent fuel. If there is adequate steam when the zirconium-based cladding reaches high temperatures (i.e., >1500 K), then the power from metal water reactions can be much larger than decay heat. Therefore, there are two competing effects on the rate of fuel degradation relative to the complete loss-of-inventory accident scenario (i.e., as described in Section 2.3.1), (1) a lower, controlled oxidation effect (i.e., due to steam starvation) and (2) a much lower convective cooling rate (i.e., because the bottom of the racks are "plugged" with water).

Finally, a third new difference in the partial loss-of-coolant inventory accident is the behavior of the hydrogen. As hydrogen is produced during fuel degradation, the hydrogen may collect and mix with oxygen in the air above the pool. Given the appropriate conditions, the hydrogen could ignite and possibly cause structural damage to the reactor building. Any damage or enhanced leakage caused by the pressurization from the hydrogen burn could increase the release of fission products and their associated adverse consequences.

As will be discussed in Sections 3.1 and 3.3, make-up or spray operation complicates the potential for water plugging the inlet to the racks. For appropriate combinations of leakage and

make-up/sprays rates and leakage location, the water addition can maintain a water level above the base plate of the racks. Consequently, the water addition in some circumstances will stop air natural circulation. If the source of water is a make-up flow that is not distributed across the assemblies, the resultant configuration will be less effectively cooled due to plugging unless the resultant water level is high ^{(b)(2) High} If the source of water is a spray flow, the effectiveness of the cooling film of water entering the assembly relative to air natural circulation is dependent upon the magnitude of the spray flow rate.

Ex. 2

3. MITIGATION OF SFP LOSS-OF-COOLANT INVENTORY ACCIDENTS

Numerous analyses of the loss-of-coolant inventory accidents have been performed using data from an operating BWR and an operating PWR. The studies analyzed a variety of scenario variations and phenomenological uncertainties to identify the most important factors affecting the accident progression and the assembly coolability. Based on the insights from the studies, actions are identified that will mitigate the consequences or enhance the coolability of a spent fuel pool accident. The topics and associated report section are,

- Section 3.1 Make-up Water and Leak Repair
- Section 3.2 Well-Organized Fuel Configurations
- Section 3.3 Emergency Sprays
- Section 3.4 Building Ventilation
- Section 3.5 Pool Configuration
- Section 3.6

Miscellaneous Other Factors

Each topic will be addressed in the sited subsection with some remarks about the application to other SFPs.

3.1 Make-up Water and Leak Repair

The most obvious solution to a loss-of-coolant inventory accident consists of leak repair and make-up water. The NRC, along with industry, has identified potential water sources to the SFP. Various size leaks were simulated in MELCOR calculations, which permitted calculation of the level response and water requirements. While not directly addressed in this study, there are obvious benefits from emergency leak repair.

Section 3.1 is subdivided into three subsections. First, the results of steady-state water level calculations are presented in Section 3.1.1. The steady-state results identify the minimum water level that prevents escalation to ignition and fuel degradation. Consequently, if the make-up flow can maintain the water level above the cited steady state conditions, then the configuration is stable until additional resources can be applied to refill the pool. Next, Section 3.1.2 shows the level response to different size leaks at a variety of elevations. The level response results yield some insight into the timing to fuel uncover and timing to the fuel heatup without any make-up flow. Section 3.1.3 shows some simple calculations to estimate the minimum make-up flow to remove the fuel decay heat. The make-up flow calculations do not account for leakage. Hence, they are applicable for scenarios where the leak is above the minimum elevation identified in Section 3.1.1. If a make-up source is available, Section 3.1.4 shows calculations for the time required to make-up the level to a coolable condition for a range of conditions. Finally, the results are summarized in Section 3.1.5, as well as suggestions to extend the insights to other SFPs.

3.1.1 Minimum Level Cooling

The separate effects water calculations were performed using the reference PWR SFP MELCOR model assuming a partially filled water configuration. The assembly decay heat removal is achieved by steam cooling and downward conduction above the water level and by boiling below the water level. The collapsed water level outside the assembly was held at a constant position. The separate effects water calculations specified various constant water levels for three levels of decay heat power. The model was initialized with nearly saturated water at a specified water level, with the remaining height covered by air. The fuel, cladding, rack, and other structures were also initialized at nearly saturated conditions. The initial and boundary conditions were specified to maintain a specified collapsed water level, which was represented as a percentage of the height of the active fuel region of the assembly in the racks. The calculations were run for a range of three decay heat powers. (b)(2)High

Ex. 2

(b)(2)High

Figure 3-1 through Figure 3-3 show the peak cladding temperatures for a range of static water levels at the high, medium, and low decay heat powers, respectively. At the high power condition, the swollen level was the highest of the three cases. (b)(2)High

Ex. 2

(b)(2)High

mechanisms. At a [redacted] collapsed liquid level, the temperature stabilized at approximately [redacted] (b)(2)High. If a peak cladding temperature of [redacted] (b)(2)High was chosen as an upper bound, then a collapsed level slightly below [redacted] would be considered as an upper bound for coolability for a high decay heat power assembly. Due to the high decay heat power, once the level dropped below [redacted] the heatup to high temperature conditions was very rapid [redacted] (b)(2)High.

Ex. 2

For the medium and low-power cases, the swollen water level was lower than the high-powered case. Consequently, the heatups occurred at higher collapsed liquid levels. The lowest collapsed water level that resulted in a peak cladding temperature less than [redacted] (b)(2)High for the medium power case and [redacted] for the low-powered case (see Figure 3-2 and Figure 3-3, respectively). Although a higher collapsed water level was required to prevent temperature excursions above [redacted] (b)(2)High than for the high-powered case, the resultant heatup rate was slower. The [redacted] water level reached [redacted] (b)(2)High for the medium-powered case and the [redacted] water level reached [redacted] (b)(2)High.

Ex. 2

The dependence of the peak cladding temperature (PCT) for a given collapsed level, as a function of specific power level are more clearly shown in Figure 3-4 through Figure 3-6. Higher decay levels cause more boiling and level swell. Hence, for scenarios with a slowly falling level (e.g., a boil-off transient), the top portion of the lower-powered assemblies would be expected to start heating first. Due to their lower decay heat level, the heatup rate would be slow. However, as the level fell lower and successively higher powered assemblies started their heat-ups, the subsequent temperature escalation rates would be much higher. Table 7 summarizes the minimum collapsed water level as a function of assembly power to remain below a temperature sometimes used for regulatory analysis (565°C) and the current best-estimate coolability limit in a steam environment [redacted] (b)(2)High.

Ex. 2

Table 7 Summary of the PCTs versus Collapsed Water Level:

(b)(2)High

Ex 1
2

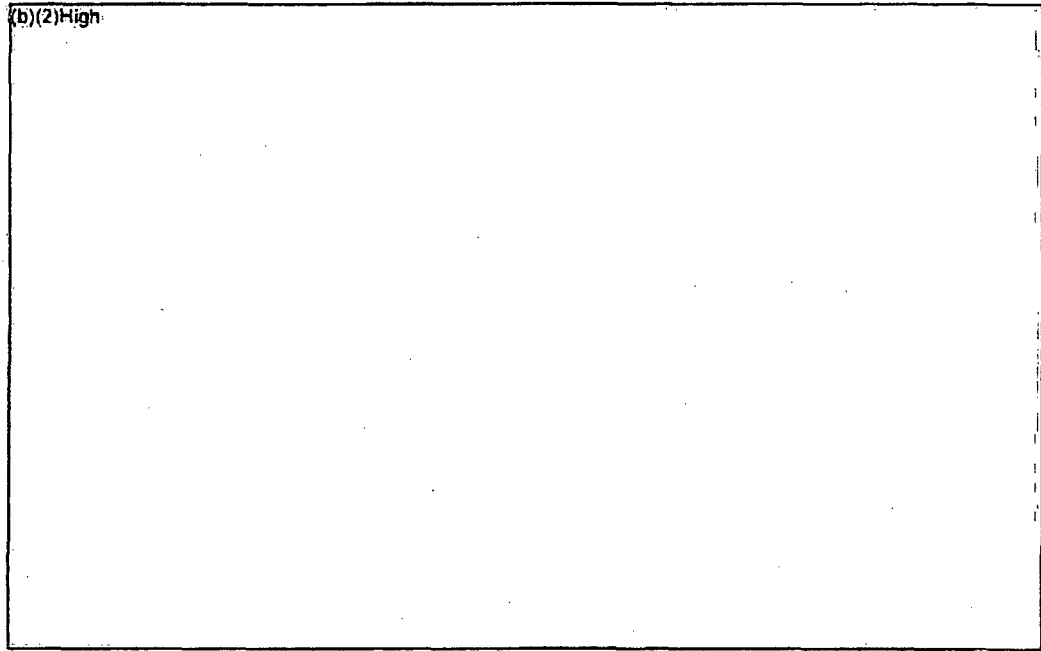
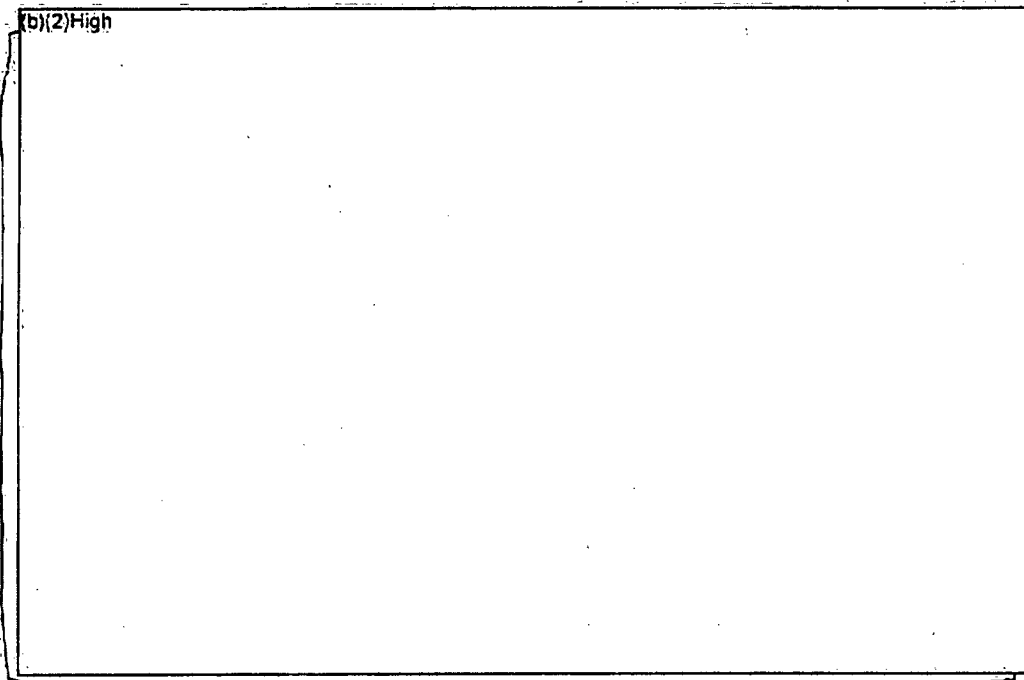


Figure 3-1 Comparison of the PCT versus a Function of the Collapsed Liquid Level Outside of the Assembly at (b)(2)High Aging Time Since the Assembly was Discharged.

Ex: 2

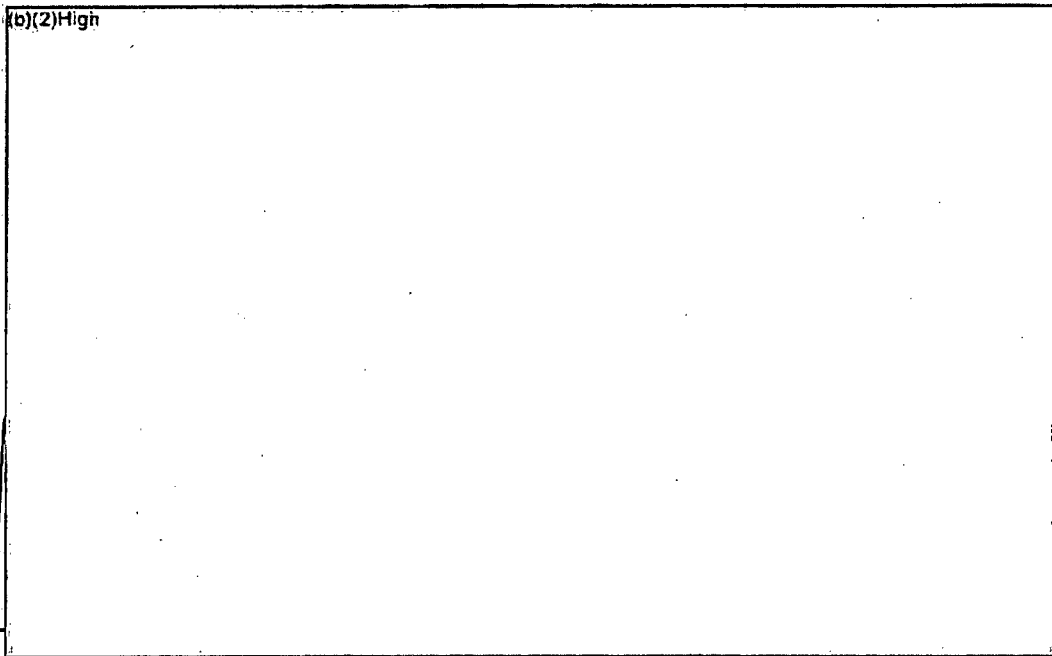
Ex. 2



Ex. 2

Figure 3-2 Comparison of the PCT versus a Function of the Collapsed Liquid Level Outside of the Assembly at (b)(2)High Aging Time Since the Assembly was Discharged.

Ex. 2



Ex. 2

Figure 3-3 Comparison of the PCT versus a Function of the Collapsed Liquid Level Outside of the Assembly at (b)(2)High Aging Time Since the Assembly was Discharged.

Ex. 2
2

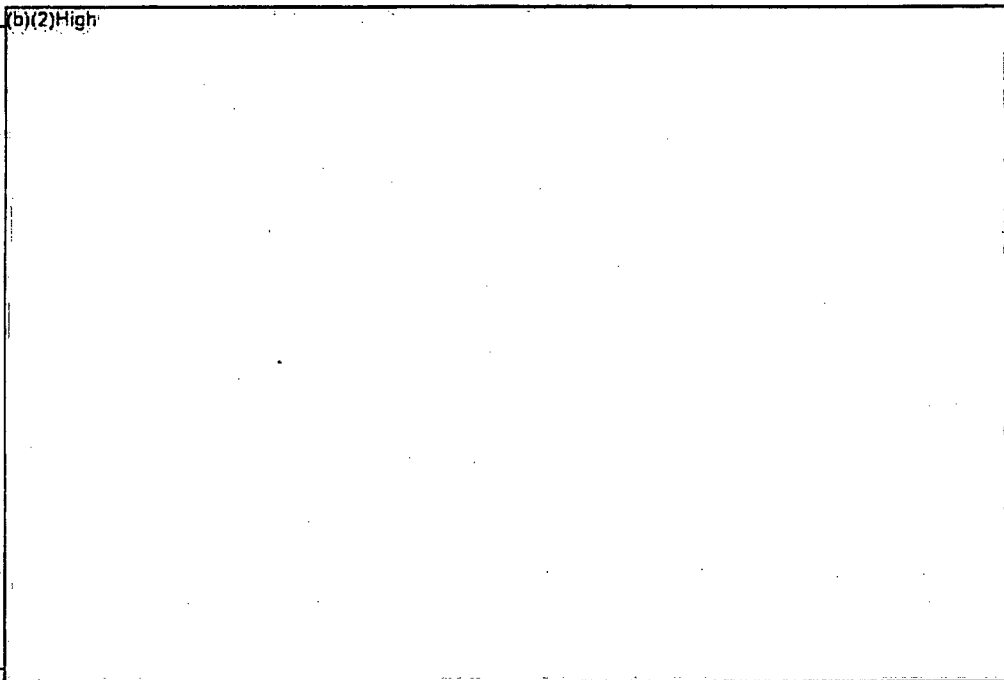


Figure 3-4 Comparison of the PCT versus a Function of the Decay Power of the Assembly at Collapsed Water Level.

Ex. 2

Ex. 2

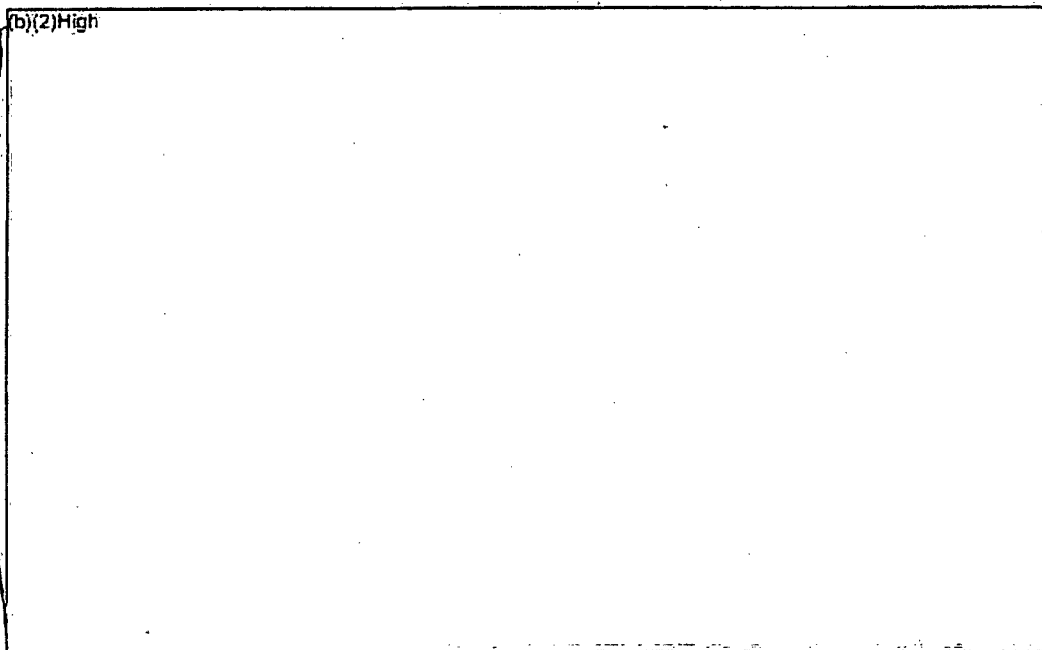
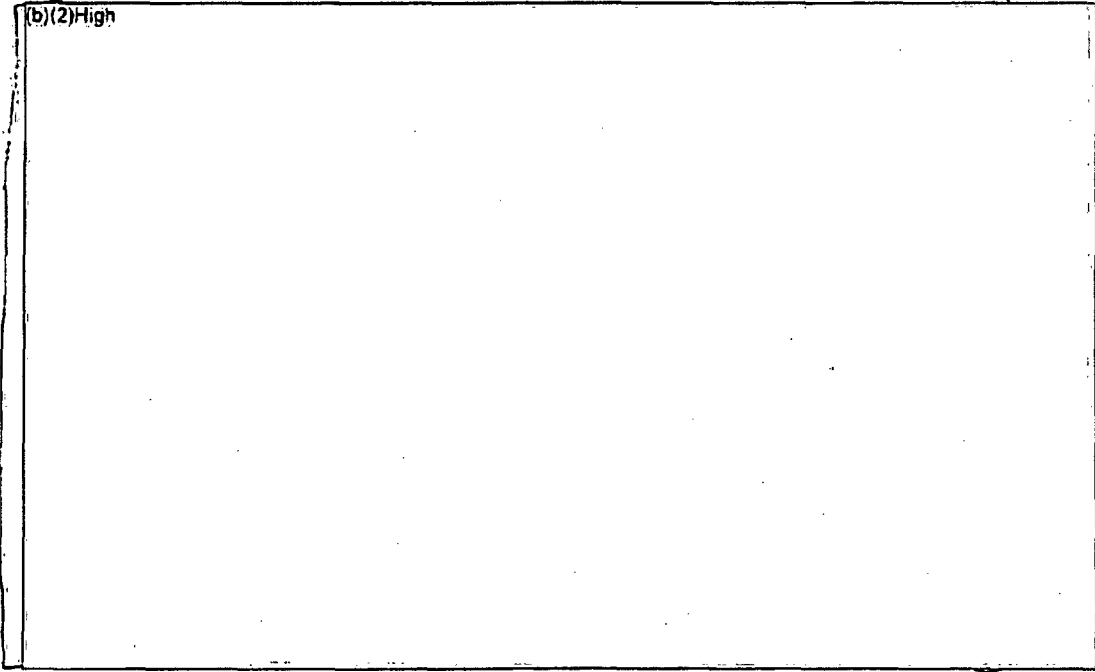


Figure 3-5 Comparison of the PCT versus a Function of the Decay Power of the Assembly at Collapsed Water Level.

Ex. 2

Ex.
2



Ex. 2

Figure 3-6. Comparison of the PCT versus a Function of the Decay Power of the Assembly at a Collapsed Water Level.

3.1.2 Level Response Timing for Non-dispersed Fuel Configuration

Reference PWR SFP calculations were performed to estimate drain-down times as a function of leak size and location. Two aging configurations were considered, (b)(2)High

Ex. 2
2

(b)(2)High

The following simplifying assumptions were used in the analysis,

- The heat capacitance of building walls, roof, and equipment was not included in the calculation. The ventilation system was assumed failed but building leakage was included.
- The pool heat removal system was assumed failed.
- There was no radial heat transfer from the high-powered to the low-powered assemblies, or between the assemblies and the empty cells or the SFP walls. As will be discussed in Section 3.2, this results in the fastest heatup of the freshly-discharged fuel.
- The MELCOR SFP model subdivided the fuel assemblies into 4 rings and modeled the empty Region I and II rack cells in 2 other rings. Ring 1 included all the fuel assemblies from the last discharge (i.e., Batch 15). Ring 2 had Batches 13 and 14; Ring 3 had Batches 11 and 12; and Ring 4 had Batches 1 through 10.⁴

The following leakage conditions were considered,

- No leakage

Ex. 2

(b)(2)High

In addition, different depths were considered for the leakage location. The lower leakage locations are described relative to the location of the fuel in the SFP racks. The following leakage locations were considered (all of which lead to a partial draindown configuration as opposed to a complete draindown),

Ex. 2
2

(b)(2)High

Ex. 2

⁴ Ring 1 simulated the assemblies from the last discharge to the SFP and had the highest powered assemblies. The decay heat of the assemblies was modeled using their average characteristics. However, the highest powered assemblies in Ring 1 had decay heat substantially above the average power. The impact of those differences was evaluated for the most limiting case (b)(2)High and is discussed with those results.

Ex. 2 Table 8 and Table 9 summarize the results of the (b)(2)High aging calculations, respectively. The four right-hand columns in the tables summarize timings to reach specific pool elevations or an (b)(2)High. The first three of those columns are specific collapsed water levels in the spent fuel pool. They include the top of the rack elevation (173"), the top of the active fuel (153"), and the mid-plane of the active fuel height (81"). For each hole leakage size, the timing to reach those particular levels are summarized in hours as a function of the leakage location. For example, the values in a particular row show the timings to particular locations for a specific leak location whereas the values in a column represent timings of different leak sizes and locations to reach a specific location. The final column shows the timing for the peak cladding temperature location to exceed (b)(2)High. The timings for this parameter ranged from

(b)(2)High

Ex. 2 Ring 1 simulated the assemblies from the last discharge to the SFP and had the highest powered assemblies. The decay heat of the assemblies was modeled using the average characteristics. However, the peak powered assembly in Ring 1 had a decay heat substantially above the average power. (b)(2)High

Ex. 2 (b)(2)High

Ex 2 Table 8 Summary of Timings to Elevations as a Function of Hole Size for a Non-Dispersed Configuration at ^{(b)(2)High} Since Shutdown.

(b)(2)High

Ex 2

- Legend:**
- Mid** Midway between the normal water level and the top of the racks (312")
 - TAF** Top of the active fuel elevation (153")
 - MAF** Middle of the active fuel elevation (81")
 - BAF** Bottom of active fuel elevation (9")

- Notes:**
- A. A non-dispersed fuel configuration places all the recently discharged fuel assemblies in one location. As will be discussed in Section 3.2, this results in the fastest heatup of the fuel.

⁵ The time is based upon the collapsed level in the open region.

Ex. 2 Table 9 Summary of Timings to Elevations as a Function of Hole Size for a Non-Dispersed Configuration at (b)(2)High Since Shutdown.

(b)(2)High

Ex. 2

Legend: **Mid** Midway between the normal water level and the top of the racks (312")
 TAF Top of the active fuel elevation (153")
 MAF Middle of the active fuel elevation (81")
 BAF Bottom of active fuel elevation (9")

Notes: A. A non-dispersed fuel configuration places all the recently discharged fuel assemblies in one location. As will be discussed in Section 3.2, this results in the fastest heatup of the fuel. For example, see Figure 3-35 in Section 3.2.2 for a comparison of the heatup timing for Case 3 (b)(2)High.

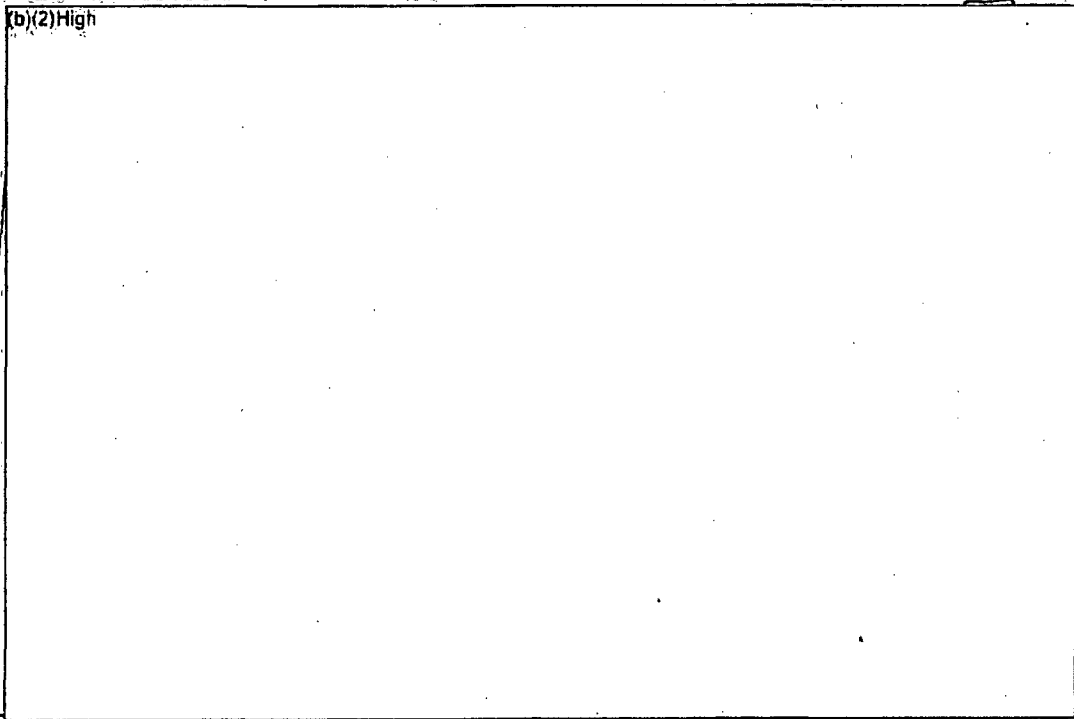
Ex. 2

Ex. 2 Figure 3-7 through Figure 3-22 graphically illustrates all the drain-down results for the (b)(2)High aging cases. For each case, the collapsed liquid and peak cladding temperature response are shown for each break location. If the leakage location was at the lower two elevations,

Ex. 2 (b)(2)High then the fuel heatups commence once the fuel is uncovered. For the higher leakage elevations, the drain-down through the leakage hole stopped before the fuel was uncovered. Subsequently, the water heated to saturation conditions (~373 K) and boiled away. Hence, the higher break elevations benefited from the additional time to heat the water to saturation conditions. The change in the level decrease rate is clearly evident on the level response figures once the water level reaches the leakage elevation. As shown by the results in Case 1 (e.g., see Figure 3-15), the level decrease rate during the boil-off phase is approximately the same as the drain rate from a (b)(2)High hole.

Ex. 2

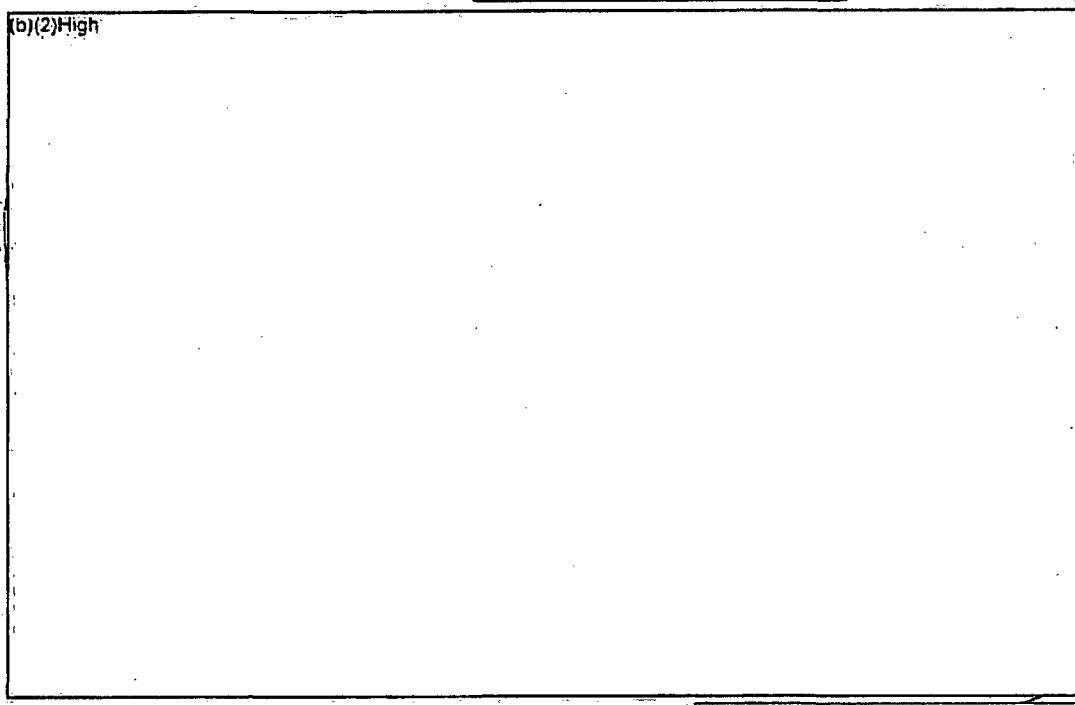
⁶ The time is based upon the collapsed level in the open region.



Ex.
2

Ex.
2

Figure 3-7 Comparison of Pool Drain Rates ^{(b)(2)High} as a Function of Leak Location ^{(b)(2)High}

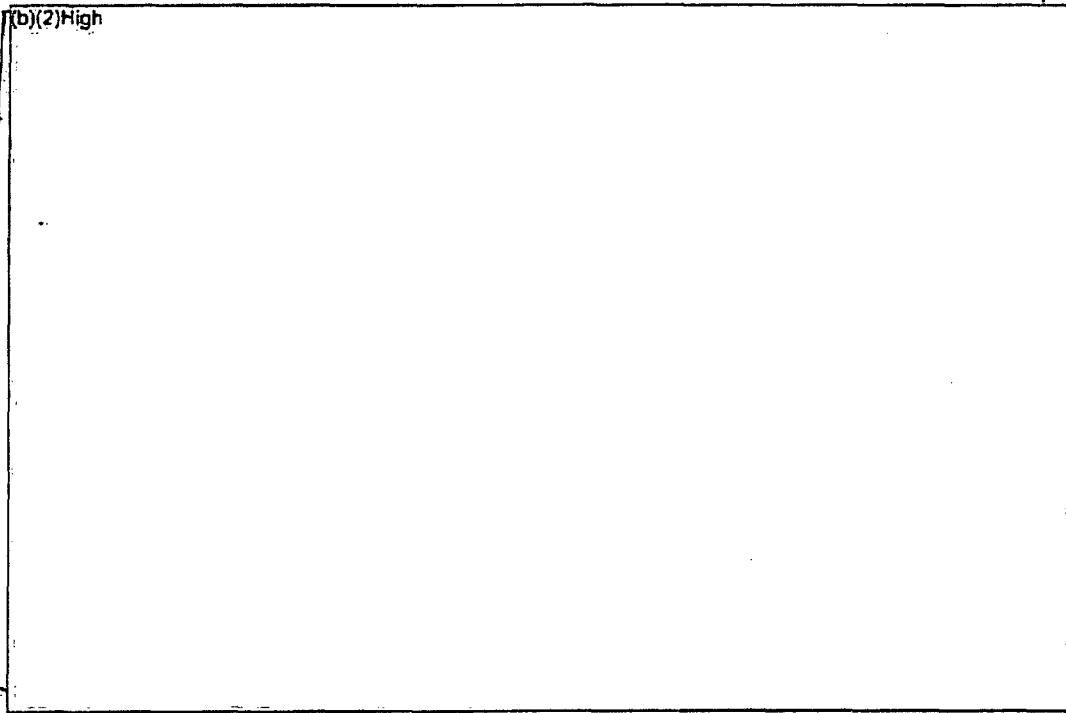


Ex.
2

Ex.
2

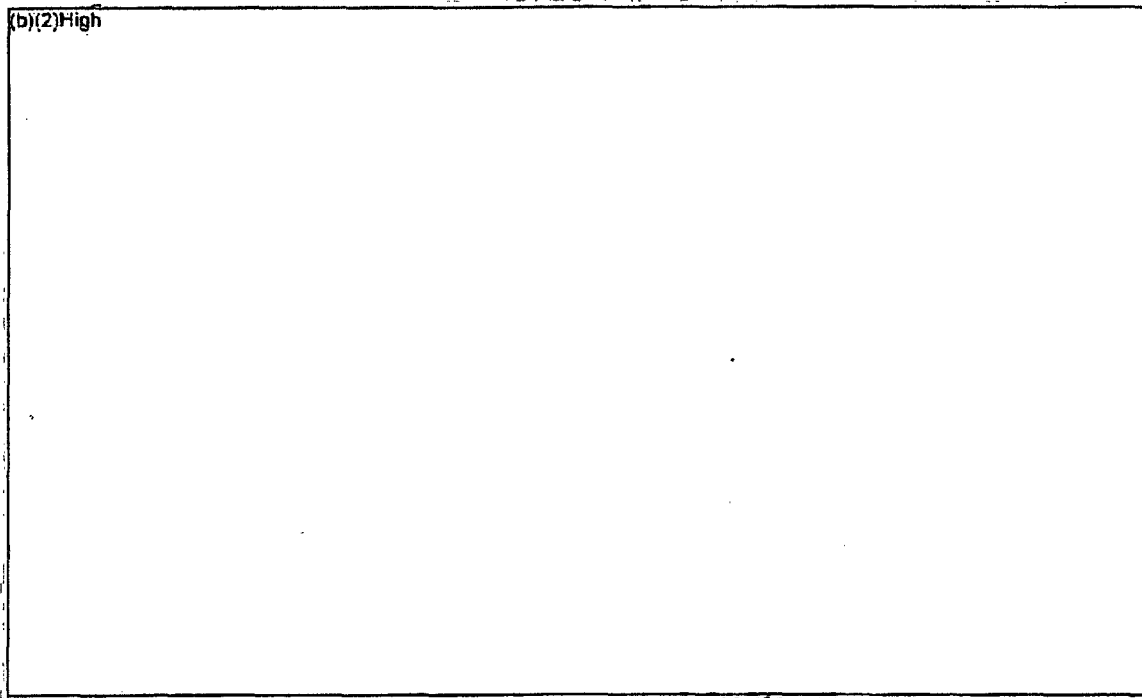
Figure 3-8 Comparison of Peak Cladding Temperatures ^{(b)(2)High} as a Function of Leak Location ^{(b)(2)High}

Ex.
2

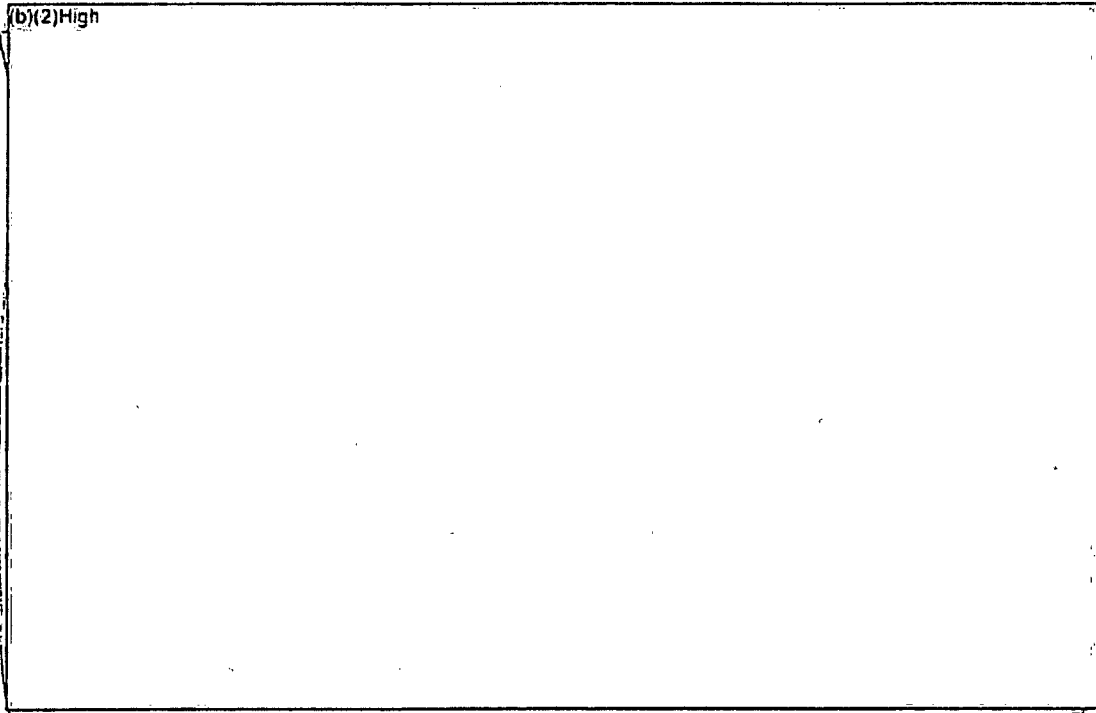


Ex. 2 **Figure 3-9 Comparison of Pool Drain Rates** (b)(2)High as a
Function of Leak Location (b)(2)High

Ex.
2

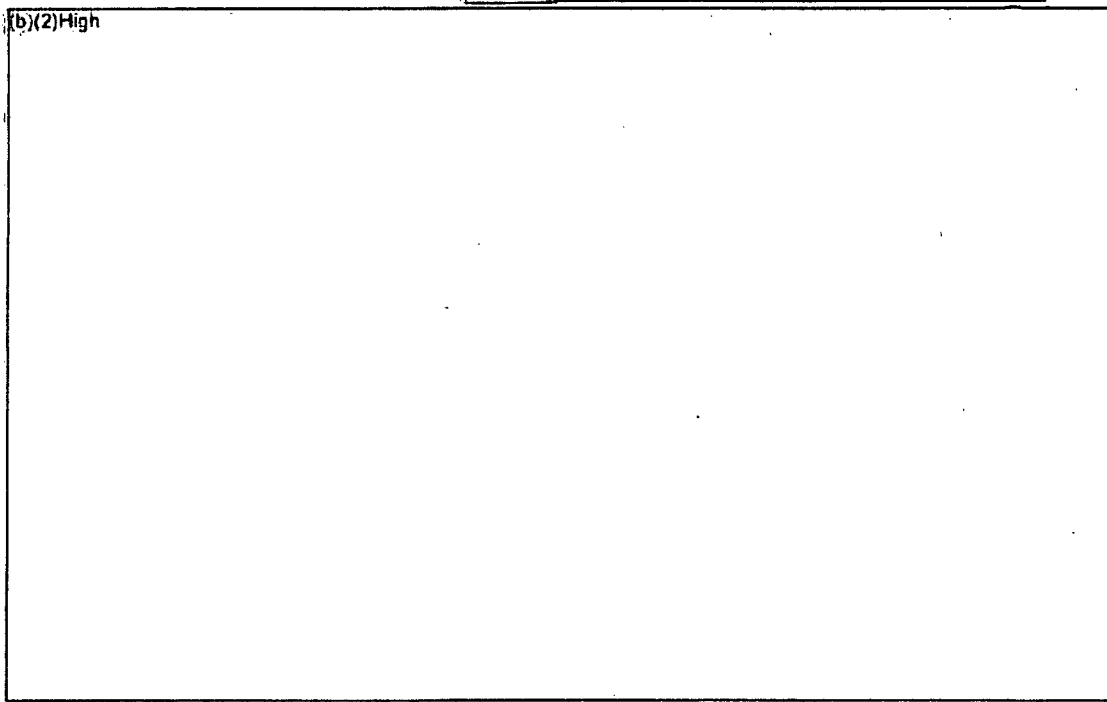


Ex. 2 **Figure 3-10 Comparison of Peak Cladding Temperatures** (b)(2)High
(b)(2)High as a Function of Leak Location (b)(2)High



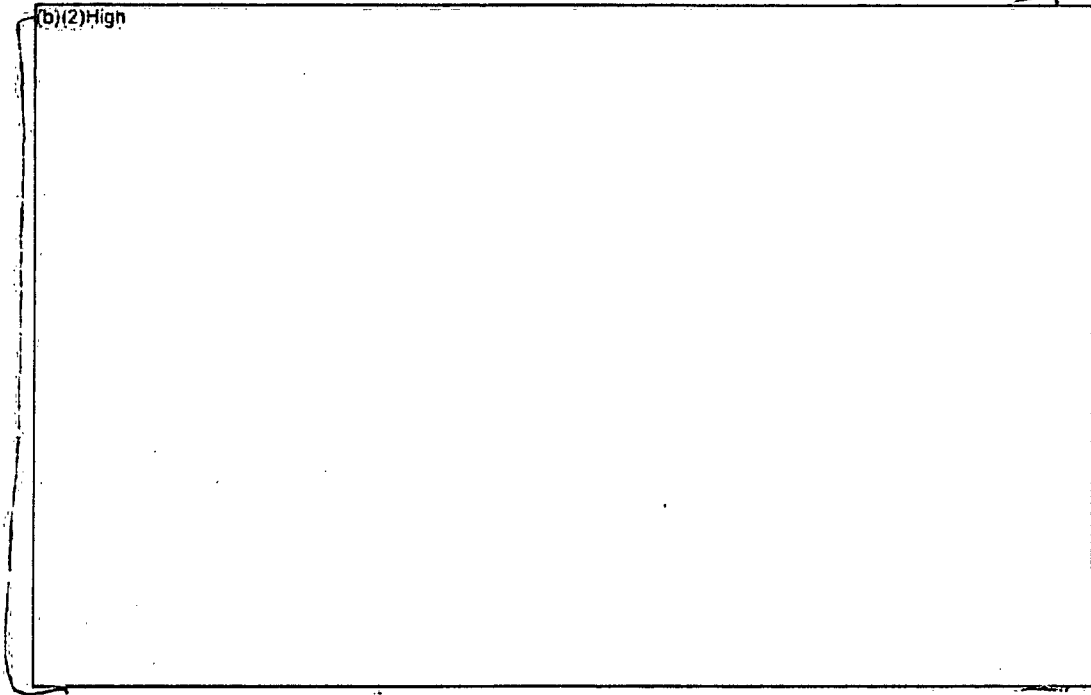
Ex.
2

Ex. Figure 3-11 Comparison of Pool Drain Rates as a Function of Leak Location (b)(2)High (b)(2)High



Ex.
2

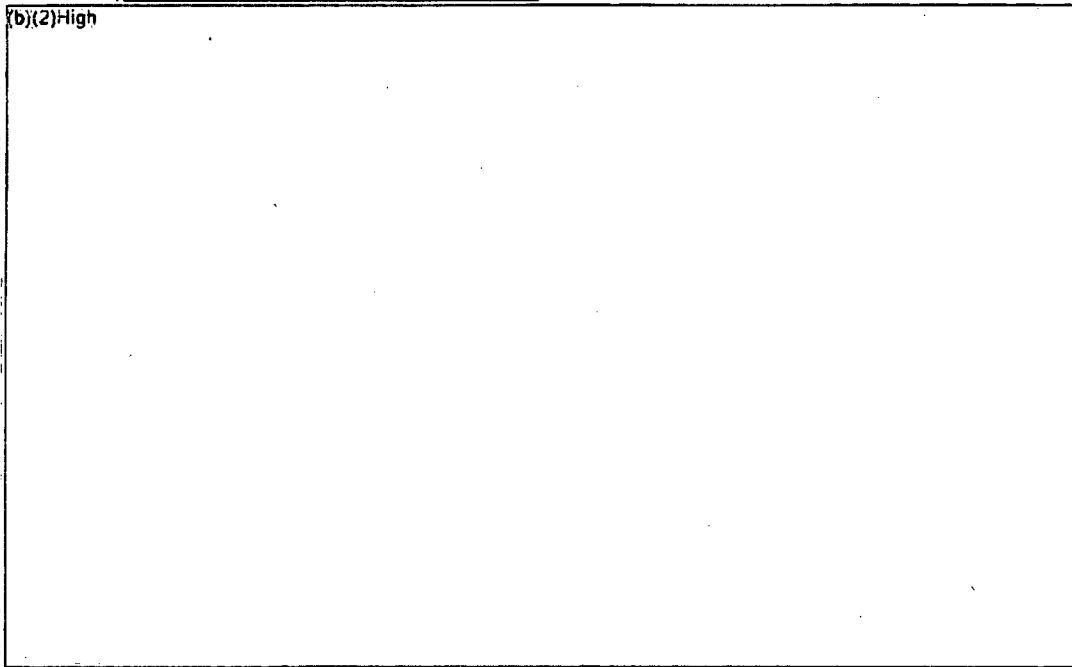
Ex. Figure 3-12 Comparison of Peak Cladding Temperatures as a Function of Leak Location (b)(2)High (b)(2)High (b)(2)High



Ex.
2

Ex. 2 Figure 3-13 Pool Drain Rates for Loss-of-Heat Removal Accident (i.e., No Leakage Hole)

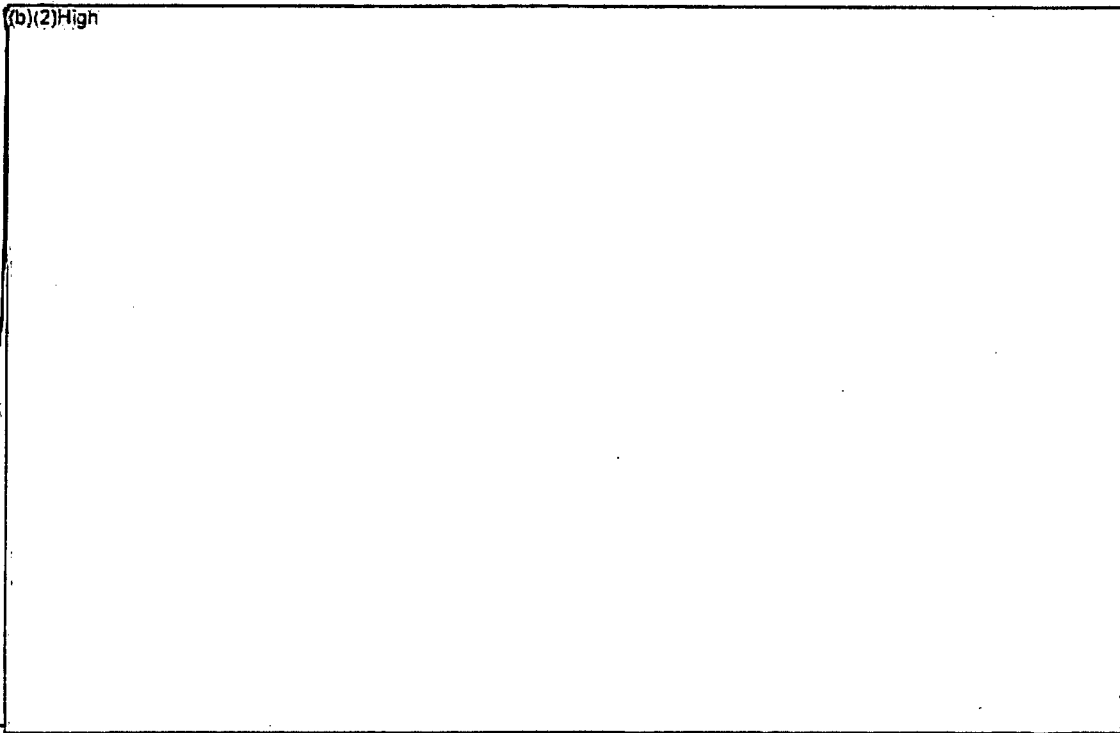
(b)(2)High



Ex.
2

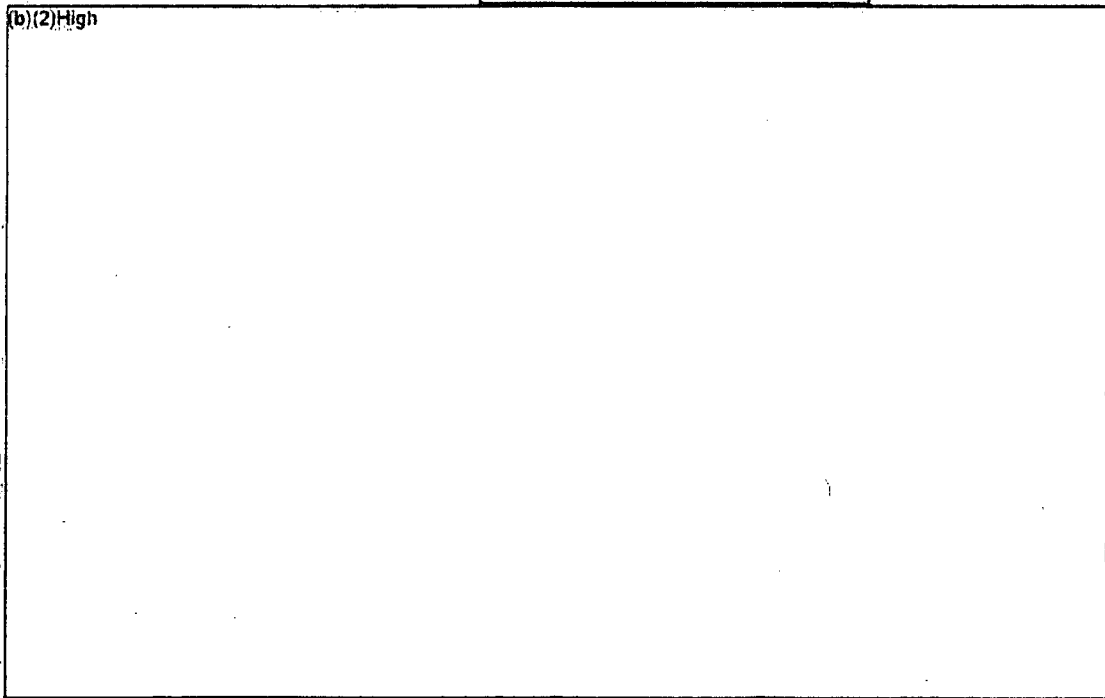
Ex. 2 Figure 3-14 Peak Cladding Temperature for Loss-of-Heat Removal Accident (i.e., No Leakage Hole)

(b)(2)High



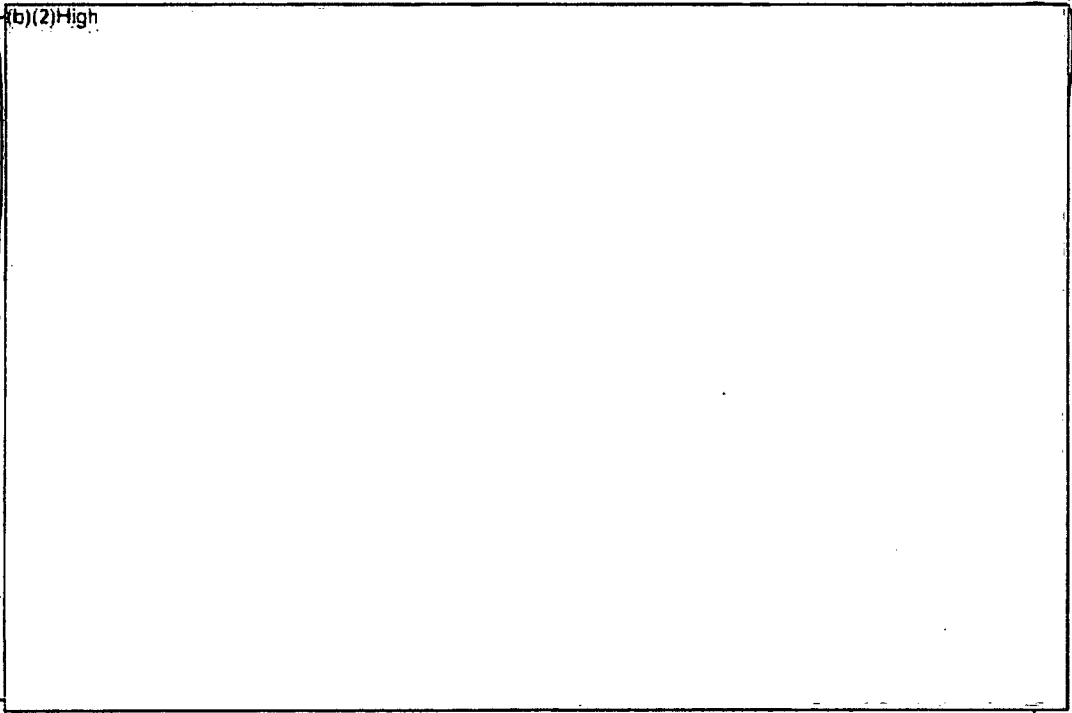
Ex.
2

Ex. 2 **Figure 3-15 Comparison of Pool Drain Rates** (b)(2)High as a Function of Leak Location (b)(2)High



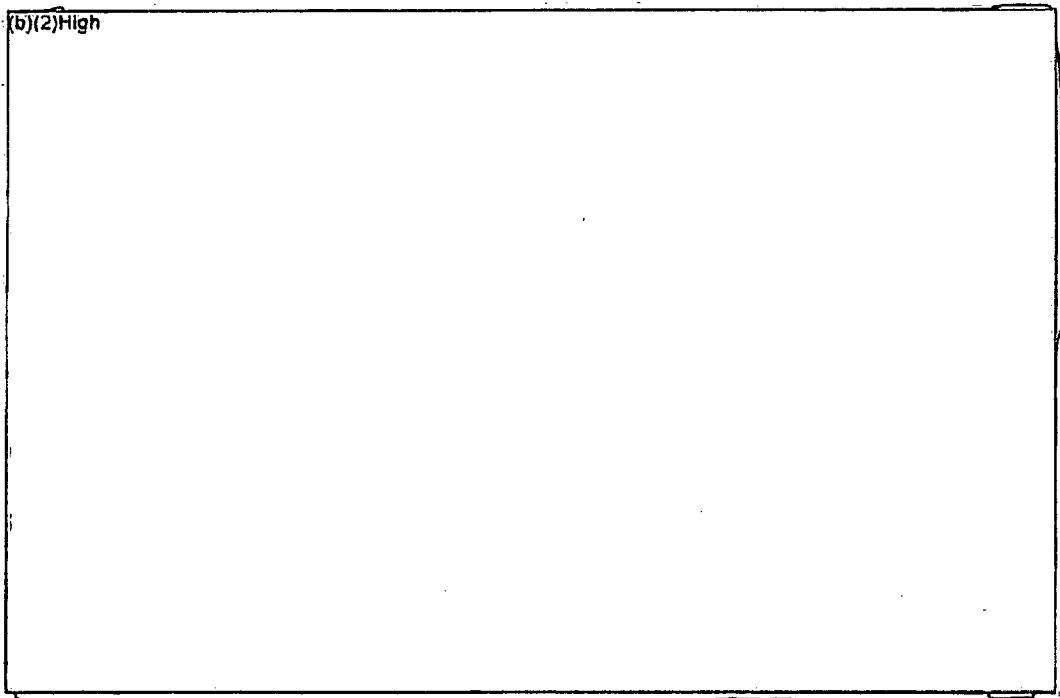
Ex.
2

Ex. 2 **Figure 3-16 Comparison of Peak Cladding Temperatures** (b)(2)High as a Function of Leak Location (b)(2)High



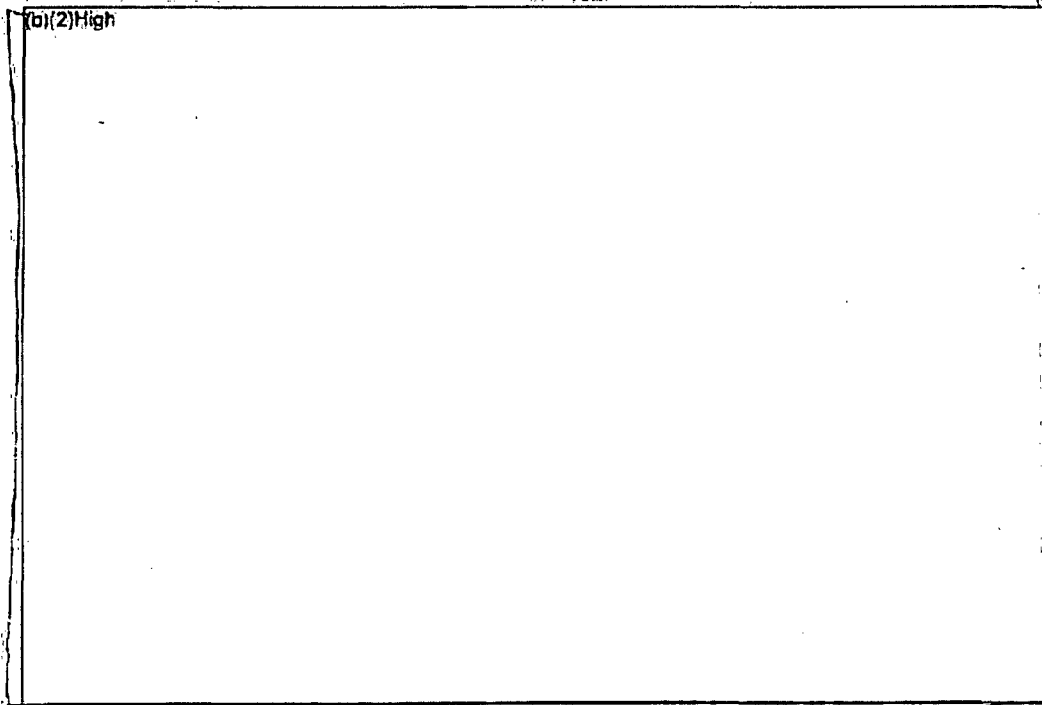
Ex.
2

Ex. 2 **Figure 3-17 Comparison of Pool Drain Rates** (b)(2)High as a
Function of Leak Location (b)(2)High



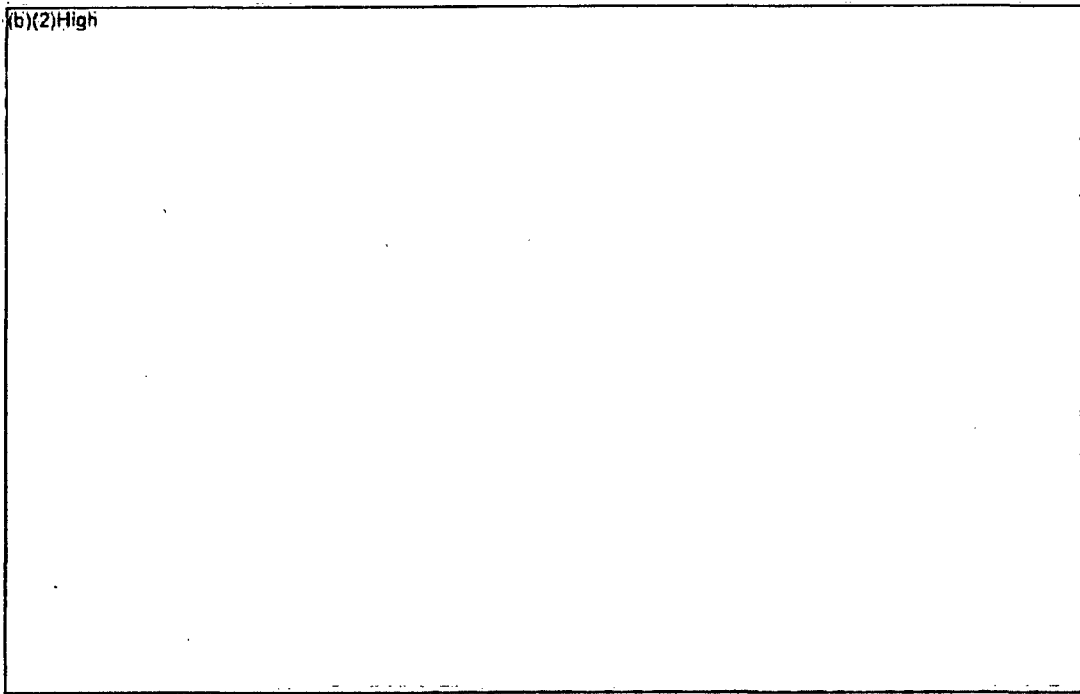
Ex.
2

Ex. 2 **Figure 3-18 Comparison of Peak Cladding Temperatures** (b)(2)High
(b)(2)High as a Function of Leak Location (b)(2)High



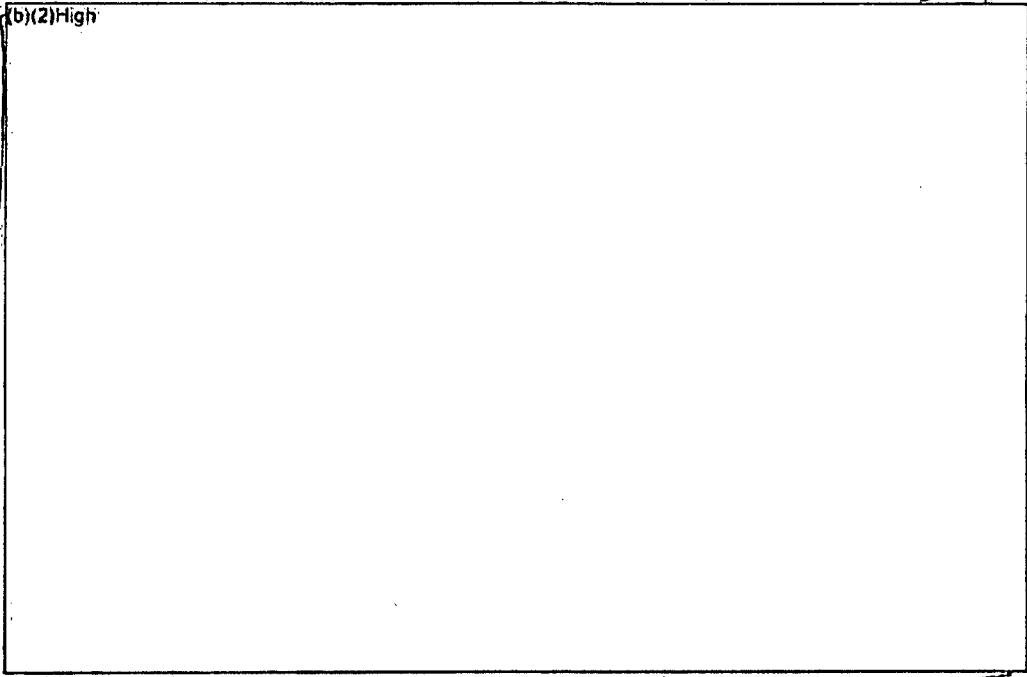
Ex.
2

Ex. 2 Figure 3-19 Comparison of Pool Drain Rates as a Function of Leak Location



Ex.
2

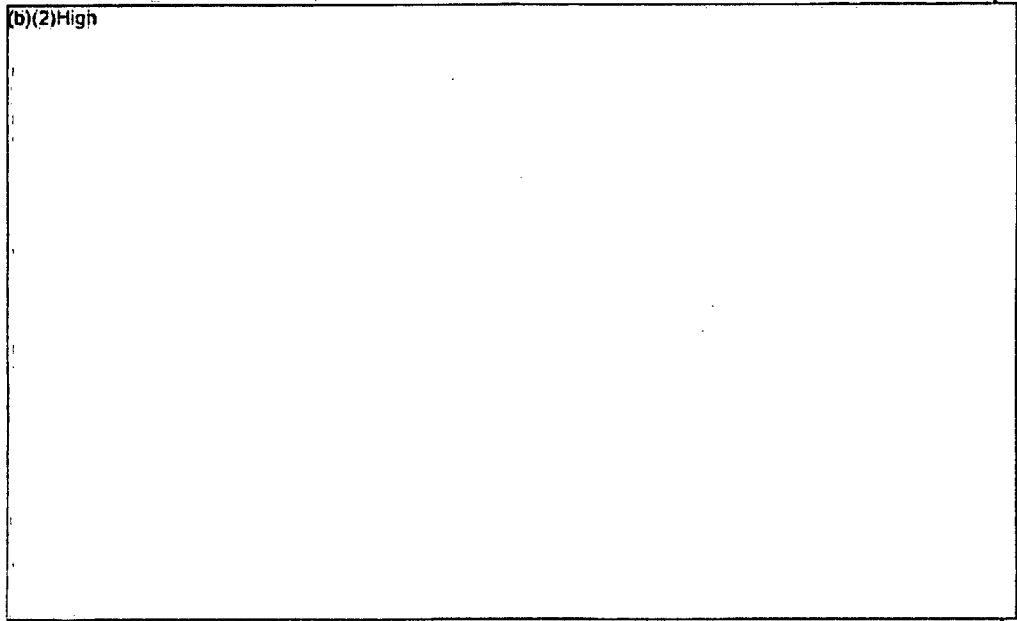
Ex. 2 Figure 3-20 Comparison of Peak Cladding Temperatures as a Function of Leak Location



Ex.
1

Ex. 2 **Figure 3-21 Pool Drain Rates for Loss-of-Heat Removal Accident (i.e., No Leakage Hole)**

(b)(2)High



Ex.
2

Ex. 1 **Figure 3-22 Peak Cladding Temperature for Loss-of-Heat Removal Accident (i.e., No Leakage Hole)**

(b)(2)High

3.1.3 Calculations for Minimum Make-up Flow

Ex. 2 Hand calculations were performed to estimate the minimum water make-up rate to the SFP assuming only a loss of heat removal or the leakage site is above [redacted] of the active fuel height (see Section 3.1). The hand calculations represent simple straight-forward energy balances that are useful for estimating the minimum flowrate for a make-up system. Depending on the time of the accident, the decay heat varies. Close to the most recent offload of fuel into the SFP, the decay heat is highest (see whole pool decay heat for the reference BWR and PWR in Figure 3-23 and Figure 3-24, respectively). Figure 3-25 and Figure 3-26 show the required flow rate to maintain the SFP level in the BWR and PWR SFPs, respectively.

Ex. 2 The following calculations illustrate the make-up flow for one point on Figure 3-25. The calculations are for the heat removal requirements (b)(2)High in the reference BWR SFP.

Assumptions:

- Ex. 2 1. Reference BWR SFP decay heat data
- 2. Last offload had (b)(2)High aging since reactor shutdown
- 3. 80°F make-up water
- 4. Decay heat removal is provided by boiling make-up water
- 5. Other modes of heat transfer are ignored.

$$\rho = 62.1 \text{ lbm/ft}^3 = 996 \text{ kg/m}^3$$

$$h_{fg} = 970.3 \text{ BTU/lbm} = 2.257 \times 10^6 \text{ J/kg}$$

$$h_{80^\circ\text{F} \rightarrow 212^\circ\text{F}} = 180.18 \text{ BTU/lbm} - 48.13 \text{ BTU/lbm} = 132.05 \text{ BTU/lbm} = 3.072 \times 10^5 \text{ J/kg}$$

$$\Delta h = h_{fg} + h_{80^\circ\text{F} \rightarrow 212^\circ\text{F}} = 1102 \text{ BTU/lbm} = 2.56 \times 10^6 \text{ J/kg}$$

Ex. 2 Reference BWR SFP whole pool decay heat (b)(2)High [redacted]

Ex. 2 Make-up Flowrate = $\frac{(b)(2)High}{(264.2 \text{ gal/m}^3)}$ $(996 \text{ kg/m}^3 * 2.56 \times 10^6 \text{ J/kg}) * (60 \text{ sec/min})$

Ex. 2 = $\frac{(b)(2)High}{(264.2 \text{ gal/m}^3)}$ [redacted]

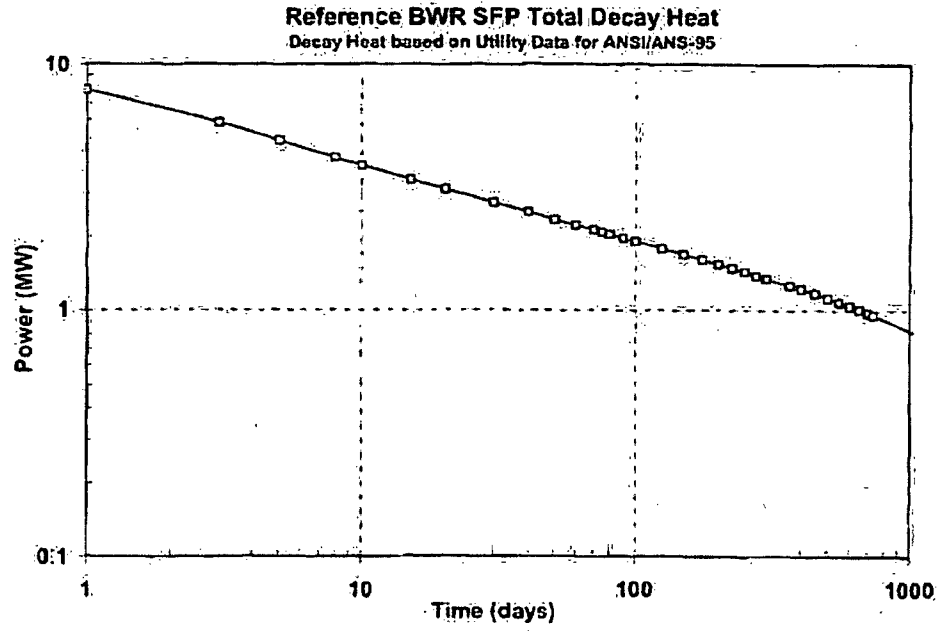


Figure 3-23 Total Pool Decay Heat Power in the Reference BWR SFP.

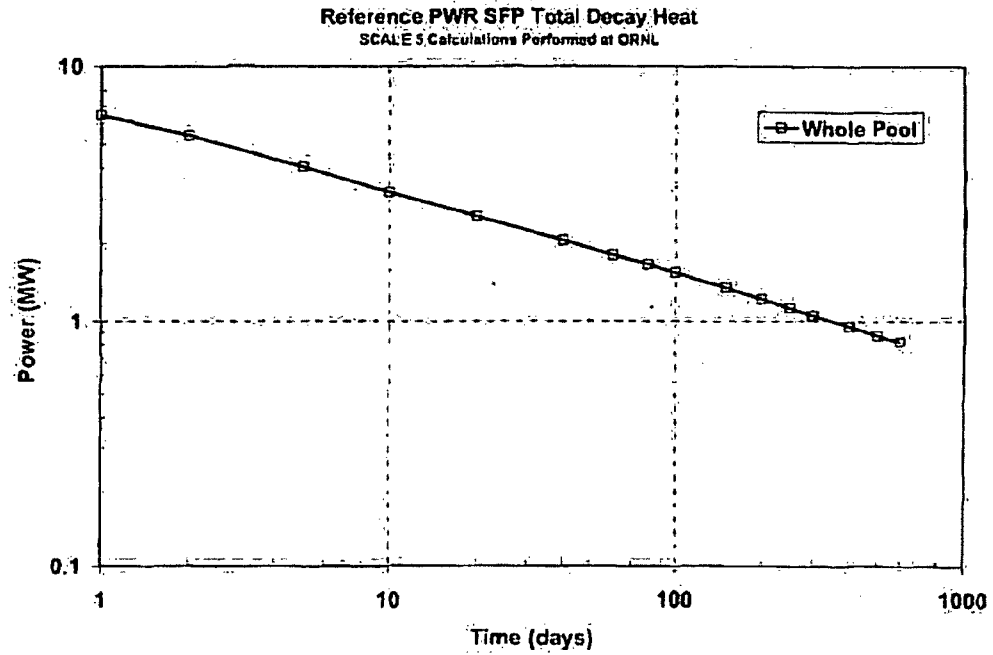


Figure 3-24 Total Pool Decay Heat Power in the Reference PWR SFP.

EX.
2

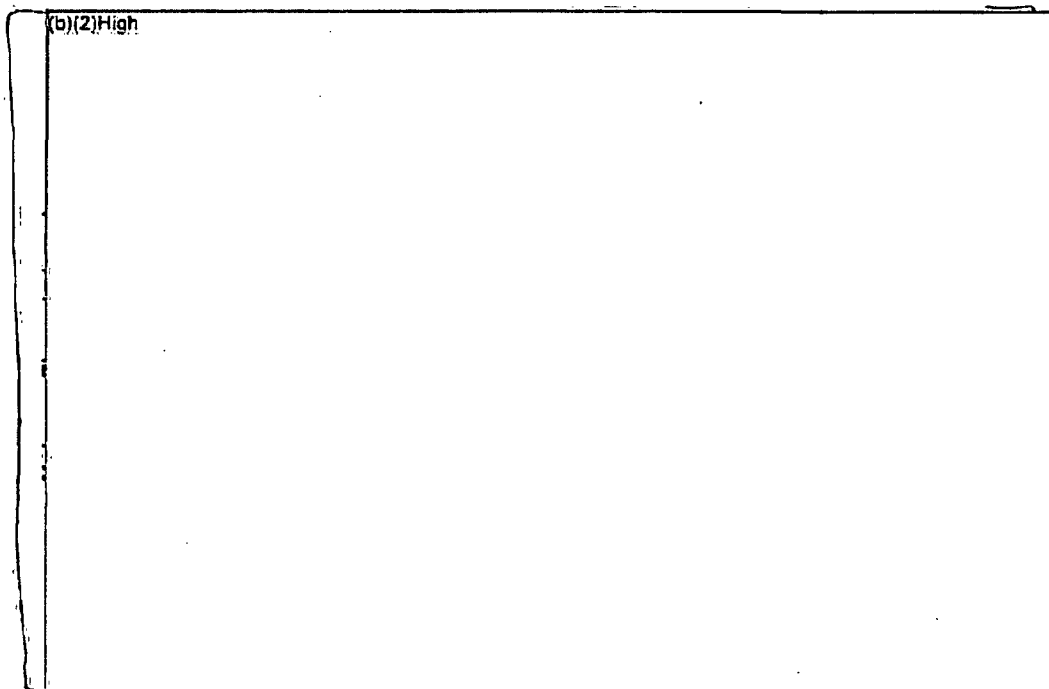


Figure 3-25 Make-up Flowrate for the Reference BWR SFP.

EX.
2

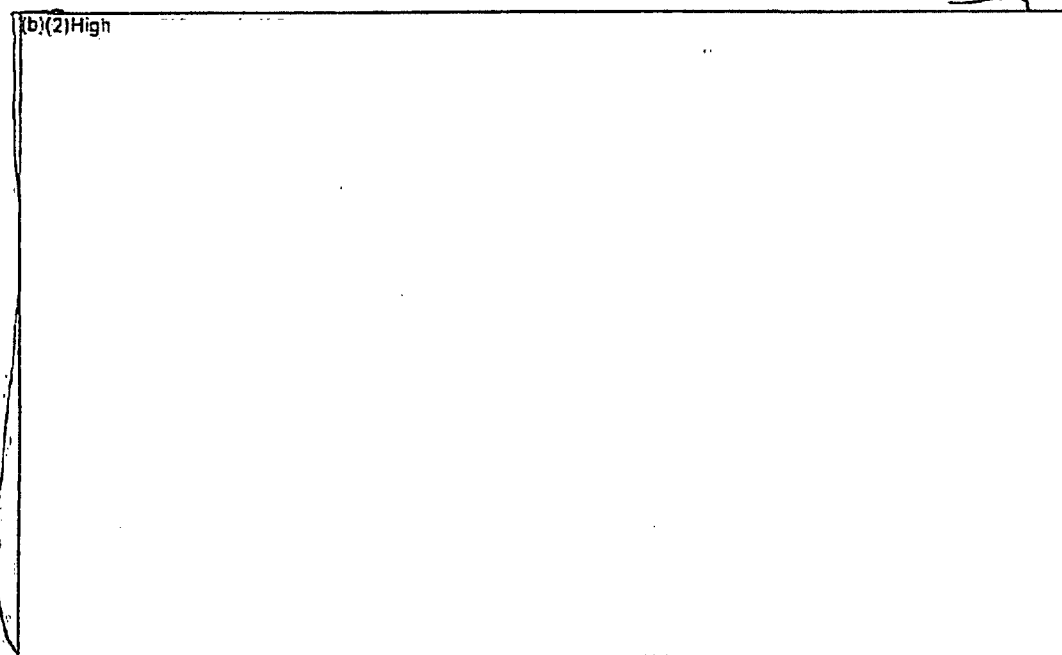


Figure 3-26 Make-up Flowrate for the Reference PWR SFP.

EX. 2

For shorter or longer outages, the step change in make-up flow (b)(2)High should be moved accordingly.

3.1.4 Calculations for Level Make-up Time

Ex. 2 Hand calculations were performed to estimate the time to make-up the water level (b)(2)High following a complete draindown and subsequent leak repair. The hand calculations represent simple calculations that are useful for estimating the minimum flowrate for a make-up system. Depending on the time of the accident, the decay heat varies. Close to the most recent offload of fuel into the SFP, the decay heat is highest (see whole pool decay heat for the reference PWR in Figure 3-24). Figure 3-27 and Figure 3-28 shows the amount of time to refill the SFP level in the reference PWR (b)(2)High respectively. Once the level reaches (b)(2)High there would be sufficient cooling (i.e., see Section 3.1.1).

The following calculations were performed to estimate the level response for various make-up flows.

Assumptions:

- 1. Reference PWR SFP decay heat data
- 2. The last offload had

Ex. 2

(b)(2)High

- 3. 80°F make-up water
- 4. A portion of the make-up flow was boiled away by the fuel decay heat based on the amount of the active fuel covered by water
- 5. As the level is restored, the sensible heat gained by the portion of the assemblies above the water level is ignored. As the level approaches the effectiveness of the steam cooling increases and reduces the sensible heat gain.
- 6. Other modes of heat transfer are ignored.

Ex. 2

$\rho = 62.1 \text{ lbm/ft}^3 = 996 \text{ kg/m}^3$

$h_{fg} = 970.3 \text{ BTU/lbm} = 2.257 \times 10^6 \text{ J/kg}$

$h_{80^\circ\text{F} \rightarrow 212^\circ\text{F}} = 180.18 \text{ BTU/lbm} - 48.13 \text{ BTU/lbm} = 132.05 \text{ BTU/lbm} = 3.072 \times 10^5 \text{ J/kg}$

$\Delta h = h_{fg} + h_{80^\circ\text{F} \rightarrow 212^\circ\text{F}} = 1.102 \text{ BTU/lbm} = 2.56 \times 10^6 \text{ J/kg}$

The reference PWR SFP whole pool decay heat (b)(2)High

(b)(2)High

Ex. 2

$Q_{\text{boil}} = \frac{(b)(2)High}{(b)(2)High} (996 \text{ kg/m}^3 * 2.56 \times 10^6 \text{ J/kg}) * (60 \text{ sec/min}) * (264.2 \text{ gal/m}^3)$

Ex. 2

(b)(2)High

Ex. 2 The reference PWR SFP whole pool decay heat (b)(2)High
(b)(2)High

Ex. 2 $Q_{boil} = \frac{\text{[redacted]}}{\text{[redacted]}} (996 \text{ kg/m}^3 * 2.56 \times 10^6 \text{ J/kg}) * (60 \text{ sec/min})$
 $* (264.2 \text{ gal/m}^3)$

Ex. 2 $= \frac{\text{[redacted]}}{\text{[redacted]}}$

$$L(t) = Level \int_0^t (GPM - Q_{boil} * \max(0, \min(1, (L(t) - BAF) / AF)) dt)$$

where,

- $L(t)$ SFP level response as a function of time
- GPM Make-up flowrate
- Q_{boil} Make-up rate based on the whole pool decay heat.
- BAF Elevation of the bottom of the active fuel (0.23 m)
- AF Active fuel height (3.66 m)
- $Level(Vol)$ SFP pool level as a function of water volume

Ex. 2 **Table 10 Summary of Timings to Restore the PWR SFP Level** (b)(2)High

(b)(2)High

Ex. 2

(b)(2)High

Ex. 2

In contrast, smaller leaks and/or leaks at higher elevations have much longer response times. [redacted]

Ex. 2 (b)(2)High

Finally, as shown in Table 10, the impact of the pool decay heat does not have a significant impact on the refilling time except for low flowrates near the minimum make-up flow.

Ex. 2

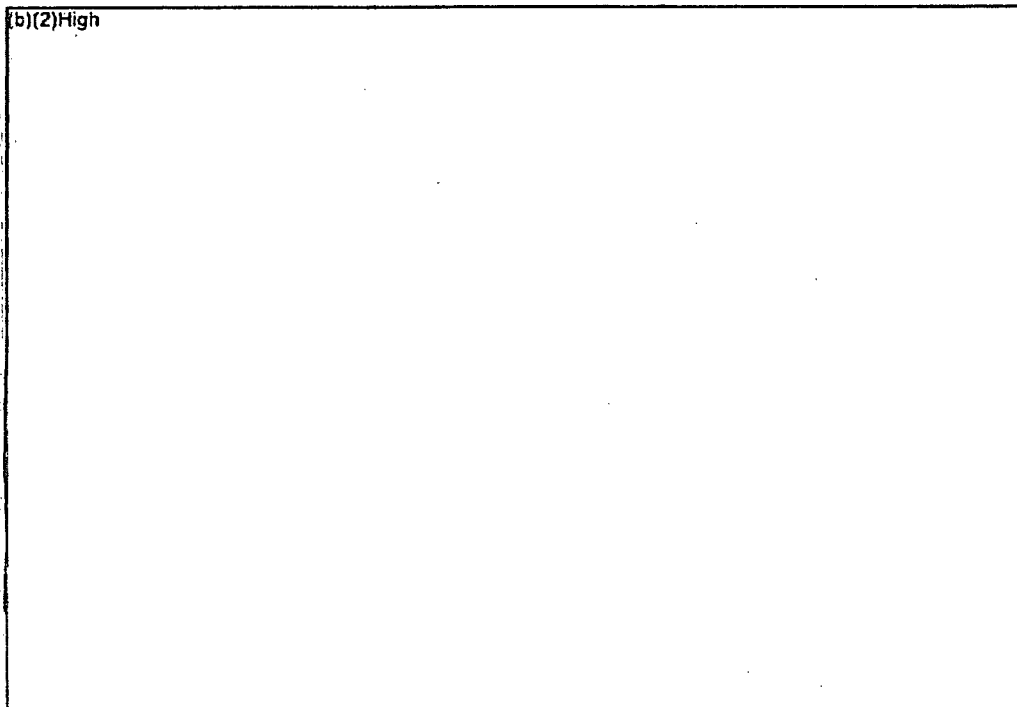
(b)(2)High

Ex. 2 (b)(2)High While the decay heat does not have a significant impact on the refilling time, it does have a significant impact on the heat-up rate and the amount of time available for a successful mitigative action. (b)(2)High

Ex. 2 (b)(2)High

The calculations presented in this section assume a uniform fuel storage configuration. The inclusion of radial heat transfer in a well-configured SFP (e.g., a 1x4 arrangement) is not straight-forward. In the PWR SFP analysis report [Wagner, 2006c], Case P2 represented a well-configured SFP (b)(2)High of the most recently discharged fuel assemblies. Case P2 simulated a (b)(2)High assembly to heat (b)(2)High without any make-up flow. The estimated timing of a peak fuel assembly in a uniform configuration was (b)(2)High (see Table 9).⁸ Both cases simulated blockage of the rack inlet by water. Consequently, a well-configured SFP provides significantly more time for mitigative actions.

Ex. 2
Ex. 2
Ex. 2
Ex. 2



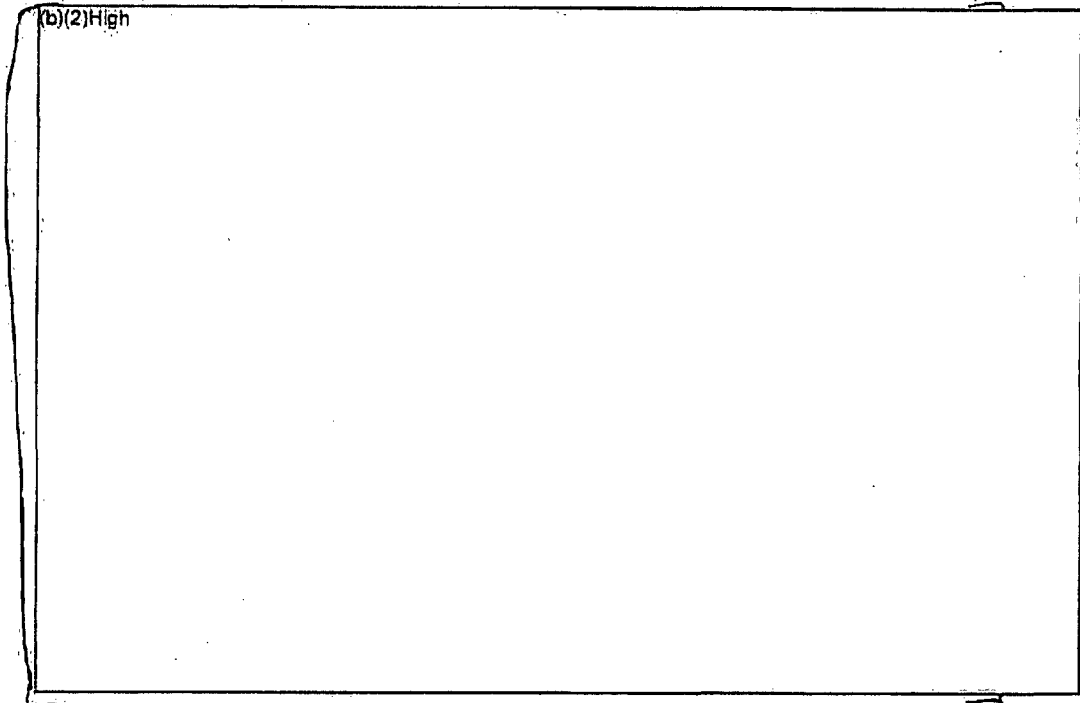
Ex. 2
2

Ex. 2 Figure 3-27 Level Response as a Function of Make-up Flow (b)(2)High following Reactor Shutdown in the Reference PWR SFP.

⁸ The heatup timing of Case P2 from the detailed PWR whole-pool model analysis with a well-configured (i.e., dispersed) assembly arrangement was based on the highest-powered assemblies from the last offload (i.e., Ring 1 versus the lower-powered assemblies in Ring 3, see Figure 3-37) [Wagner, 2006c]. In contrast, the simplified whole-pool model results with a uniform or poorly configured assembly arrangement that were presented in Table 8 and Table 9 represented the average decay power of the last discharge batch. Based on decay heat scaling arguments, the estimated timing of the peak powered assembly in a uniform configuration to heat to:

Ex. 2 (b)(2)High

Ex.
2



Ex.2 Figure 3-28 Level Response as a Function of Make-up Flow (b)(2)High following Reactor Shutdown in the Reference PWR SEP.

3.1.5 Summary of Make-up Flow Requirements and Extension to Other Sites

As stated previously, the most obvious and effective solution to a loss-of-coolant inventory accident consists of leak repair and make-up water. The results presented in the previous sections show that (a) the water level must be maintained (b)(2)High (b) the time available is dependent upon the leakage size and location and the amount of aging since shutdown, and (c) relatively modest amounts of water are needed to remove the SFP decay heat, if the leak is (b)(2)High

Ex. 2

Ex. 2

Ex. 2

If the leak is not repaired and lies (b)(2)High then the additional make-up flow is required to reestablish the level. For example, Figure 3-29 shows the leak flowrate as a function of pool elevation for a leak at the bottom of the SFP. (b)(2)High

Ex. 2

(b)(2)High As will be shown in Section 3.3, a spray system would be more effective than a make-up system for large leak rates.

For application to other SFPs, the minimum water level analysis in Section 3.1.1 for the reference PWR is applicable. The timing to drain the SFP is dependent on the pool size, the hole size, and the decay heat load. The timing values in Section 3.1.2 are applicable to the reference PWR SFP with its size dimensions (260,000 gal, 970 m³) and pool decay heat powers (b)(2)High

Ex. 2

(b)(2)High Alternate draining and heatup analyses would be required to predict the drain rates in pools with substantially different characteristics. However, the flow rate versus elevation shown in Figure 3-29 would be valid for any SFP and could be used in a calculation to estimate the drain rate for different sized pools.

Alternate hand calculations can be performed for the make-up flow for extension to other SFPs using the example in Section 3.1.3. (b)(2)High

Ex. 2

(b)(2)High As the fuel ages, the relative amount of the decay heat power from the last offload steadily decreases. After two years (i.e., the fuel cycle duration for the BWR reference plant), the relative contribution from the last discharge is only 34% of the total pool decay heat. In the absence of SFP decay heat calculations, Figure 3-30 and Figure 3-31 can be used to estimate the decay power of the various offloads in the SFP as a function of aging time. The reference BWR fuel cycle was 2 years. The burn-up was not available but was estimated to be approximately 50 GWd/MTU in the most recent batch. The reference PWR fuel cycle length varied considerably but the most recent cycles were approximately 2 years. The average burn-up of the assemblies in the last batch was ~50 GWd/MTU. The large variations in the decay heat power within a fuel cycle, which is particularly evident in the last fuel discharge, were whether the assemblies were burned at high power for two cycles (i.e., the high values) or were burned for three cycles with the last cycle being at low-power.

⁹The total pool decay powers cited above and used in the calculations for Section 3.1.2 do not include the heat load from assemblies in the SFP during refueling that will be returned to the reactor. The 260,000 gallon volume accounts for the space occupied by the fuel and racks.

One final consideration should be mentioned. If there was a leak that completely drains the SFP, then adding make-up water could cover the bottom of the rack and preclude natural circulation flow. Depending upon several factors (e.g., fuel age, storage configuration, presence of a flow downcomer, adequate ventilation, etc.), the fuel could be coolable with air ventilation. Once the air convection is stopped with the make-up flow, the heat removal decreases and the fuel will heat more quickly. Hence, with heat removal due to air convection, the make-up flow must fill the pool (b)(2)High before the fuel heats to ignition conditions, which may require a very high capacity flow system. As will be discussed later, a uniform spray flow that provides top-down cooling could provide sufficient cooling at a much lower flowrate.

Ex. 2

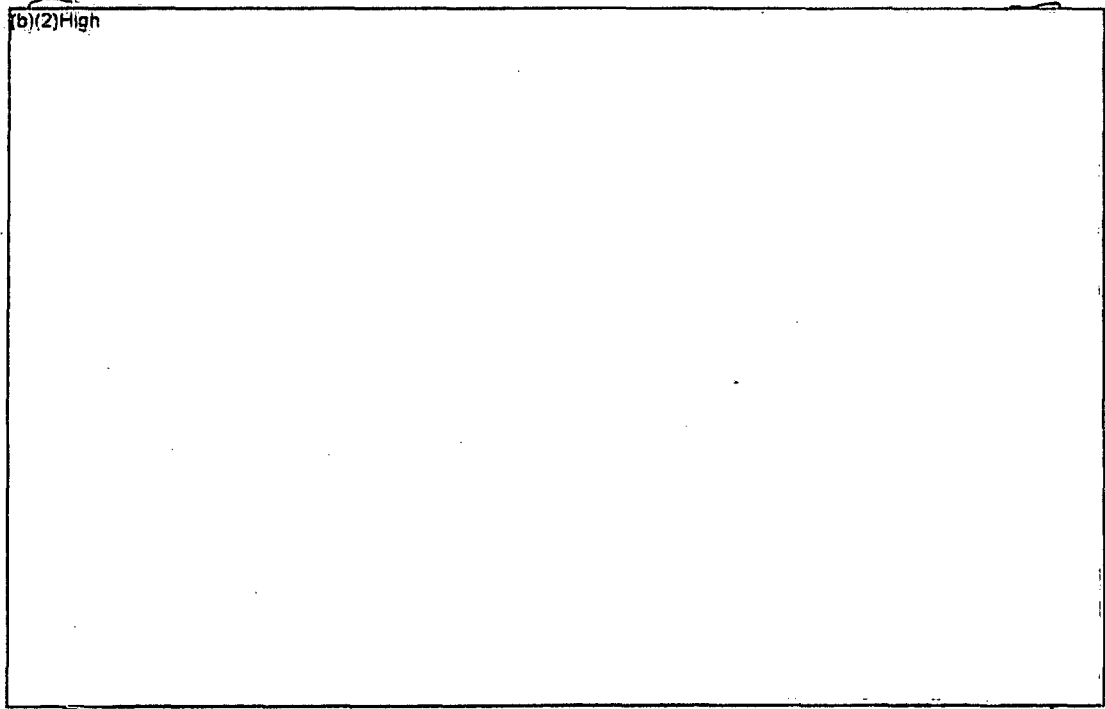


Figure 3-29 Comparison of Leakage Rates versus Water Level Height as a Function of Leak Size.

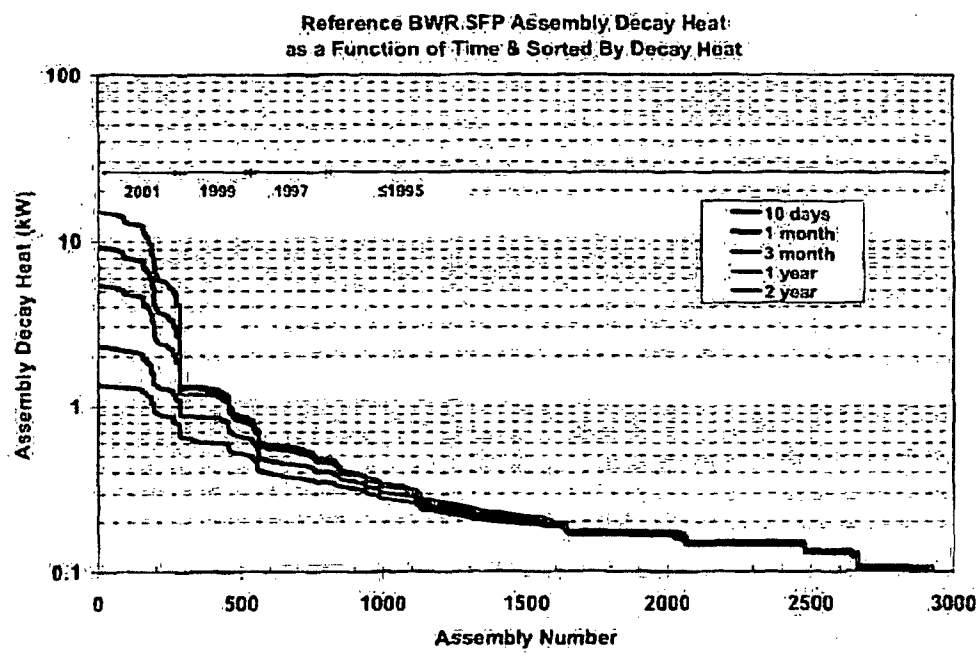


Figure 3-30 Comparison of the Reference BWR SFP Assembly Decay Heat Rates as a Function of Time and Sorted by Decay Power.

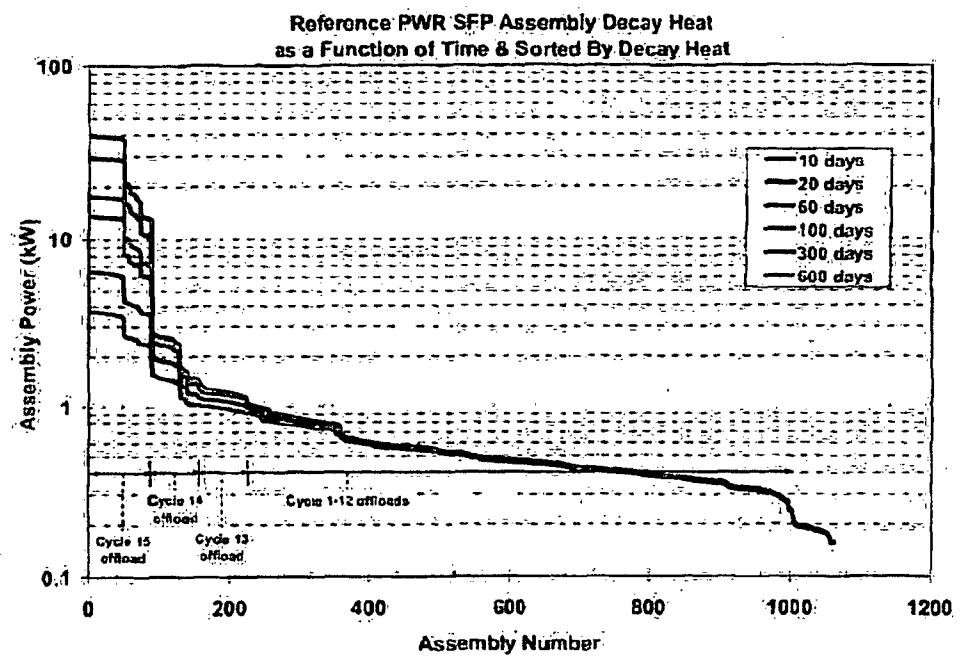


Figure 3-31 Comparison of the Reference PWR SFP Assembly Decay Heat Rates as a Function of Time and Sorted by Decay Power.

3.2 Well-Organized Fuel Configurations

A well-organized fuel configuration in the SFP is the most valuable passive improvement. The general philosophy of a well-organized fuel configuration consists of surrounding recently discharged, high decay heat power assemblies with low-powered assemblies or empty rack cells. The impact is beneficial to both complete and partial loss-of-coolant inventory accidents. For complete loss-of-coolant accidents, many separate effects calculations were performed for both reference plants to quantify the effect of the configuration on the assembly coolability. The impact of a well-organized configuration on partial loss-of-coolant accidents was quantified using whole pool calculations rather than through separate effects calculations due to the additional complications of tracking the level response. The analysis of the BWR SFP reference plant concentrated on the existing fuel configuration (i.e., circa 2002), which was neither well nor poorly configured. Calculations were performed with the base BWR SFP model, which reflected the actual configuration and a sensitivity configuration where the radial coupling between high- and low-powered assemblies was reduced by a factor of 10 (i.e., a poorly configured SFP). In contrast, PWR SFP whole pool analyses used both well-configured (i.e., dispersed) and poorly configured (i.e., non-dispersed) configurations. The configuration analyses for the reference plants for the complete and partial loss-of-coolant inventory results are discussed in Sections 3.2.1 and 3.2.2, respectively. The application of these concepts to other SFPs is discussed in Section 3.2.3.

3.2.1 Summary of Well-Configured Patterns in Complete Loss-of-Coolant Inventory Accidents

Figure 3-32 shows the fuel configurations considered in the MELCOR separate effects analyses. The least coolable configuration places all the recently discharged assemblies together in a uniform pattern. In a uniform pattern, there is no radial heat transfer between assemblies. Consequently, all heat removal must occur axially, which is limited by the convective flow rate in the assembly. The most effective pattern placed four empty cells around each high-powered assembly. This requires the most space in the SFP and consequently may not be practical. Alternately, a 1x4 pattern with four low-powered assemblies surrounding one high-powered assembly may be achievable at most sites.

Table 11 shows the gains from a uniform pattern of recently discharged assemblies to other better configured arrangements. If the most recently discharged, highest-powered assemblies are surrounded by assemblies at or below the median assembly decay power, there are substantial gains in the minimum amount of aging for coolability for a checkerboard or 1x4 pattern. Similarly, if the highest-powered assemblies are surrounded with empty cells, the improvements are also significant. In summary, spent fuel assemblies stored in a contiguous pattern (i.e., uniformly high-powered region) are not coolable (b)(2)High

Ex. 2 (b)(2)High in a 1x4 configuration. The checkerboard pattern provides a moderate
Ex 2 improvement in coolability (b)(2)High. It should be noted that other patterns can be postulated that would also give benefits between those cited (e.g., 1x2, 1x3).

The separate effect calculations cited in Table 11 include some key assumptions that were separately investigated in sensitivity studies. The key assumptions are summarized below:

- The separate effects configurations were initiated with a complete loss-of-coolant inventory. There is no water in the SFP.
- The decay heat power for the high-powered assembly was the peak value from the reference BWR or PWR SFP decay heat analysis. The decay heat power for the low-powered assembly was the median value in the reference BWR or PWR SFP inventory from the decay heat analysis. In both the BWR and PWR analysis, there was considerable variability in the decay heat power of the last offload. For example, the decay heat powers of the last offload of the reference BWR ranged from 9.34 kW to 2.66 kW at one month of aging (Figure 3-30). Similarly, the reference PWR peak assembly decay power ranged from 21.6 kW to 8.30 kW at 40 days. The primary factor effecting the short-term (i.e., <1 year) decay heat power is the assembly fission power in the last fuel cycle (Figure 3-31). The total burn-up was a secondary factor affecting the short-term decay power in the reference plant decay heat calculations.
- The inlet temperature was assumed to be 300 K. The importance of adequate ventilation is further discussed in Section 3.4.
- The assemblies are assumed to be in the center of the rack, away from edge effects and not over a rack foot (see Section 3.6).
- There is an initial oxide layer that is within the range of values found in BWR and PWR spent fuel assemblies ([Lanning] and [O'Donnell]).

Table 11 Summary of BWR and PWR Coolability Aging Estimates for Assemblies in Air.

Ex 2

(b)(2)High

Notes:

- A. The calculations assumed a complete and rapid loss-of-coolant inventory from the SFP. There are many other assumptions in these calculations that are carefully outlined in the previous studies but they illustrate the relative gains achievable for well-configured pools.
- B. The BWR results with adjacent empty cells are based on a slightly older modeling approach but are believed to be representative.

Figure 3-36 shows an example of the reference BWR SFP in a well-configured arrangement using repeating 1x4 patterns. The most recently discharged "orange" and "red" assemblies are surrounded by the older "blue" assemblies in the SFP in 1x4 patterns. (b)(2)High

Ex.
2

(b)(2)High
(b)(2)High Hence, 600 high-powered assemblies (i.e., red and orange), or approximately two core offloads, can be accommodated in 1x4 patterns.¹⁰ The 1200 lowest powered assemblies were placed around the most recent offload (i.e., up to 300 red assemblies in a 1:4 ratio). The next 1200 lowest powered assemblies were placed around the next most recent offload. This represents a well-configured arrangement from a thermal-hydraulic perspective, but does not account for criticality concerns (or other constraints).

A similar example of a well-configured layout for the reference PWR SFP is shown in Figure 3-37. In this example, the most-recently discharged fuel (i.e., identified as Batch 15a and 15b in Rings 1 and 3) is placed in a 1x4 pattern with the lowest powered assemblies in the SFP (Batches L1 through L7 in Ring 2). The next most recent offload (i.e., identified as Batch 14a and 14b in Rings 4 and 6) are placed in a 1x4 pattern with the next oldest (Batches L8 through L10 in Ring 5). The whole pool analysis, which was based on the configuration shown in Figure 3-37, actually gave better coolability than was expected from the 1x4 separate effects analyses for three reasons. First, the highest powered assemblies in Rings 1 and 3 were coupled to the lowest powered assemblies in Ring 2. The average decay power of the assemblies in Ring 2 was 0.37 kW versus the 0.5 kW SFP median value used in the comparable separate effect analyses. Second, the resultant ratio of Ring 1 and 3 assemblies to Ring 2 was the equivalent of 5.1 low-powered assemblies for every high-powered assembly due to additional assemblies at edges and corners of the repeating 1x4 configuration. Previous BWR separate effects calculations show that additional cooling benefits with additional surrounding assemblies (e.g., 1x4x8x12 configuration had better cooling than the 1x4x8, which was better than the 1x4 configurations, [Wagner, 2003]). Finally, as a related benefit, the 1x4 configuration with the highest powered assemblies in Ring 1 were placed in a "checkerboard pattern" with the 1x4 configurations with the Ring 3 assemblies using Ring 2 as the low-powered assemblies for both sets of 1x4 patterns. The average assembly decay power in Ring 3 only had 46% of the decay power in the Ring 1 assemblies. Hence, the heat load from Ring 1 high-powered assemblies into Ring 2 would further expand into the portion of Ring 2 assemblies attributed to a 1x4 pattern around the Ring 3 assemblies.

Ex.
2

(b)(2)High

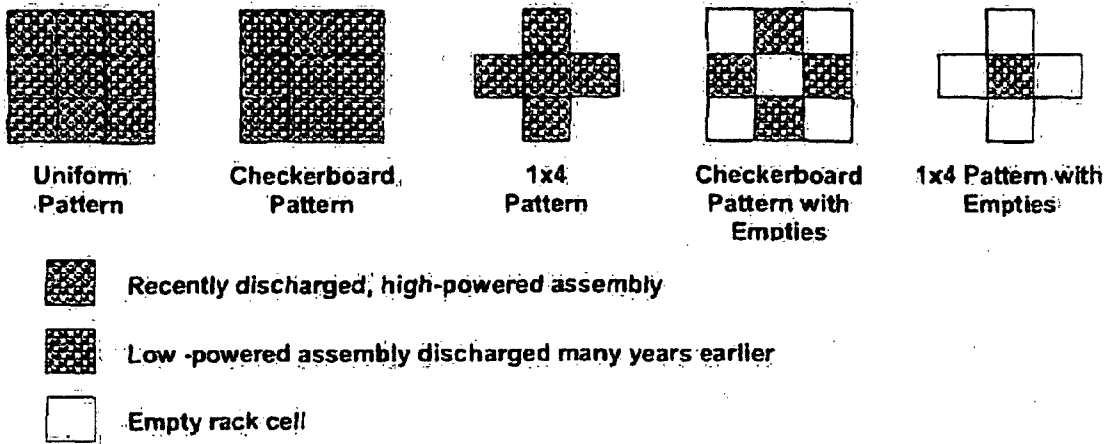


Figure 3-32 Fuel Configurations Considered in the MELCOR Separate Effects Models.

3.2.2 Summary of Well-Configured Patterns in Partial Loss-of-Coolant Inventory Accidents

As discussed above, the impact of a well-organized configuration on partial loss-of-coolant accidents was quantified using whole pool calculations rather than through separate-effects calculations due to the additional complications of tracking the level response. In the complete loss-of-coolant inventory accidents, some of the power from the high-powered assemblies was transferred radially into low-powered assemblies. At quasi-steady conditions, the additional heat load or power from the high-powered assembly was convected out of the low-powered assembly. At limiting conditions near the threshold of coolability, almost 80% of the center assembly power was transferred to the four peripheral assemblies in a 1x4 configuration. Consequently, the decay power becomes distributed across the configuration. In contrast for a partial loss-of-coolant inventory accident, heat (or power) that is transferred from the high-powered assembly to the low-powered assembly can not be convected away, once the water level has dropped below the point of effective steam cooling. Therefore, the benefit of a well-configured pattern in a partial loss-of-coolant inventory accident is temporal. The low-powered assemblies initially act as an additional heat sink that absorbs energy from the high-powered assembly. However, once the low-powered assemblies heat up, their benefit as a heat sink diminishes. Nevertheless, as will be shown below, the additional time for mitigative actions due to a well-configured pattern is significant.

The analysis of the BWR SFP reference plant concentrated on the existing fuel configuration (i.e., circa 2002), which was neither well nor poorly configured. As shown in Figure 3-33, the most recently discharged assemblies (i.e., the highest decay heat) are distributed somewhat randomly but generally not concentrated in large contiguous regions. An analysis of the existing configuration was performed and the highest powered assemblies were grouped according to their coupling to other high-powered assemblies versus low-powered assemblies. The base coupling model of the existing configuration included high-powered assemblies with high (i.e., ~4 sides or like a 1x4 pattern), medium (i.e., 1-3 sides or like a checkerboard pattern), and low (i.e., ~0 sides or like a uniform pattern) coupling to low-powered assemblies. Additional sensitivity calculations were performed where the radial coupling between high- and low-powered assemblies was reduced by a factor of 10 (i.e., a poorly configured SFP).¹¹

A comparison of the peak cladding temperature response for the base case and degraded view factor cases is show in Figure 3-34 for the reference BWR SFP. (b)(2)High

Ex. 2.

(b)(2)High

(b)(2)High

A comparison of the

¹¹ Mechanically, the view factor between the high- and low-powered assemblies was reduced by a factor of 10. The radial view factors for a high-powered assembly to the low-powered assemblies in a 1x4, checkerboard, and uniform patterns are approximately 1, 0.25, and 0. Consequently, a factor of ten reduction in the view factor changes the high-coupled regions to much closer to a uniform configuration (i.e., a view factor of 0.1). This was a simplified approach to examine a non-dispersed storage configuration without having to rebuild the MELCOR input to reflect a different fuel layout. However, it should be noted that even a view factor of 0.1 can transfer a significant amount of power at high temperatures following ignition due to the fourth power dependency on thermal radiation.

Ex 2 Ring 3 peak temperature response shows both configurations heated similarly until high
Ex 2 temperature radiation became effective at transferring heat away from the high-powered fuel.
Ex 2 The poorly configured case heated (b)(2)High (i.e., temperature of cladding failure and the gap
Ex 2 fission product release) (b)(2)High versus much later in the dispersed configuration. In fact,
Ex 2 the first fission product failure location in the dispersed case changed from Ring 3 to Ring 7,
Ex 2 which had fuel from the second most recent offload but was more uniformly configured. Since
Ex 2 Ring 7 assemblies had a lower decay heat power, the heatup rate of Ring 7 was much slower
Ex 2 than Ring 3. A comparison of the results (b)(2)High for dispersed and
Ex 2 non-dispersed cases are summarized in Table 12. Both (b)(2)High cases show
Ex 2 increased coolability from a well-configured SFP as evidenced by the increased timing to the
Ex 2 start of the fission product releases (b)(2)High

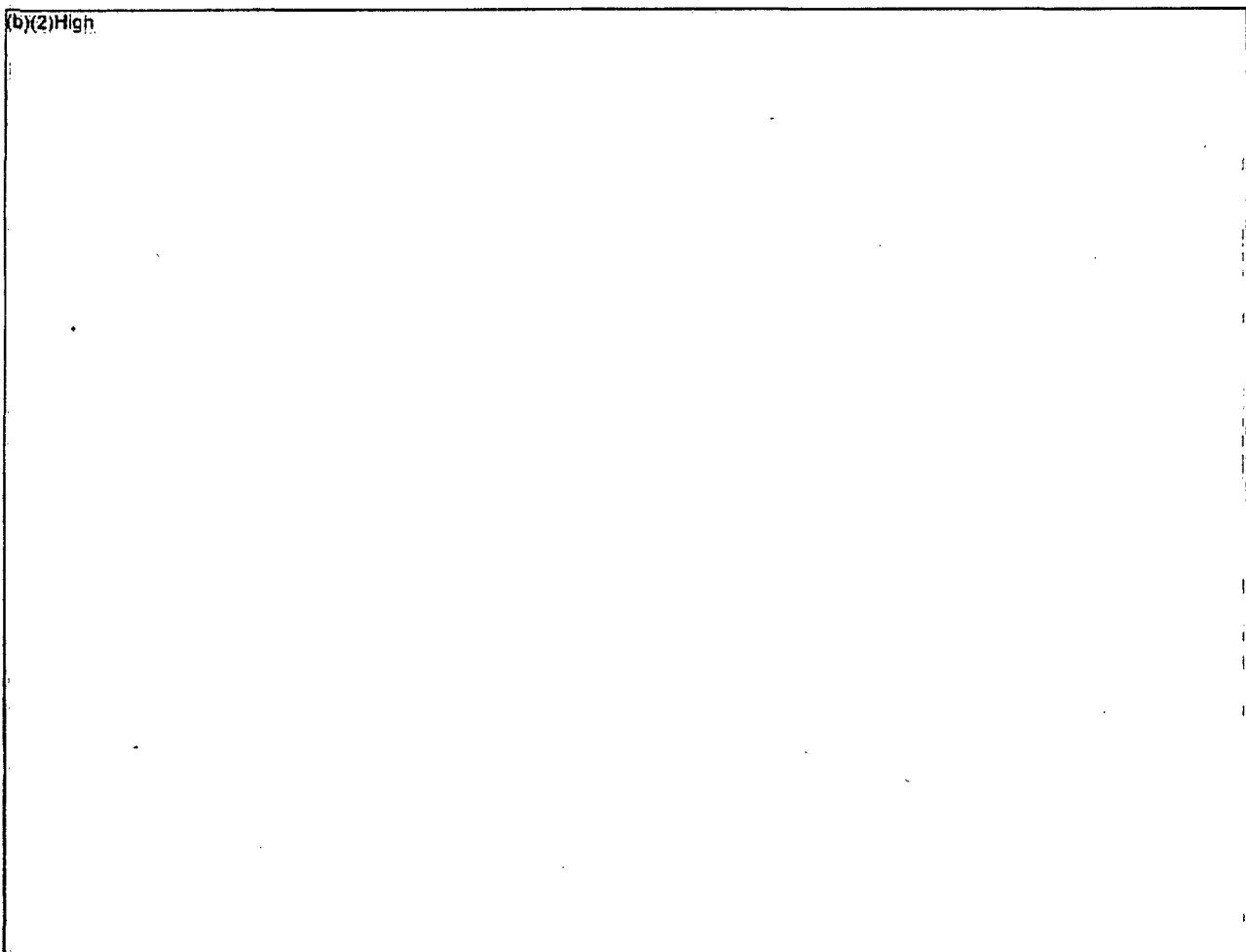


Figure 3-33 Reference BWR Spent Fuel Decay Heat Level at 1 Month after Discharge to the SFP (circa 2002).

Ex. 2
2

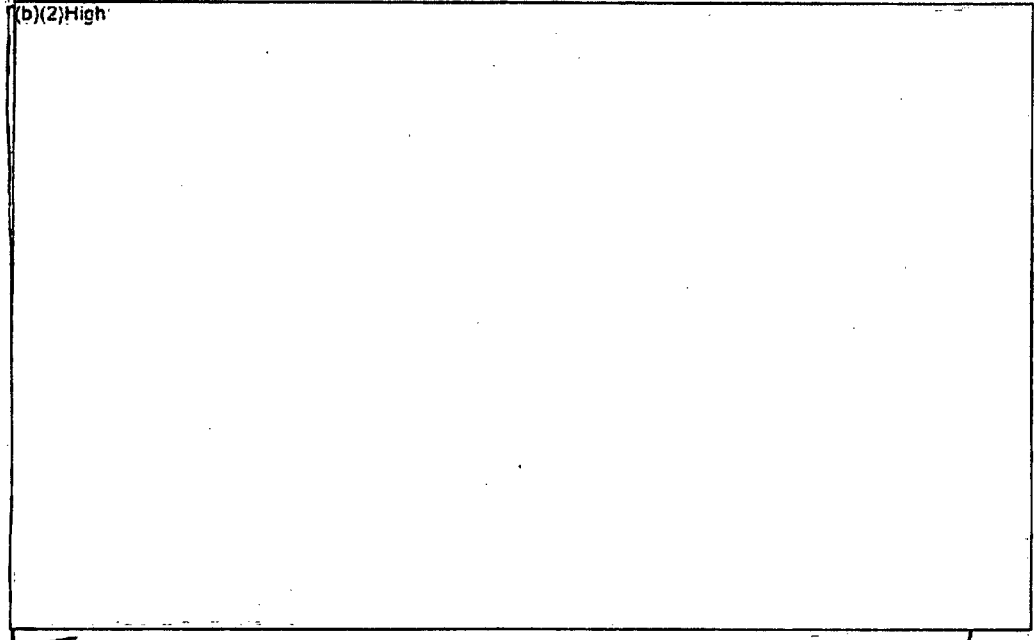


Figure 3-34 Comparison of the Peak Cladding Temperature for a Partial Loss-of-Coolant Accident in the Reference BWR SFP for Partially Dispersed and Non-Dispersed Fuel Configurations.¹²

Ex. 2 Next, a comparison of a well-configured and poorly configured PWR SFP is presented. The most recently discharged fuel had age (b)(2)High which is a much higher relative decay heat than the previous reference BWR case. (b)(2)High

Ex. 2 (b)(2)High In the dispersed case, the reference PWR is arranged in a checkerboard pattern of 1x4 configurations with the most recently discharged fuel as shown in Figure 3-37.¹³

Ex. 2 (b)(2)High there was essentially no steam cooling in this case versus some steam cooling in the previous BWR cases. A comparison of the peak temperature response shows both configurations heated similarly until high temperature radiation became effective at transferring heat away from the high-powered fuel. (b)(2)High

Ex. 2 (b)(2)High Similar to the BWR results, the PWR results

Ex. 2 showed a substantial time benefit even for the much more severe case (b)(2)High (b)(2)High

¹² Both Ring 3 and 7 are shown in Figure 3-34 for comparison to Table 12.

¹³ The combined checkerboard and 1x4 patterns are perhaps more clearly illustrated Figure 3-36 in the well-organized BWR SFP configuration.



Ex.
2

Figure 3-35 Comparison of the Peak Cladding Temperature for a Partial Loss-of-Coolant Accident in the Reference PWR SFP for Dispersed and Non-Dispersed Fuel Configurations.

EX. 2
EX. 2

Table 12

Summary of Reference BWR
with the Leak Location

(b)(2)High
(b)(2)High
Active Level Results.

Since Discharge Partial Loss-of-Cool

(b)(2)High

EX.
2

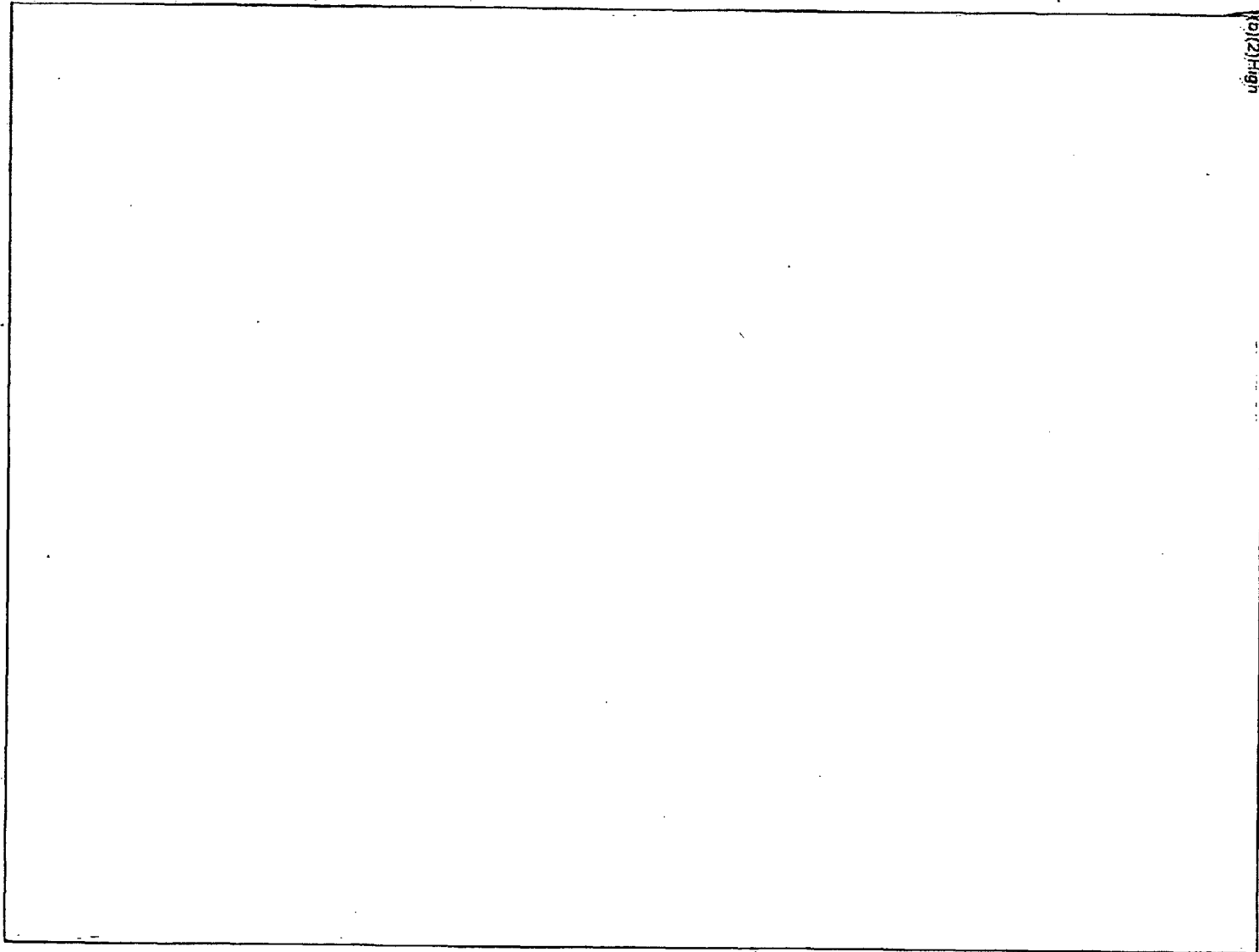
3.2.3 Extension of Well-Configured Patterns to Other Sites

The following guidelines are provided for the extension of the well-configured patterns to other sites.

- The following guidelines rank the impact of various configurations on the coolability of the assemblies.

Configuration		Ranking
1x4-empties		Best
1x4		
Checkerboard with empties		Good
Checkerboard		Moderate
Uniform		Worst

- A checkerboard pattern with the 1x4 patterns as shown in Figure 3-36 further spreads out the highest-powered assemblies and enhances coolability.
- As will be discussed in Section 3.5, a contiguous opening on at least one corner of the SFP provides a downflow region for cool air. Figure 3-36 and Figure 3-37 show contiguous open regions on all four sides of the SFP.



(b)(2) High

Ex.
2

Figure 3-36. Example of the Reference BWR SFP in a Well-Configured Arrangement using Repeating 1x4 Patterns.

(b)(2)HIGH

Ex.
2

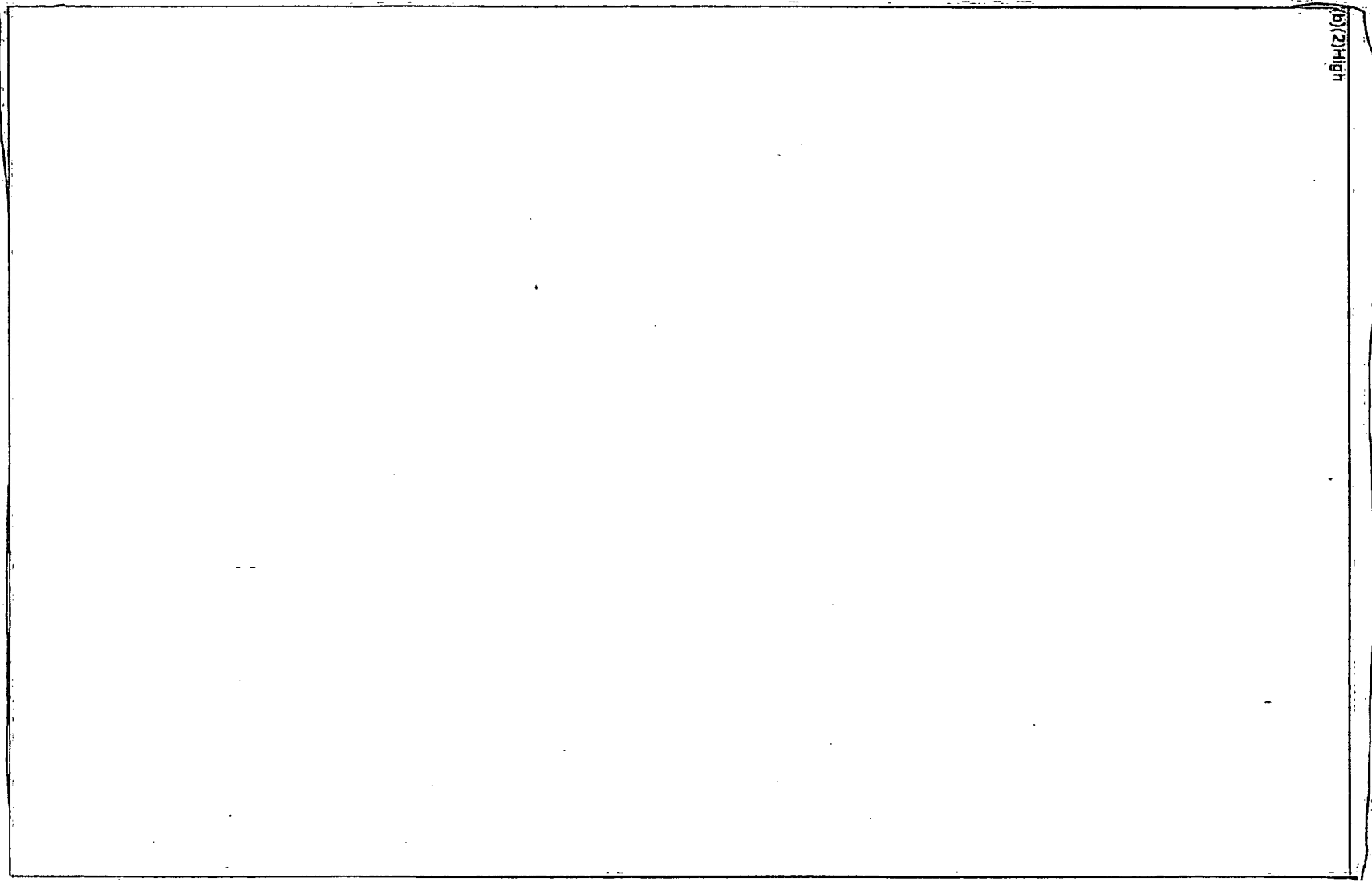


Figure 3-37 Example of the Reference PWR SFP in a Well-Configured Arrangement using Repeating 1x4 Patterns.

3.3 Emergency Sprays

A focused study was performed to estimate the emergency spray effectiveness in SFP loss-of-coolant inventory accidents [Wagner, 2006a]. The conditions considered in the study were specified with guidance from the NRC. The spray analyses did not seek to study implementation feasibility, fuel geometry disruption, spray droplet size effects, or variations in the pool or building geometry. Nevertheless, the study provides some key insights into the effectiveness of the sprays for a range of conditions.

Section 3.3 is subdivided into three subsections. First, Section 3.3.1 shows simple hand calculations that were initially performed to estimate the spray requirements. The hand calculations do not address complications such as radial heat transfer for well configured assembly arrangements, removal of sensible heat, and cooling outside the canister for BWRs. Nevertheless, they appear to be a conservative starting point for sizing spray system requirements. Section 3.3.2 shows the results of the spray effectiveness study using MELCOR. Finally, the results are summarized in Section 3.3.3 as well as suggestions to extend the findings to other SFPs.

3.3.1 Hand Calculations for Minimum Spray Flow

Ex. 2 As discussed in Section 3.1, the required make-up flow rates can be very large if the leak is (b)(2)High and can not be repaired. However, if the make-up flow could be provided directly into the individual assemblies via a spray system, then adequate assembly cooling might be provided with a much smaller flow rate. Hand calculations were performed to calculate the heat removal capacity of the spray flow by completely vaporizing the injected water. Based on the peak decay heat assembly, the amount of spray required for the entire pool was calculated as described below. The peak powered assembly is used because ignition must be prevented in the limiting assembly to prevent possible propagation to the other assemblies. If the limiting assembly ignites, then the additional exothermic power and corresponding high temperatures from the ignition oxidation reactions can substantially increase the heat flux to the surrounding assemblies.

Ex. 2 The calculations made assumptions about the spray nozzle overlap factor and that only flow within the canister was effective. It was further assumed that the peak assembly spray flow must be projected across the whole pool. (b)(2)High (b)(2)High. The calculations were considered as potentially conservative since radial heat transfer for a well-configured pool was not considered nor was heat removal from spray flow in the annulus between the BWR canister and the rack. The MELCOR calculations presented in Section 3.3.2 address those limitations.

Assumptions:

1. Reference BWR SFP data
- Ex. 2 2. (b)(2)High
3. 80°F spray water
4. 33% spray coverage inefficiency/overlap

5. Only flow within the canister cross-section is effective
6. Make-up based on peak assembly decay heat projected across entire pool
7. No radial heat transfer to adjacent assemblies (i.e., a uniform configuration)

$$\rho = 62.1 \text{ lbm/ft}^3 = 996 \text{ kg/m}^3$$

$$h_{fg} = 970.3 \text{ BTU/lbm} = 2.257 \times 10^6 \text{ J/kg}$$

$$h_{80^\circ\text{F} \rightarrow 212^\circ\text{F}} = 180.18 \text{ BTU/lbm} - 48.13 \text{ BTU/lbm} = 132.05 \text{ BTU/lbm} = 3.072 \times 10^5 \text{ J/kg}$$

$$\Delta h = h_{fg} + h_{80^\circ\text{F} \rightarrow 212^\circ\text{F}} = 1102 \text{ BTU/lbm} = 2.56 \times 10^6 \text{ J/kg}$$

Ex. 2

(b)(2)High

BWR SFP Assembly Pitch = 6.28"

BWR SFP Canister ID = 5.4¹⁴

Inside canister area to cell pitch ratio = $(5.4'' \times 5.4'') / (6.28'' \times 6.28'') = 0.739$

Whole Pool Size = $480'' \times 424'' = 203,520 \text{ in}^2 = 131.3 \text{ m}^2$ (Cross-sectional area)

Equivalent number of SFP rack cells in entire SFP cross-section
= $203,520 \text{ in}^2 / (6.28'' \times 6.28'') = 5160$ equivalent cells

Ex. 2

Spray Flowrate

(b)(2)High

$$\begin{aligned} & (996 \text{ kg/m}^3 \times 2.56 \times 10^6 \text{ J/kg}) \times (60 \text{ sec/min}) \\ & \times (264.2 \text{ gal/m}^3) \times 1.33_{(\text{overlap})} \times 1.35_{(\text{chan. ratio})} \times 5160 \text{ equiv. cells} \end{aligned}$$

Ex. 2

(b)(2)High

The results for a range of decay heat levels for the reference BWR and PWR SFPs are shown in Figure 3-38 and Figure 3-39, respectively. The corresponding assumptions for the minimum spray flow in the reference PWR SFP were,

1. Reference PWR data (see Figure 3-24 for the reference PWR SFP decay heat power)
2. 80°F spray water
3. 33% spray coverage inefficiency/overlap
4. Make-up based on peak assembly decay heat projected across entire pool
5. (b)(2)High

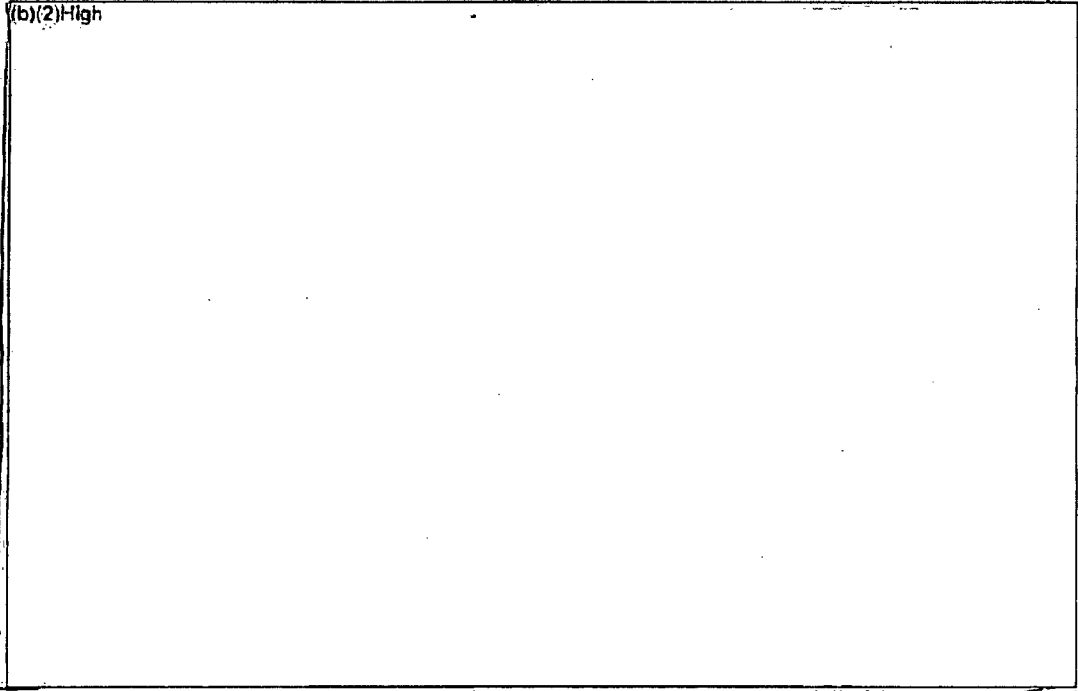
Ex. 2

(b)(2)High

Ex. 2

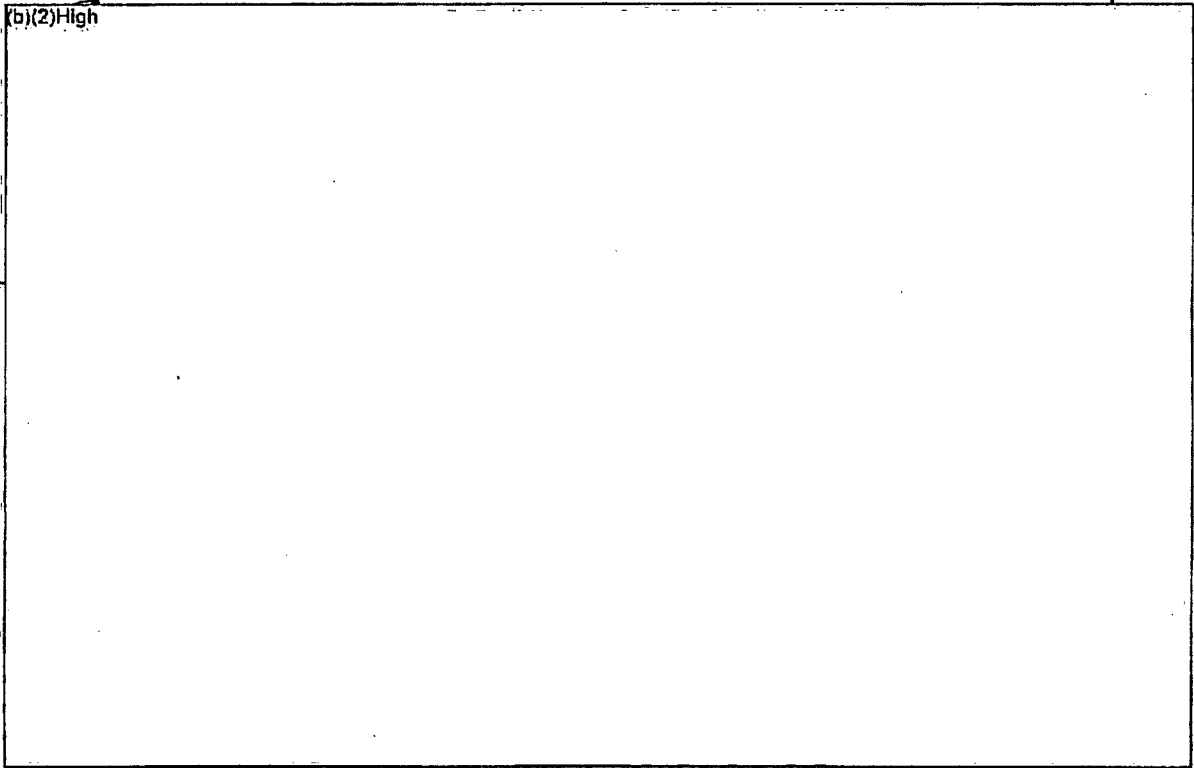
(b)(2)High

¹⁴ This is an approximate value for the BWR canister ID. More accurate GNF GE-11 data from the SNL SFP program show variable thickness across the length of the canister with an ID in the active fuel region of 5.28".



EX.
2

Figure 3-38 Hand Calculations to Estimate Spray Heat Removal Requirements for the Reference BWR SEP.



EX
2

3.3.2 MELCOR Calculations for Minimum Spray Flow

The MELCOR spray calculations were performed in two steps. First, whole pool calculations were performed to get the overall response in the SFP. The results from the whole pool calculations were then used as boundary conditions for a separate effects model that included a detailed nodalization to track the spray flow as it penetrated into the assembly. The basic spray flow modeling assumptions that were prescribed for the analysis are summarized in Section 3.3.2.1. The results of the whole pool calculations are summarized in Section 3.3.2.2. Finally, the results of the detailed separate effects spray model are given in Section 3.3.2.3.

3.3.2.1 Basic Assumptions in the MELCOR Spray Analyses

- Ex. 2. Based on input from the NRC, a delay time of (b)(2)High was assumed for spray initiation. Also
Ex. 2. based on input from the NRC, a spray flow rate of (b)(2)High was selected for the majority of calculations. Note that the flow rates referenced in these analyses refer to the spray flow rate entering the pool, not the spray flow rate that the system is capable of providing (i.e., they do not include a spray overlap factor or a delivery inefficiency). The spray flow entering the SFP was assumed to be evenly distributed over the cross-section of the spent fuel pool. The reference BWR SFP has a cross-sectional area of 40 ft (12.2 m) by 35.3 ft (10.8 m).
Ex. 2. This results in a spray flow rate of roughly (b)(2)High per rack cell.

3.3.2.2 SFP Water Level Response with Sprays

- Ex. 2. An assortment of whole pool calculations were run to establish boundary conditions for the separate effects calculations. Figure 3-40 and Figure 3-41 show typical results (b)(2)High.
Ex. 2. (b)(2)High The most interesting result of calculations was the resultant water level (see summary in Table 13) (b)(2)High.
Ex. 2. (b)(2)High
Ex. 2. (b)(2)High For the range of hole sizes and spray flow rates considered in the study, the long-term water level spanned conditions that would allow air flow (i.e., the inlet is not plugged) versus cases where the inlet would be plugged. (b)(2)High had a relatively high level that would cover the inlet to the racks and partially cover the bottom of the fuel (a water level of >16"). In contrast, the (b)(2)High had a very low water level and would be ensured to have air natural circulation flow (b)(2)High.
Ex. 2. (b)(2)High As discussed in Section 2.3, the phenomena and thermal response for non-spray cases with the inlet plugged by the water level is much different than the response when there is air flow in the assembly. Most importantly, air natural convective heat removal is prevented when the inlet is blocked. However, the spray calculations with a plugged inlet showed a much less significant impact after the spray initiation. The spray flow source provided an active heat removal mechanism that reduced the necessity of convective air flow.

Table 13 Summary of the Steady-State Water Levels as a Function of Leakage Hole Size and Spray Flow Rate.

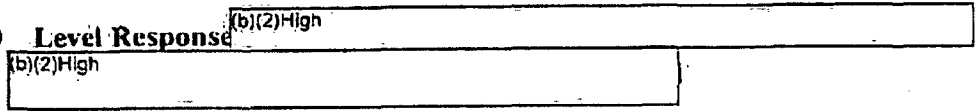
(b)(2)High

Ex. 2

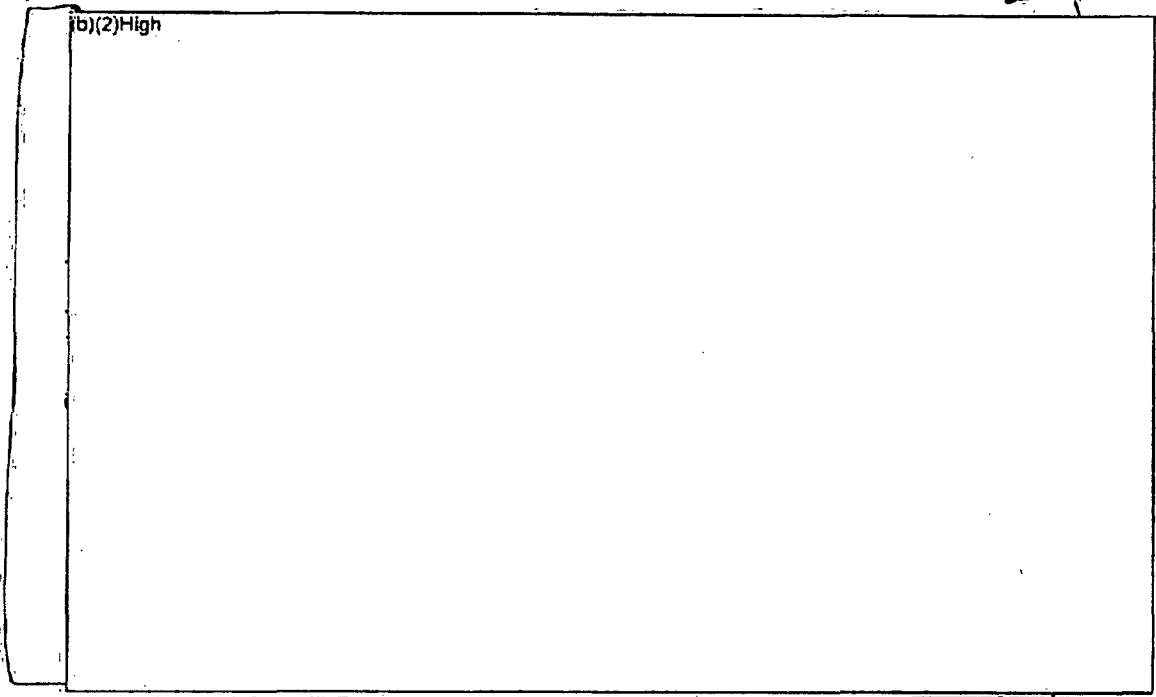
E

Figure 3-40 Level Response

Ex. 2



Ex
2



Ex. 2 **Figure 3-41 Comparison of the Leak Rate and Spray Flowrate Response** (b)(2)High
(b)(2)High

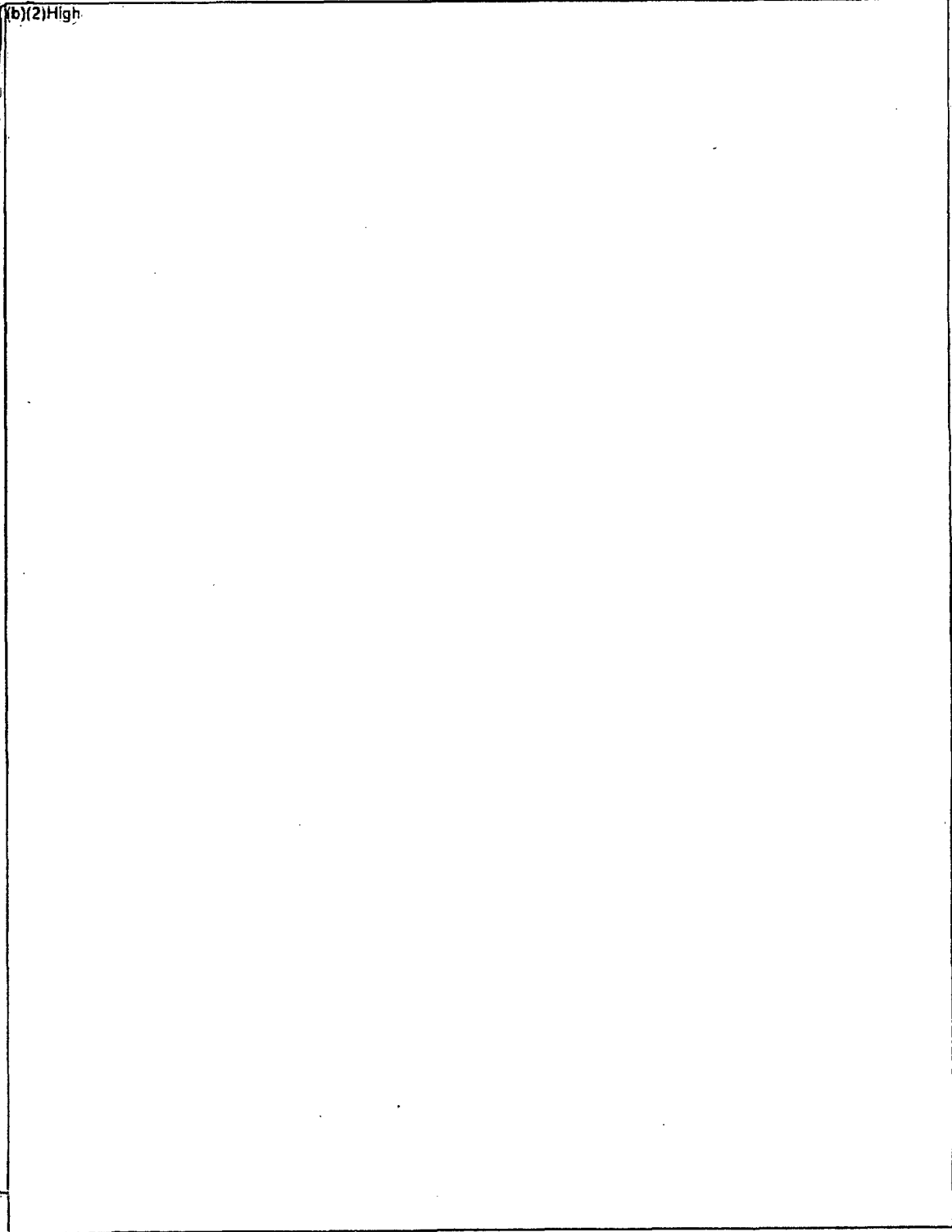
3.3.2.3 Separate Effects Spray Calculations

Ex. 2 Table 14 summarizes the highlights of separate effects spray calculations. Calculations were performed for the uniform, checkerboard, and 1x4 configurations. For each configuration, parametric calculations were performed with variations in one or more of the scenario or modeling attributes. The variations in the calculations included fuel configuration (uniform, checkerboard, and 1x4), aging time of the peak powered assembly, leak size (b)(2)High, spray flow rate (b)(2)High, and air flow (some configurations that were expected to have air flow also had a sensitivity calculation where the inlet was plugged with water).

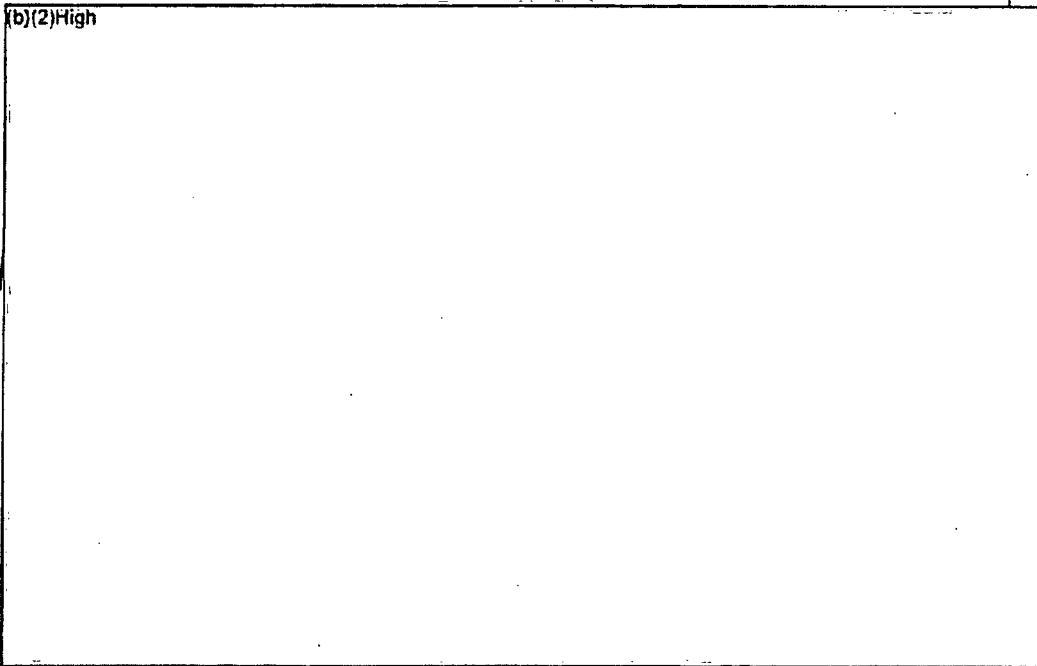
Ex. 2 For fuel which has been favorably configured in a 1x4 pattern, a spray flow rate (b)(2)High provided adequate cooling for the fuel assemblies (b)(2)High. If the fuel was Ex. 2 configured in a checkerboard pattern, it is also coolable (b)(2)High but only if the inlet or Ex. 2 plugged. Under the same conditions, fuel which is not favorably configured (i.e., uniform fuel Ex. 2 loading) is not coolable (b)(2)High. The uniform fuel configuration becomes Ex. 2 coolable at (b)(2)High following shutdown (b)(2)High (see Ex. 2 Figure 3-42) and (b)(2)High (see Figure 3-43). If the spray flow rate is Ex. 2 increased (b)(2)High the uniform configuration is coolable (b)(2)High and Ex. 2 fluctuating near coolability limits (b)(2)High (see Figure 3-44).

Table 14 Summary of Separate Effects Spray Calculation Results.

(b)(2)High



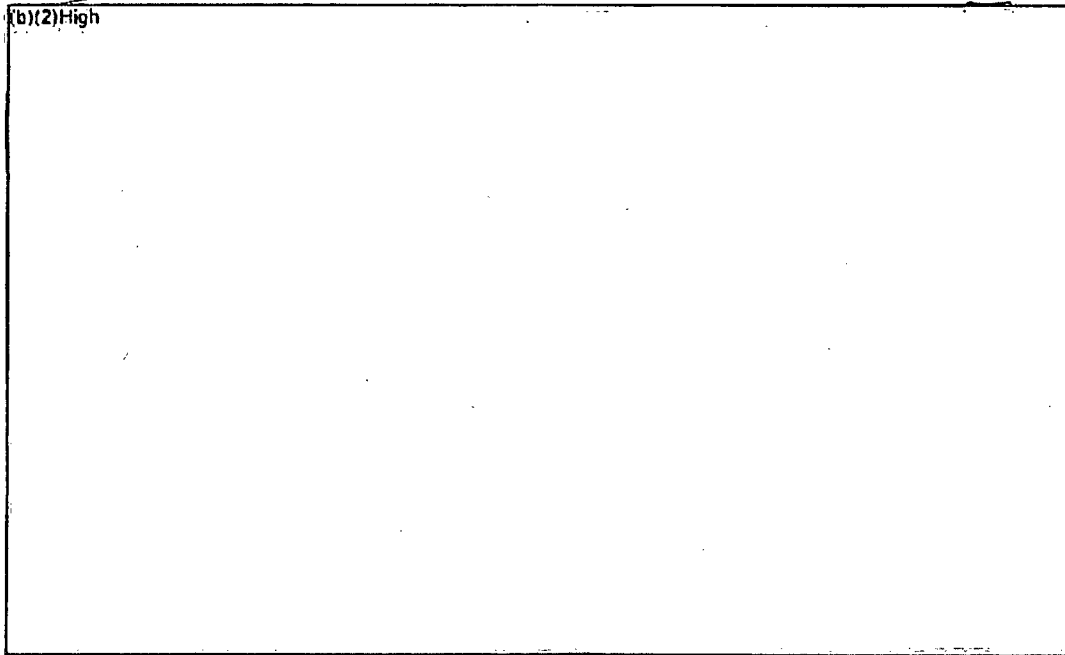
Ex.
2



Ex.
2

Figure 3-42. Comparison of the Peak Cladding Temperatures for the Uniform Configuration with Various Aging Periods and a Whole Pool Spray Flow

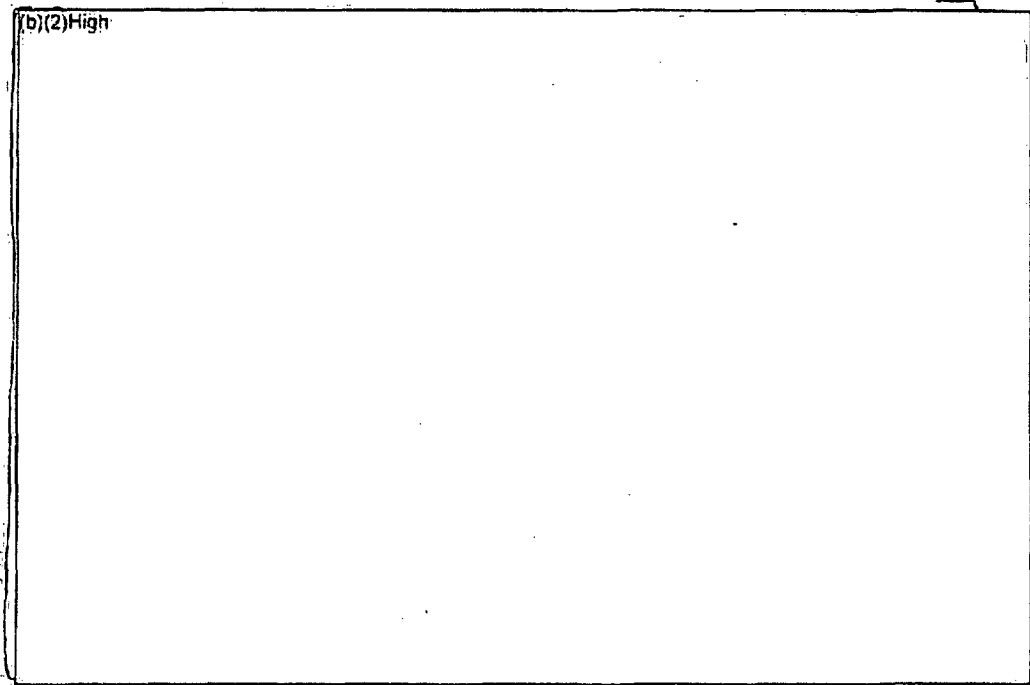
(b)(2)High



Ex.
2

Figure 3-43. Comparison of the Peak Cladding Temperatures for the Uniform Configuration with Various Aging Periods and a Whole Pool Spray Flow

(b)(2)High



Ex. 2
2

Figure 3-44 Comparison of the Peak Cladding Temperatures for the Uniform Configuration with Various Aging Periods and a Whole Pool Spray Flow

(b)(2)High

3.3.3 Summary of Spray Flow Requirements and Extension to Other Sites

Ex. 2 In summary, spray flow rates on the order of (b)(2)High do provide benefit, in that they can either delay or preclude an oxidation transient for a range of conditions. The extent of this benefit is dependent on the conditions of interest. For fuel which has been favorably configured in a 1x4

Ex. 2 pattern, a spray flow rate (b)(2)High provided adequate cooling for the fuel assemblies at

Ex. 2 (b)(2)High. If the fuel was configured in a checkerboard pattern, it is also

Ex. 2 coolable (b)(2)High but only if the inlet is not plugged. Under the same conditions, fuel which is not favorably-configured (i.e., uniform fuel loading) becomes coolable at (b)(2)High

Ex. 2 (b)(2)High. For shorter decay times, sprays will delay the onset of rapid cladding oxidation and subsequent fuel damage.

There are several important factors to be considered when applying these results. First, the reported flowrate in the MELCOR calculations could be considered as the minimum flux at the elevation of the racks. The reported flowrates do not include spray nozzle overlap inefficiencies. The spray flows do, however, assume the entire pool is covered (e.g., the cask region and gaps between the racks and walls are also being sprayed). Although there are only (b)(2)High rack cells in the reference BWR SFP and (b)(2)High spent assemblies, the specified spray flow was further assumed to be evenly spread across the entire SFP cross-sectional area (i.e., an equivalent size of 5160 cells). Consequently, the effectiveness of the spray flowrate is affected by the overall size of the SFP. For application of the reference BWR results to other configurations, the net flux

Ex. 2 into the rack cell should be used (b)(2)High

The hand calculations in Section 3.3.1 included a 33% inefficiency factor for spray overlap and neglected any benefit from spray entering the annulus between the canister and the rack. If these inefficiencies are removed and the decay power is adjusted (b)(2)High then the calculated minimum flowrate is (b)(2)High (see Figure 3-45), or approximately the same value as calculated by MELCOR for cooling (see Figure 3-42). The MELCOR calculations showed a sharp thermal profile where the top of the fuel rods were cooled by the liquid spray but the fuel rods below the spray penetration depth were hot. The radial heat transfer from the hot rods heated the canister and rack wall. The spray flow in the annulus also boiled away, thereby also removing heat from the lower portion of the assembly.

Ex. 2
Ex. 2

Ex. 2 In contrast, the MELCOR calculation showed that (b)(2)High in a uniform, or non-favorable configuration. The comparable hand calculation that included heat transfer to the annulus and neglected the spray inefficiencies predicted (b)(2)High (see lower line in Figure 3-45). It might be argued that (b)(2)High MELCOR result was somewhat coolable, although judged unstable. The modified hand calculation that included heat transfer to the annulus and neglected the spray inefficiencies required (b)(2)High or somewhat closer to the MELCOR result (b)(2)High. Nevertheless, the modified hand calculations were judged as non-conservative at this high power, high flow condition and therefore should only be used as a scoping aid. For example, the MELCOR calculations provide more realistic representation of radial heat transfer, counter-current flow limiting, liquid pass-through in the annulus, film boiling heat transfer rates, etc., that refine the simplistic hand calculation assumption of 100% boiling efficiency. In summary, the MELCOR calculations provide a more mechanistic representation of the physics and therefore are the best guidance for coolability thresholds.

Ex. 2
Ex. 2
Ex. 2
Ex. 2

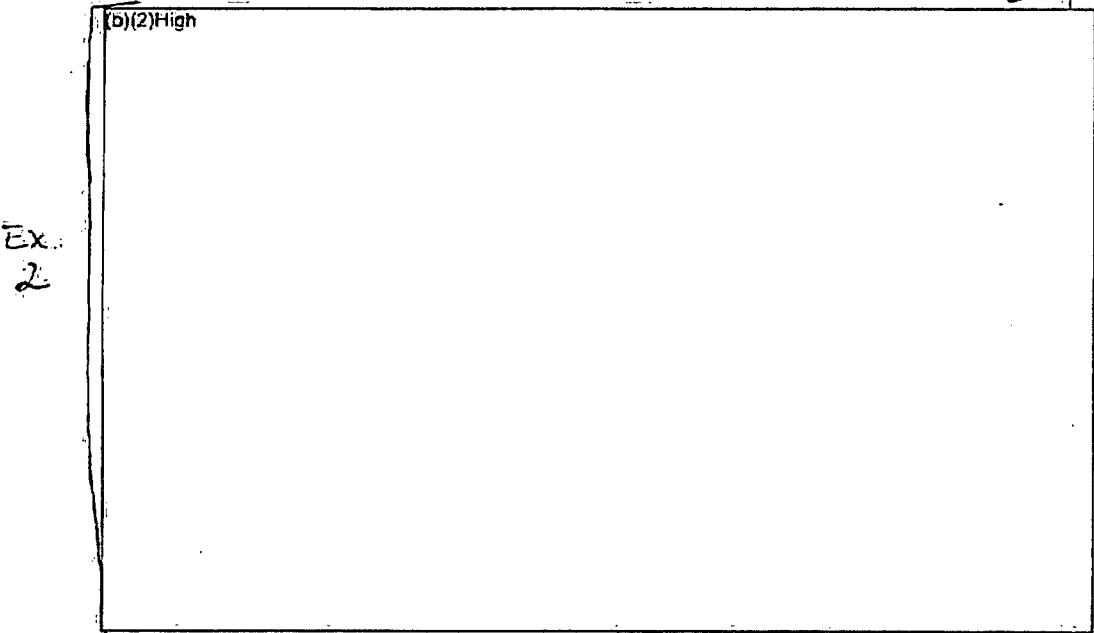


Figure 3-45 Base and Modified Hand Calculations to Estimate Spray Heat Removal Requirements for the Reference BWR SFP.

No PWR spray calculations were made in this study. Based on a comparison of the results from the BWR and PWR hand calculations in Section 3.3.1, the required spray flux per rack cell or per unit area can be calculated.

Ex. 2 For the BWR (b)(2)High (from Section 3.3.1 per unit area but no spray inefficiencies and no radial heat transfer to the annulus between the canister and rack cell wall),

Ex. 2 BWR Spray Flow = (b)(2)High (996 kg/m³ * 2.56 x 10⁶ J/kg) * (60 sec/min) / (264.2 gal/m³) / (5.4" x 5.4")

Ex. 2 (b)(2)High

Ex. 2 (b)(2)High

Ex. 2 For the PWR (b)(2)High with no spray inefficiencies,

Ex. 2 PWR Spray Flow = (b)(2)High (996 kg/m³ * 2.56 x 10⁶ J/kg) * (60 sec/min) / (264.2 gal/m³) / (9.04" x 9.04")

Ex. 2 (b)(2)High
Ex. 2 (b)(2)High

Ex. 2 Consequently, from a flux per unit area perspective, the reference PWR requires less spray flow than the reference BWR (b)(2)High (see Figure 3-47). Although this relatively small difference in fluxes seems contradictory to the overall results cited in Section 3.3.1 (b)(2)High the reference BWR pool dimensions were 48% larger than the reference PWR. Consequently, a smaller flowrate was required to cover the PWR SFP.

Figure 3-46 shows a comparison of the BWR hand-calculation results from above and those from Section 3.3.1 to the MELCOR spray calculation results. The hand calculations assume a uniform storage configuration whereas MELCOR results are shown for uniform, checkerboard, and 1x4 configurations: (b)(2)High the MELCOR uniform configuration results (b)(2)High

Ex. 2 (b)(2)High were coolable (b)(2)High which agrees well with the hand calculations presented in this section (i.e., the lower blue curve in Figure 3-46). To be coolable

Ex. 2 (b)(2)High in a uniform configuration, the MELCOR calculations required (b)(2)High which compares best with the hand calculations presented in Section 3.3.1 that have more conservative assumptions. The correlation of the MELCOR results to the two different hand calculations suggest that more complex physics are present than is treated in either of the hand calculations. Consequently, the best conclusion that can be made from these comparisons is that the Section 3.3.1 calculations, which have several conservative assumptions, bound the MELCOR uniform configuration results. However, when well-configured arrangements are considered (i.e., such radial heat transfer effects were not included in the hand calculations), the MELCOR results for 1x4 and unplugged checkerboard arrangements require significantly less spray flow for coolability than the uniform configurations (i.e., see the MELCOR 1x4 and unplugged checkerboard results in Figure 3-46).

For extension of results to other SFPs, the following findings to improve coolability were identified,

1. The MELCOR calculations showed the spray system would improve the coolability of the checkerboard and uniform configurations and also improved the coolability of the 1x4 configuration, even if the inlet was blocked by water.

Ex. 2

2. The spray injection system benefits from a well-configured layout. The 1x4 assemblies were coolable (b)(2)High with the specified flowrate as was the checkerboard configuration if the rack inlet was not plugged by water. The uniform configuration was not coolable, though additional time for mitigative action was gained.

Ex. 2

3. Only BWR SFP spray calculations were performed using MELCOR. However, simple scaling arguments show that the required PWR spray flux (i.e., gpm/ft²) was similar (b)(2)High (see Figure 3-47).¹⁵

4. The deployment of the spray system requires consideration of spray overlap and pool size. The effective flow to an individual assembly for the same total spray flowrate could vary significantly based on the pool size and spray overlap. For example, the reference PWR SFP was 48% smaller than the reference BWR SFP.

Ex. 2

5. The MELCOR results offer the best guidance for other SFPs when scaled per unit cell (b)(2)High

Ex. 2

Ex. 2

Ex. 2

Ex. 2

6. The hand calculations presented in this section compared well to the MELCOR result (b)(2)High. However, the hand calculation (b)(2)High was non-conservative relative to the MELCOR result (b)(2)High

Ex. 2

Consequently, the MELCOR calculations provide a more mechanistic representation of the physics and therefore are the best guidance for coolability thresholds. For the two conditions examined (b)(2)Low the Section 3.3.1 hand calculations had additional conservatism that bounded the MELCOR results.

¹⁵ The BWR spray hand calculations used the canister ID as the effective cross-sectional area for spray flow. The MELCOR calculations showed heat removal benefit from the spray water entering the annular region between the canister and the rack wall. Consequently, the BWR spray flow is expected to be more effective than shown in this hand calculation. If the entire rack pitch cross-sectional area is used in the BWR calculations (i.e., inside the canister and the gap between the canister and the rack wall) (b)(2)High

Ex. 2

(b)(2)High. However, these differences are small relative to other variations and uncertainties (e.g., see discussion above in context with Figure 3-46).

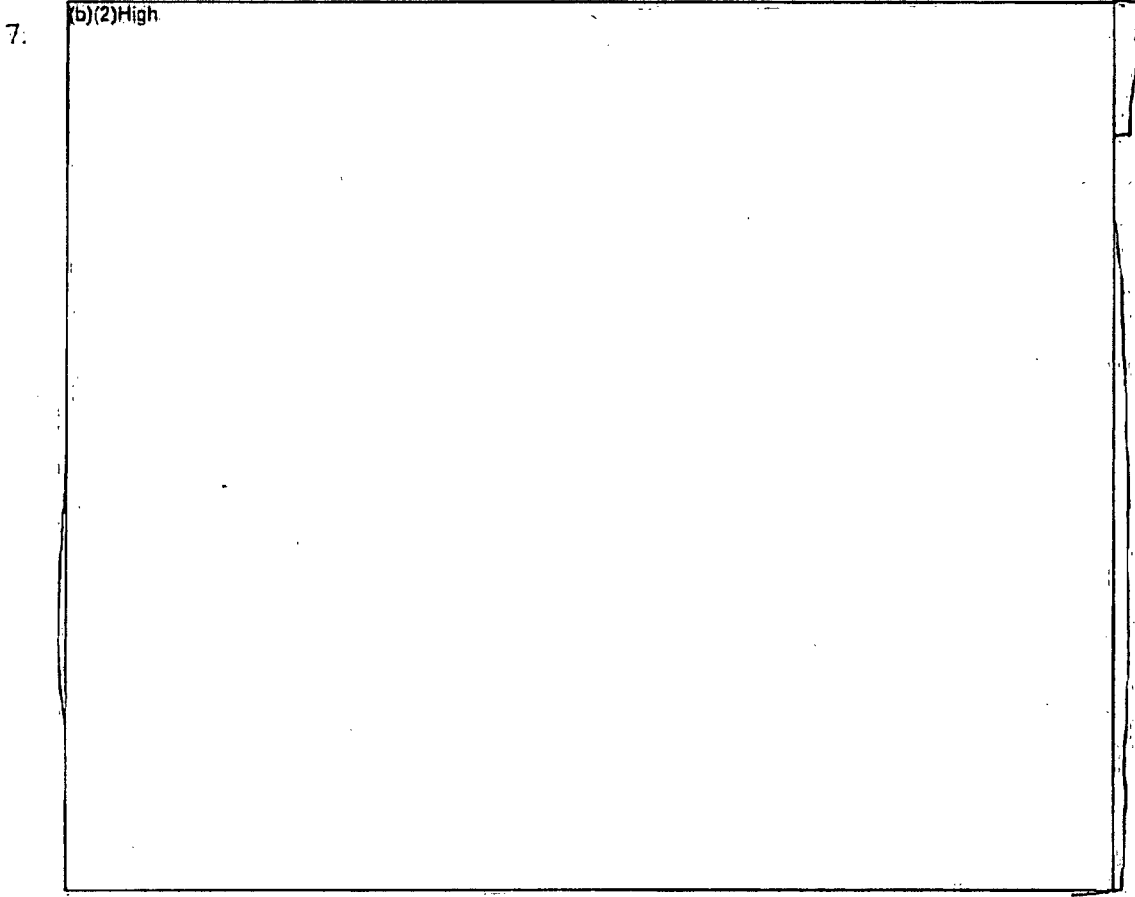


Figure 3-46 Base and Modified Hand Calculations to Estimate Spray Heat Removal Requirements for the Reference BWR SFP (Uniform Configuration).

EX. 2

¹⁶ As shown in Section 3.1.1, the fuel will remain coolable with a water level (b)(2)High (b)(2)High. Consequently, the spray will initially remove the sensible heat from that region. However, the detailed MELCOR spray calculations showed the sprays could be effective at cooling the fuel even if all the water had completely drained away and there had been some heatup of the top of the fuel [Wagner, 2006a].

Ex.
2

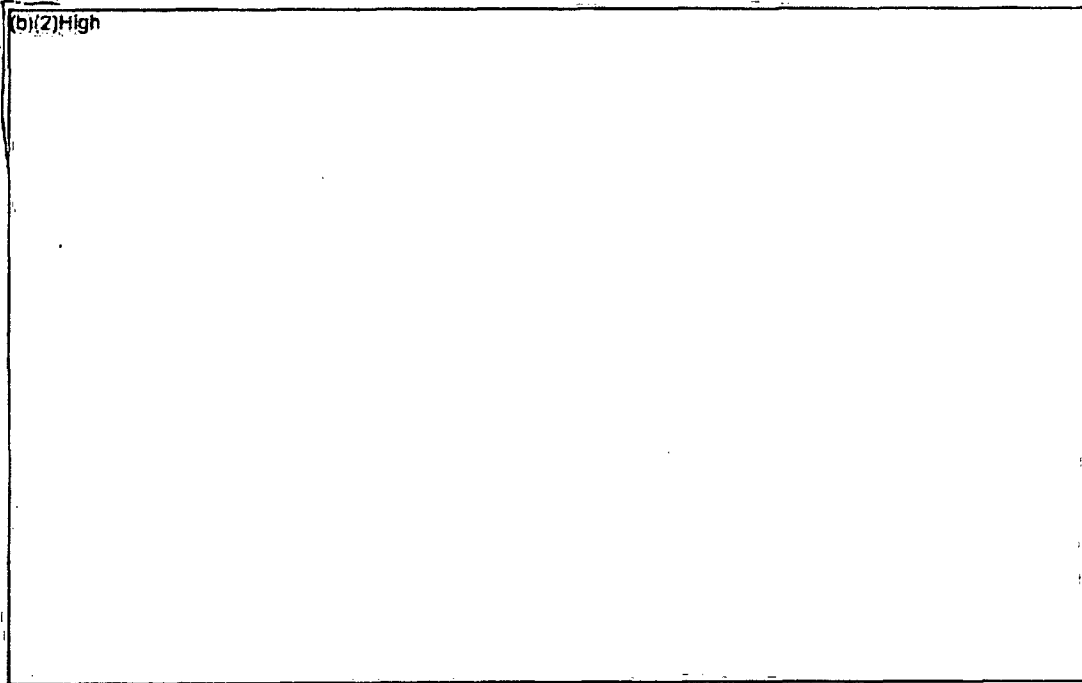


Figure 3-47 Minimum BWR and PWR Spray Flux (Uniform Configuration).

3.4 Building Ventilation

In complete loss-of-coolant inventory scenarios, air circulation patterns develop that circulate air into the SFP and through the spent fuel assemblies. If the building heat removal is inadequate, the room will heat as well as the air circulating through the spent fuel pool racks. At steady conditions, the decay heat power of the SFP must be removed by the ventilation system and/or building leakage. In the reference plant SFPs, the total pool decay heat ranges from ~3 MW at 20 days to <1 MW at one year. In the absence of in addition to a forced ventilation system, the ideal ventilation configuration would supply cool air at the bottom of the room with the SFP and exhaust air from above the SFP. (b)(2)High

(b)(2)High

(b)(2)High In both the reference plants, nominal leakage and heat loss through the walls and ceiling provided a significant amount of heat removal. (b)(2)High

Ex. 2

(b)(2)High

In partial loss-of-coolant inventory conditions where there is no air flow through the assemblies, the role of ventilation is not a significant factor for coolability. The assembly heat removal occurs by boiling below water level and steam cooling above. Sustained coolability is much more difficult to achieve in partial loss-of-coolant inventory accidents without make-up water or sprays. (b)(2)High

Ex. 2

(b)(2)High

(b)(2)High It might seem intuitive to inhibit ventilation for a partial loss-of-coolant inventory accident to retain any released fission products. However, the by-product of steam oxidation with zirconium-based cladding and stainless steel racks in the SFP is hydrogen. (b)(2)High

Ex. 2

(b)(2)High

Therefore, the benefits of preventing hydrogen burns and potential building damage needs to be weighed against increased retention of released fission products. The potential benefit of increased fission product retention with reduced ventilation only applies to an accident which is mitigated prior to a hydrogen burn.

Ex. 2
Ex. 2

To demonstrate the importance of ventilation on the complete loss-of-coolant inventory response, Section 3.4.1 shows the results of the computational fluid dynamics (CFD) analysis of the reference PWR fuel storage building. The amount of ventilation was varied (b)(2)High (b)(2)High by specified amounts. The CFD results show the impact (b)(2)High on the natural ventilation rate, the building temperature, and the peak temperature in the spent fuel racks. As the ventilation rate decreases, the building temperature rises as well as the temperature under the racks. Section 3.4.2 shows the results from separate effects calculations that assessed the impact of the inlet temperature on the peak cladding temperature and amount of aging for coolability. A summary of an analysis of the governing equations for convective heat removal illustrates that a 50 K increase in the inlet temperature results in a much higher increase in the peak cladding temperature, thereby emphasizing the importance of the adequate building ventilation.

3.4.1 Flow Patterns in the Reference PWR Fuel Storage Building

The FLUENT CFD code was used to perform the simulations of complete loss-of-coolant inventory accidents in the reference PWR SFP [Khalil]. FLUENT is a state-of-the-art commercial CFD code that solves the fundamental Navier-Stokes equations for mass, momentum, and energy through a finite volume approach. The FLUENT models of the spent fuel pool and the fuel storage building consisted of over 490,000 finite volume cells. The individual fuel racks were modeled as anisotropic porous media. The principal objective of the FLUENT calculations was to study the steady state flow patterns above, below and around the spent fuel racks for different scenarios.

The CFD calculations simulated the steady state profiles that would develop after a complete loss-of-coolant inventory: (b)(2)High

Ex. 2 (b)(2)High

Ex. 2 The CFD results show a flow pattern of hot air exiting from the assemblies at the top of the racks (see Figure 3-48). The hot gases form a plume which then rises to the building ceiling. Once the plume hits the ceiling, it spreads radially and mixes within the hot gas layer at the top of the room. The room remains thermally stratified as hot gases preferentially leak out the large, open ceiling ventilation units. Meanwhile, cool air enters (b)(2)High to replace the exiting hot gases. The cool air fills the lower regions of the building, overflows to the SFP floor elevation, and sinks into the SFP to replace exiting hot gases. The cool air flow flows underneath the racks through the cask area and open rack cells and then spreads radially under the racks. The hydrostatic pressure difference between the cold gases outside the racks and the hot gases inside the assemblies drives the airflow through the racks.

Ex. 2 Table 15 summarizes the results for the air mass flow into the building (b)(2)High

(b)(2)High The cool air was drawn into the main room and down into the SFP. Some of the air dropped below the racks and was heated in the assemblies while a portion swept across the top of the racks and mixed with the hot plume exiting the racks. After the air streams combined, the hot gas plume rose to the ceiling and formed a hot gas layer. The hot gases near the ceiling subsequently leaked through the ventilation units on the roof of the fuel storage building. The FLUENT calculations achieved quasi-steady conditions when the flow through the fuel storage building became steady. (b)(2)High

Ex. 2 (b)(2)High

Table 15. Key Calculated Results Using FLUENT.

(b)(2)High

Ex. 2

In the next two columns of Table 15, the maximum temperature in the racks and the air above the SFP for each case are shown. (b)(2)High

(b)(2)High

Ex. 2

(b)(2)High It was concluded that other non-linear thermophysical effects led to the larger increase in the fuel response and can be explained by looking at the temperature dependence in some of the terms affecting the convective heat removal capability [Wagner, 2005b]. (b)(2)High

Ex. 2

(b)(2)High

As the SFP heated to quasi-steady conditions, a hot plume rose out of the SFP and formed a hot gas layer next to the refueling room ceiling. Below the hot gas layer, the gas temperature remained cool. A counter current flow developed where hot gases leaked out of the refueling room and cool gases entered. The cool gas in the lower portion of the refueling room preferentially sank into the SFP to replace the gas discharged in the hot air plume. (b)(2)High

Ex. 2

(b)(2)High

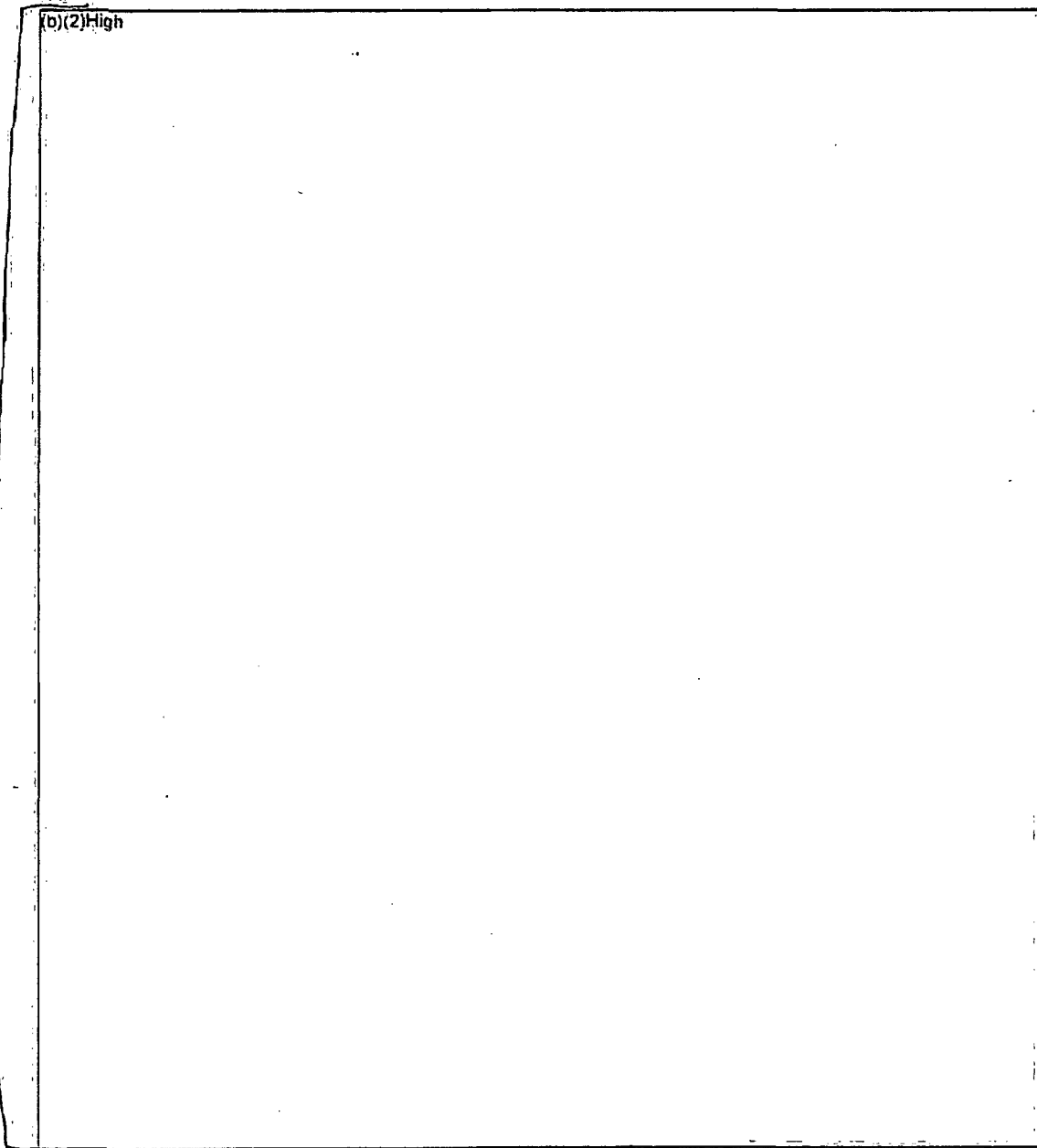


Figure 3-48 Flow Patterns into the SFP From FLUENT Calculations With Open Roll Door.

3.4.2 Separate Effect Sensitivity Analysis of Inlet Temperature

The separate analysis also showed a strong dependence of the peak cladding temperature as a function of the inlet temperature. The base case calculations assume that the inlet temperature remained at 300 K.¹⁷ Using an inlet temperature of 300 K, the uniform configuration for the reference PWR was coolable (b)(2)High. As shown in Figure 3-49, a change in inlet temperature had a dramatic effect on the PCT response: (b)(2)High.

Ex. 2

Ex. 2

MELCOR calculations were then performed to evaluate the coolability of the assembly for 350 K and 400 K inlet temperature cases. Figure 3-50 and Figure 3-51 show variable aging responses for 350 K and 400 K inlet temperatures, respectively. (b)(2)High.

Ex. 2

(b)(2)High To understand the reasons for this large impact, it is worth examining the governing equations for the convective heat removal rate as a function of temperature.

The convective heat removal rate is linearly dependent on $\rho_{outside}$, the overall density difference ($\rho_{outside} - \rho_{inside}$), the overall enthalpy difference and ($h_{exit} - h_{outside}$), and other constants. With some simplifying assumptions and power fits to the thermophysical properties, it can be shown that the convective heat removal varies with temperature as follows,

$$q_{flow} \propto (T_{inside}^{-2.66}) * (1/T_{outside} - 1/T_{inside}) * (T_{exit} - T_{outside}) \quad (\text{Eqn. 3-1})$$

Equation 3-1 is somewhat awkward to assess the sensitivity of the convective heat removal rate without specific data. However, if the 300 K and 350 K inlet cases have similar temperature profiles through the assembly, the following parameters can be set,

Ex. 2

(b)(2)High

Using Eqn. 3-1, the ratio of the convective heat removal rates for the two cases is

Ex. 2

(b)(2)High

(Eqn. 3-2)

Ex. 2 Hence, this simple analysis suggests that the 300 K inlet case removes more heat than the 350 K inlet case.

In reality, due to non-linear temperature profiles, inertial flow losses, and oxidation effects, the comparisons are more complicated than shown in the evaluation of the governing equations. MELCOR performs a mechanistic solution of the governing equations with these effects and can

¹⁷ The MELCOR calculations included in this section were performed with an earlier version of the code that does not include breakaway oxidation kinetics. The MELCOR calculations are representative of the impact of higher inlet temperature on the coolability. However, the inclusion of breakaway kinetics and a steam oxidation layer would slightly impact the quantitative values.

be used to assess the impact of the inlet temperature on the PCT.¹⁸ Using an example from some MELCOR calculations, the results from two 300 K inlet temperature cases are compared to a 350 K case (see Figure 3-52). The convective heat removal rates (b)(2)High cases as a function of exit temperature were compared (b)(2)High. The peak exit gas temperatures from the two 300 K cases bracketed the result from the 350 K inlet case. The 350 K temperature inlet case required a 242 K higher exit temperature to achieve the same amount of heat removal from the assembly, which is qualitatively consistent with the trends observed in the analysis of the governing equations. Similarly, the ratio of powers to achieve the same exit conditions were,

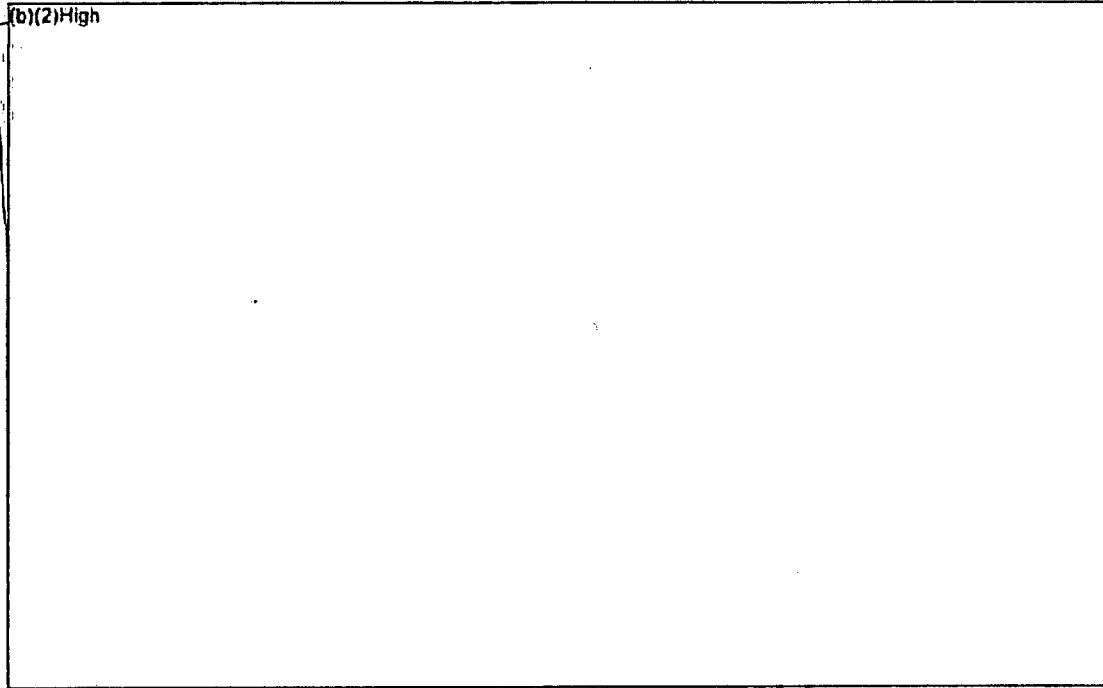
Ex. 2 (b)(2)High (Eqn. 3-3)

Ex. 2 which, is in good agreement with (b)(2)High from Equation 3-2.

Ex. 2 Similar to the uniform configuration, increasing the inlet temperature to 350 K also had a significant effect on the 1x4 configuration. As shown in Figure 3-53 (b)(2)High 300 K inlet temperature is compared to various results with a 350 K inlet temperature. (b)(2)High

Ex. 2 (b)(2)High

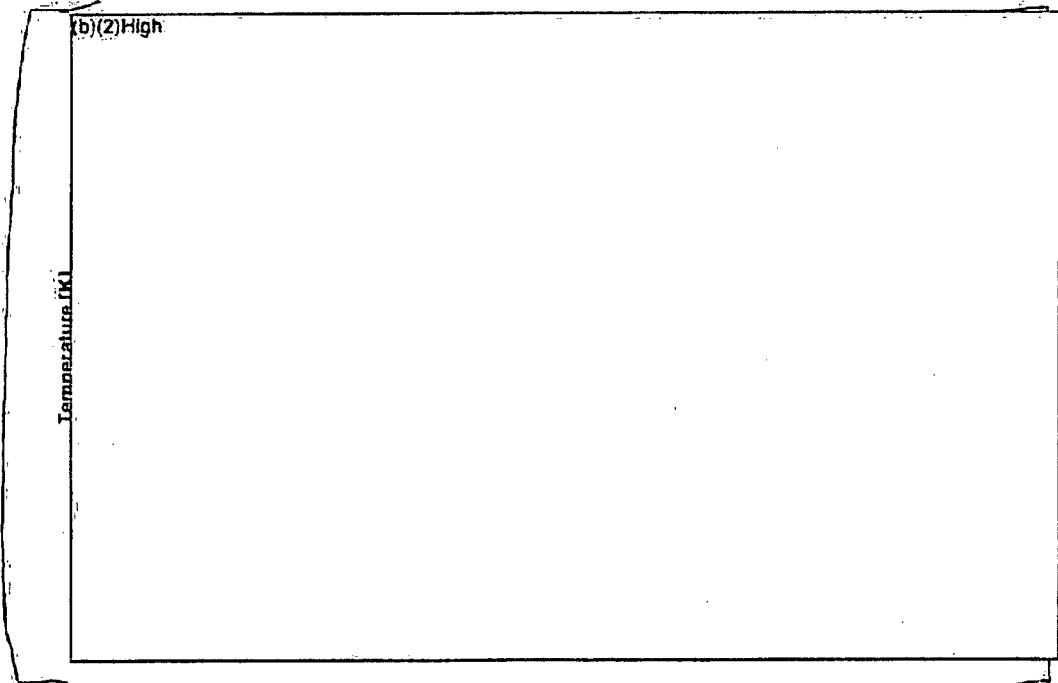
¹⁸ In addition to the convective heat removal, MELCOR also calculates oxidation of the assembly cladding, the canister, and the steel components. Oxidation introduces a transient power source that is not included in the hand calculations.



Ex.
2

Ex. 2 **Figure 3-49 Comparison of the PCT versus the Assembly Inlet Temperature Aging Time Since the Assembly was Discharged for the Uniform Configuration.**

(b)(2)High



Ex.
2

Figure 3-50 Comparison of the PCT versus the Aging Time at an Assembly Inlet Temperature of 350 K.

Ex.
2

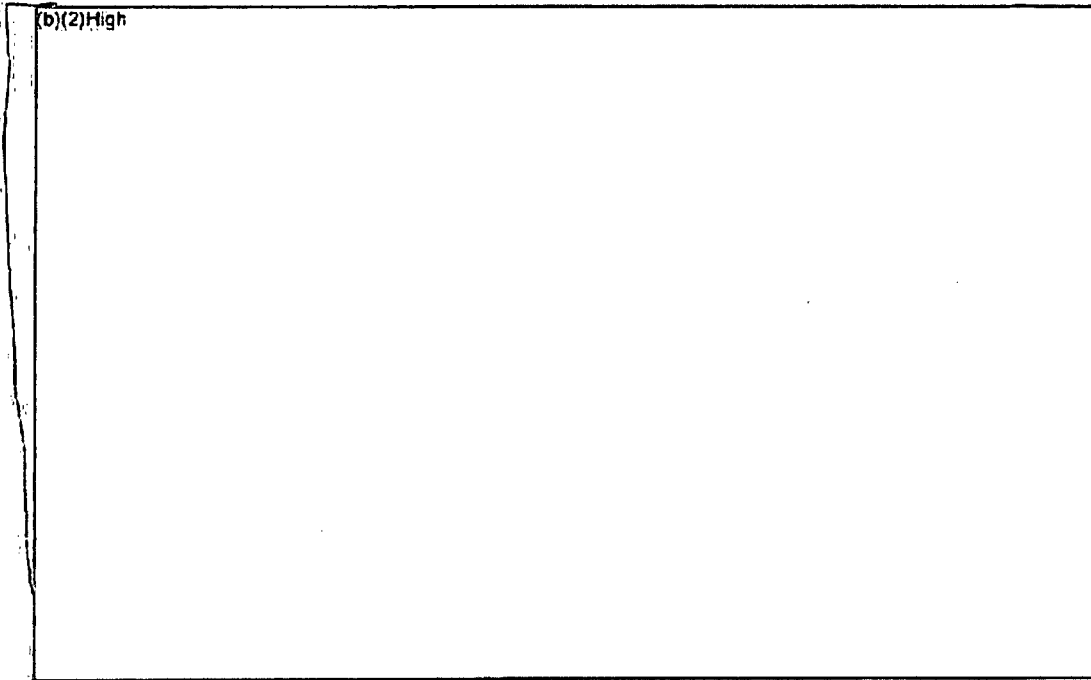


Figure 3-51. Comparison of the PCT versus the Aging Time at an Assembly Inlet Temperature of 400 K for the Uniform Configuration.

Ex
2

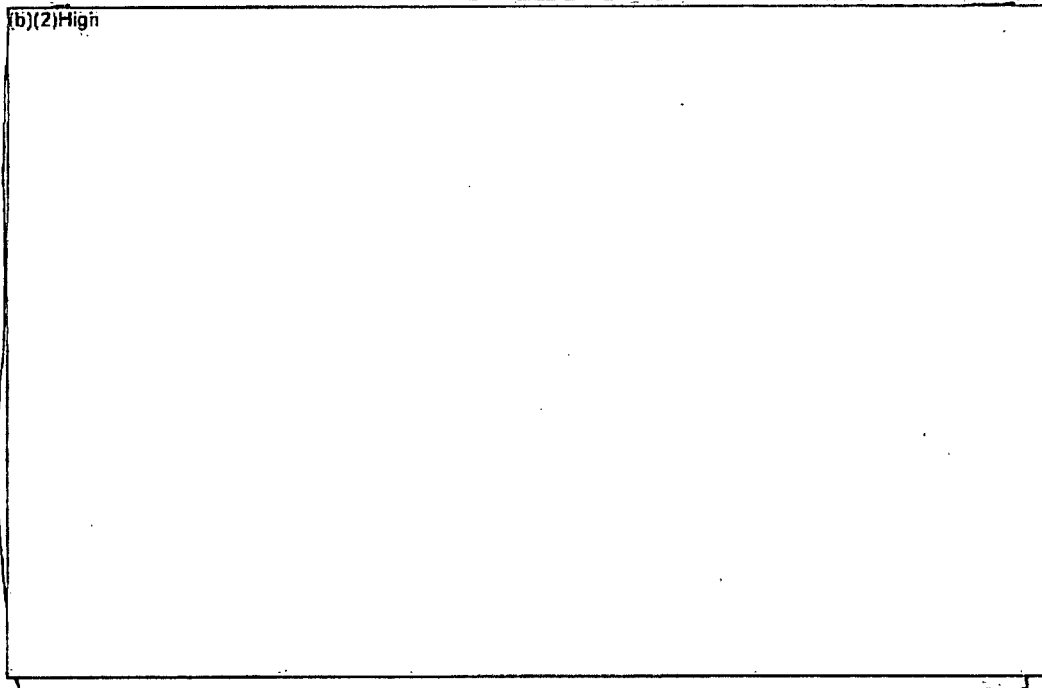
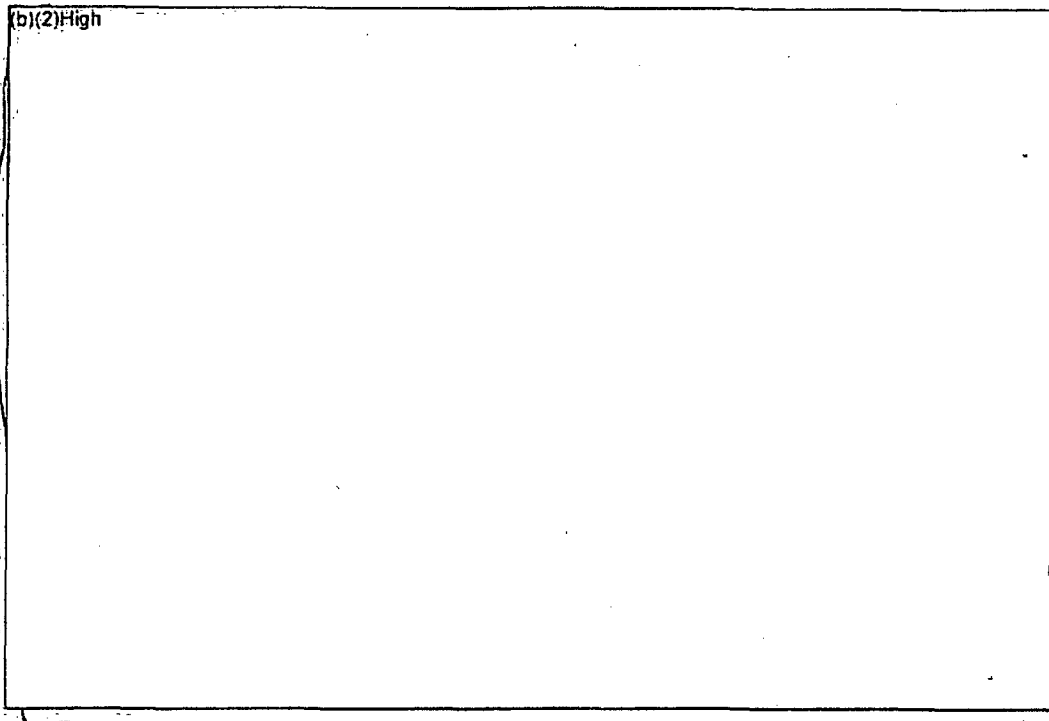


Figure 3-52. Comparison of the Convective Heat Removal Rates at 300 K versus 350 K Inlet Temperatures as a Function of Exit Temperature.



Ex. 2

Figure 3-53 Comparison of the PCT versus the Aging Time at an Assembly Inlet Temperature of 350 K in a 1x4 Configuration.

3.4.3 Impact of Ventilation on Integral Whole Pool Calculations

A series of three complete loss-of-coolant inventory calculations were performed for the reference PWR SFP using MELCOR [Wagner, 2006c]. (b)(2)High

Ex. 2

(b)(2)High

(b)(2)High The spent fuel was well-configured as shown in Figure 3-37 with the highest-powered assemblies in 1x4 patterns with the lowest-powered assemblies. The 1x4 patterns of the highest-powered assemblies were further distributed in a checkerboard arrangement with the 1x4 patterns of the lowest-powered assemblies from the last offload (e.g., clearly shown in Figure 3-36). The three cases are similar to the ones discussed in Section 3.4.1 but included (a) a high decay heat level (b)(2)High

Ex. 2

(b)(2)High (b) the nominal building leakage; (c) the full accident progression and drain down timing, and (d) better calculations of the fuel response (i.e., detailed assembly geometry models and physics models for radiation, oxidation, and radial assembly-to-assembly heat transfer). Hence, they are also included for reference.

Ex. 2

The water level fell very rapidly (b)(2)High The water level fell to the top of the SFP racks (b)(2)High

Ex. 2

(b)(2)High As a result of the loss of water cooling, the fuel rods began to heatup in all regions of the SFP (b)(2)High

(b)(2)High

Ex. 2 (b)(2)High

The reference PWR fuel storage building has a few key features that will promote convective heat removal during a complete loss-of-coolant inventory accident. (b)(2)High

(b)(2)High

(b)(2)High In. (b)(2)High the nominal building leakage was estimated from a National Institute of Standards and Testing paper to be ~1 m² [Persily].²⁰ Consequently, all cases were supplemented by other sources of leakage that were estimated to be equivalent (b)(2)High

Ex. 2 (b)(2)High The other sources of leakage include the wall joints, doors, pipe chases, and other penetrations (~1 m²). Since the building is well insulated, the leakage paths are the primary mechanisms for heat removal.

Ex. 2 It is important to note that the locations (b)(2)High (b)(2)High are ideally situated for natural circulation flow. Hot air exiting the

Ex. 2 SFP will rise to the ceiling (b)(2)High Simultaneously, cool outside air will enter (b)(2)High and other leakage locations to replace the hot air leakage. As shown in Figure 3-48, the cool air remains at the bottom of the SFP room and sinks into the SFP. The cool air travels under the racks and is subsequently heated in the spent fuel assemblies. If the only leakage pathways were at a low elevation, then the natural circulation flow would be less effective. The room would fill with hot gases. (b)(2)High

Ex. 2 (b)(2)High

Cases C5, C7, and C6 parametrically investigated (b)(2)High building leakage configurations. The resultant total building ventilation flow is shown in Figure 3-54. As pointed out in Section 3.4.1, the building ventilation flow was limited by (b)(2)High

Ex. 2 (b)(2)High and by leakage through the roof ventilation units when (b)(2)High (b)(2)High Consequently, the flow did not simply scale (b)(2)High (b)(2)High

The resultant gas temperature entering the SFP was the most important impact of the ventilation rate. Figure 3-55 shows the temperature of the gas entering the SFP. As discussed in Section 3.4.2, the inlet gas temperature has a strong, non-linear impact on the peak cladding

Ex. 2 (b)(2)High (b)(2)High

Ex. 2 (b)(2)High

²⁰ The nominal building leakage was distributed uniformly by the building wall and roof surface area. The equivalent amount of roll door leakage was estimated by comparing the ventilation flow with only nominal leakage versus (b)(2)High

Ex. 2 (b)(2)High

EX. 2

(b)(2)High

EX. 2 The impact of the higher SFP gas inlet temperature between the (b)(2)High cases resulted in higher peak cladding temperatures throughout the SFP. The impact on the Ring 1 assemblies (i.e., the highest powered assemblies and most susceptible to igniting) was mitigated by increased radial heat transfer to Ring 2 and reduced radial heat transfer from Ring 3 to Ring 2.

EX. 2

(b)(2)High

(b)(2)High Hence, it was concluded that the increased heat removal due to radial radiative exchange partially mitigated the adverse impact of an increased gas inlet temperature. Nevertheless, the (b)(2)High ventilation condition left the SFP assemblies at a higher temperature and more susceptible to ignition than the (b)(2)High case.

Table 16 Summary of Ventilation Sensitivity Study Specifications and Results.

EX. 2

(b)(2)High

Ex.
2

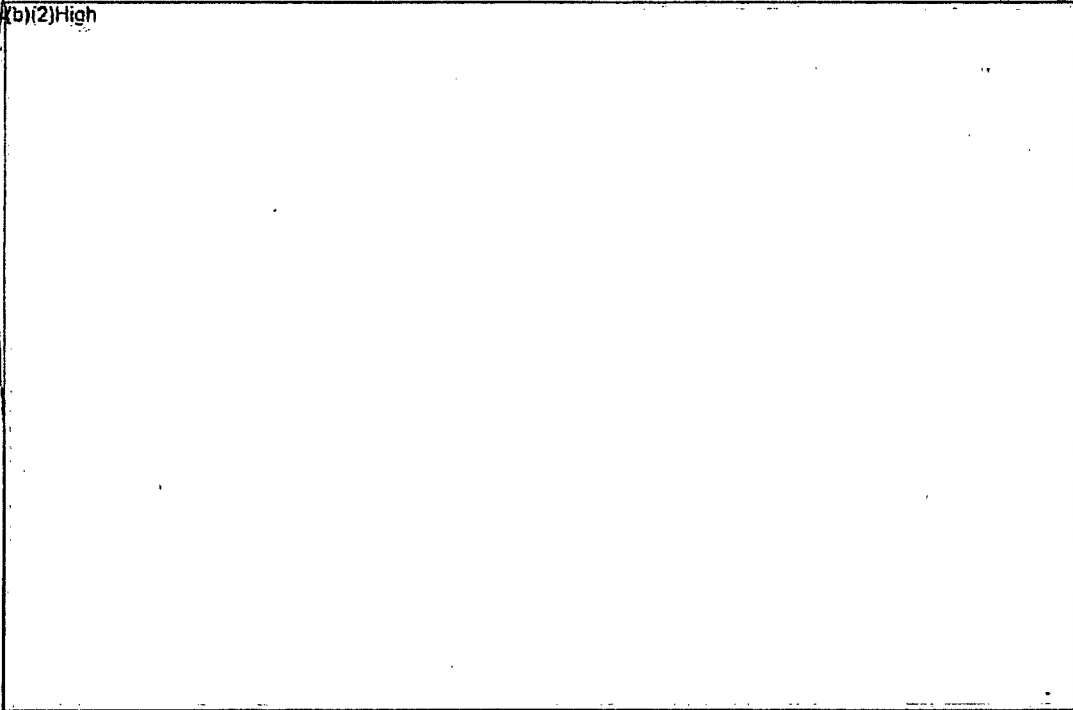


Figure 3-54 Comparison of the SFP Building Ventilation Flows

Ex.
2

(b)(2)High
(b)(2)High

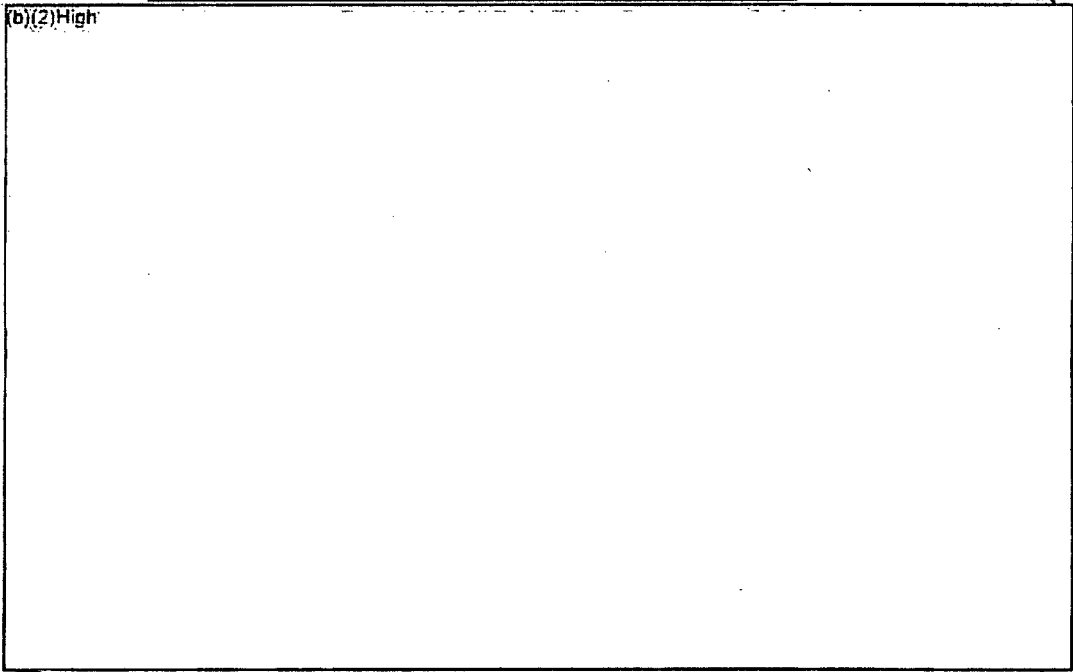


Figure 3-55 Comparison of the Gas Temperatures Flowing into the SFP

Ex.
2

(b)(2)High
(b)(2)High

Ex. 2

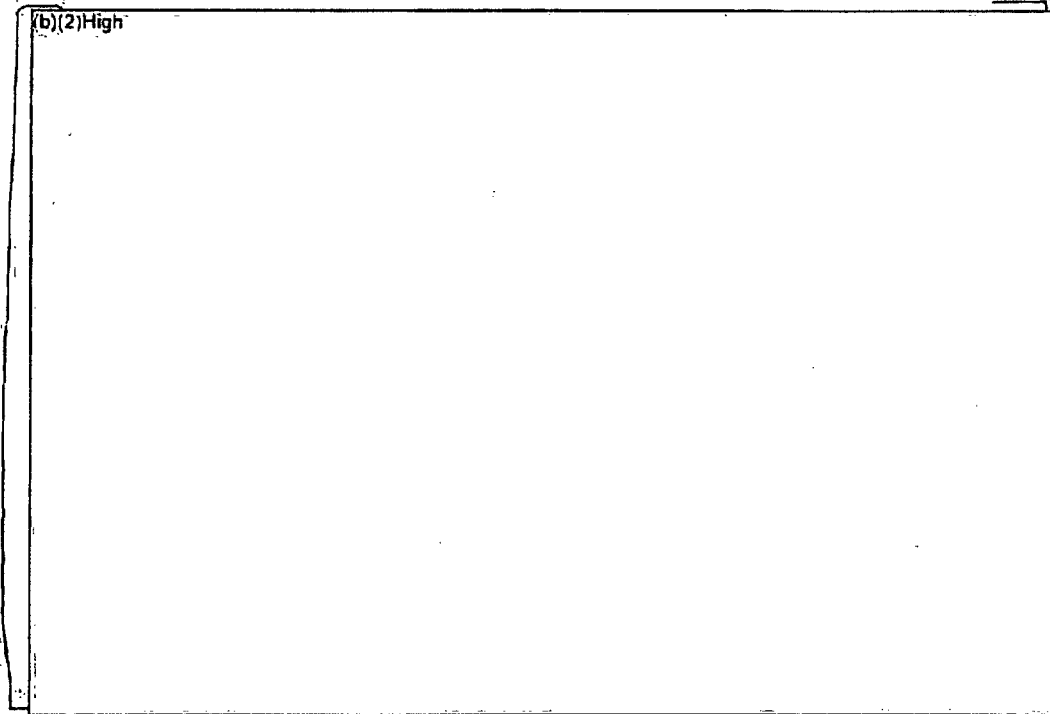


Figure 3-56 Comparison of the Peak Cladding Temperature Responses

(b)(2)High

Ex. 2

(b)(2)High

3.4.4 Summary of Ventilation Findings and Extension to Other Sites

In summary, a robust ventilation flow is needed in complete loss-of-coolant inventory accidents to remove the SFP decay heat. Without adequate heat removal, the room will heat-up causing the hot gas layer to drop into the SFP. The separate effect calculations in Section 3.4.2 showed the strong, nonlinear impact of the inlet temperature on the assembly cladding temperature response. In the CFD calculations in Section 3.4.1, it was shown that a robust, natural circulation flow could be developed by opening doors. In particular, the natural flow patterns in the reference plants were enhanced due to the supply flow from below the SFP and an exhaust location above the SFP.

As discussed in Section 3.4, the role of ventilation is not a significant factor for coolability in the partial loss-of-coolant inventory conditions. However, if the accident proceeds to fuel damage, very large amounts of hydrogen can be generated, which will result in hydrogen burns and building damage. It might seem intuitive to inhibit ventilation for a partial loss-of-coolant inventory accident to retain any released fission products. However, the by-product of steam oxidation with zirconium-based alloy cladding and stainless steel racks in the SFP is hydrogen.

(b)(2)High

Ex. 2

(b)(2)High

The potential benefit of increased fission product retention with reduced ventilation

only applies to an accident which is mitigated prior to a hydrogen burn. In contrast, intentionally enhanced leakage could preclude hydrogen burns, permit re-isolation at a later time, and generically benefits the complete loss-of-coolant configuration, if the water level in the pool is unknown.

The application of the ventilation findings to enhance spent fuel coolability should be guided by the following insights from the SFP analyses.

Ex. 2

- In an otherwise unmitigated complete loss-of-coolant inventory accident, a well-configured pool can be air coolable if there is adequate ventilation. As shown in Section 3.4.3, the reference PWR SFP was air coolable with adequate ventilation and a well-configured layout. (b)(2)High If the ventilation was inadequate, then the room gradually heated, which caused heatup of the spent fuel to failure conditions.
- The specification of the required amount of ventilation is complicated by many factors. Is the ventilation flow due to a mechanical system or open doors? What are the nominal flow leakage characteristics of the building? What is the relationship of leakage area versus elevation and location? What is the flow resistance through the passive leakage sites? What are the building heat loss characteristics? What is the temperature of the supply and exhaust air?

These issues were addressed in the reference plants through CFD and MELCOR code calculations. However, some first-order heat removal requirements can be estimated as follows:

$$V_{exit} = \frac{\dot{m}}{\rho_{exit}} = \frac{Q}{\rho_{exit} \int_{T_{in}}^{T_{ex}} dh(T)} \quad (\text{Eqn. 3-4})$$

- where,
- V_{exit} Volumetric flow
 - \dot{m} Ventilation mass flow through the fuel storage building
 - ρ_{exit} Ventilation exhaust gas density
 - Q Pool decay heat power
 - $h(T)$ Gas enthalpy, which is a function of temperature
 - T_{in} Ventilation supply temperature
 - T_{exit} Ventilation exhaust temperature

Using Eqn. 3-4 for the reference PWR (which has approximately 10% lower SFP decay power than the reference BWR), the heat-removal ventilation requirements were calculated (see Figure 3-57 and Figure 3-58). It was assumed that the ventilation flow removes all the decay heat from the SFP (i.e., there is no building heat loss). (b)(2)High

Ex. 2

(b)(2)High

Ex. 2

(b)(2)High

- If emergency make-up flow or sprays are activated, then the importance of the ventilation for spent fuel heat removal is diminished. The emergency make-up flow could plug the inlet of the SFP racks with water, thereby preventing air natural circulation. Furthermore, the sprays, if uniformly applied at a reasonable flowrate²², will keep the gas temperature in the SFP relatively low (e.g., see [Wagner, 2006a]). Enhanced ventilation is useful to provide cooling prior to spray activation and hydrogen control following spray initiation.
- If a partial loss-of-coolant inventory accident occurs, then ventilation is not important for the spent fuel heat removal. Additional ventilation will limit the buildup of combustible gases but also enhances fission product release to the environment. (b)(2)High

Ex. 2

(b)(2)High

(b)(2)High The potential benefit of increased fission product retention with reduced ventilation only applies to an accident which is mitigated prior to a hydrogen burn. In contrast, intentionally enhanced leakage could preclude hydrogen burns, permit re-isolation at a later time, and generically benefits the complete loss-of-coolant configuration, if the water level in the pool is unknown.

Ex. 2

(b)(2)High

Ex. 2

²² A spray flowrate (b)(2)High was used in a reference BWR SFP analysis [Wagner, 2006a], which kept the gas temperature in the SFP cool (i.e., near the spray temperature for the air going under the racks).

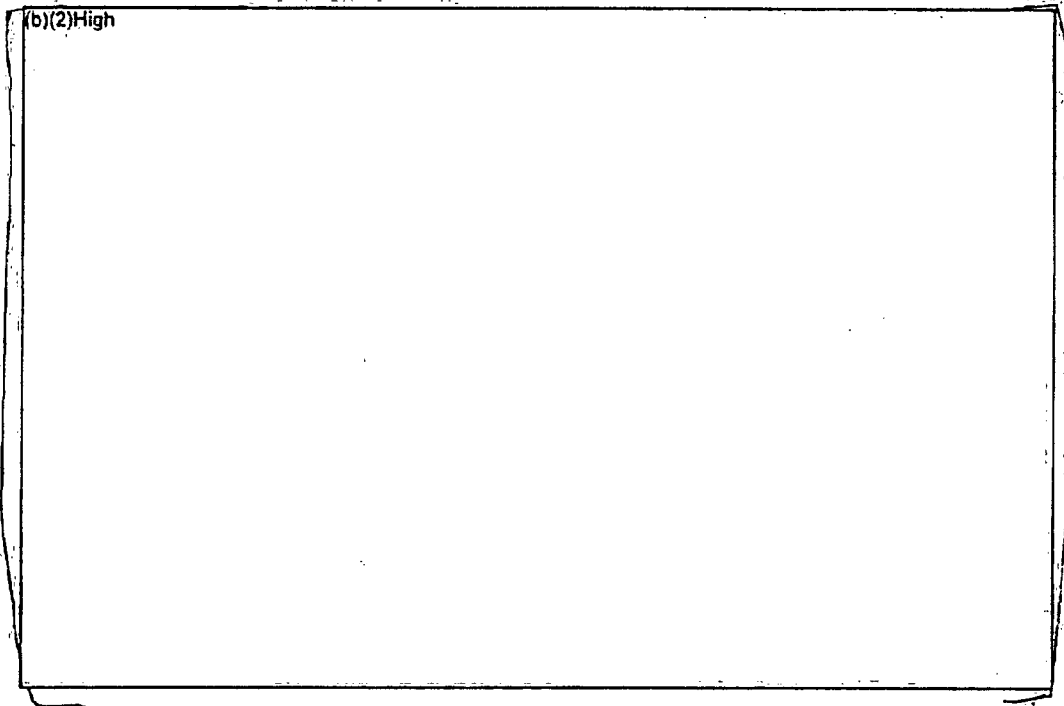


Figure 3-57 Hand Calculation of Ventilation Requirements for the Reference PWR SFP (SI Units).

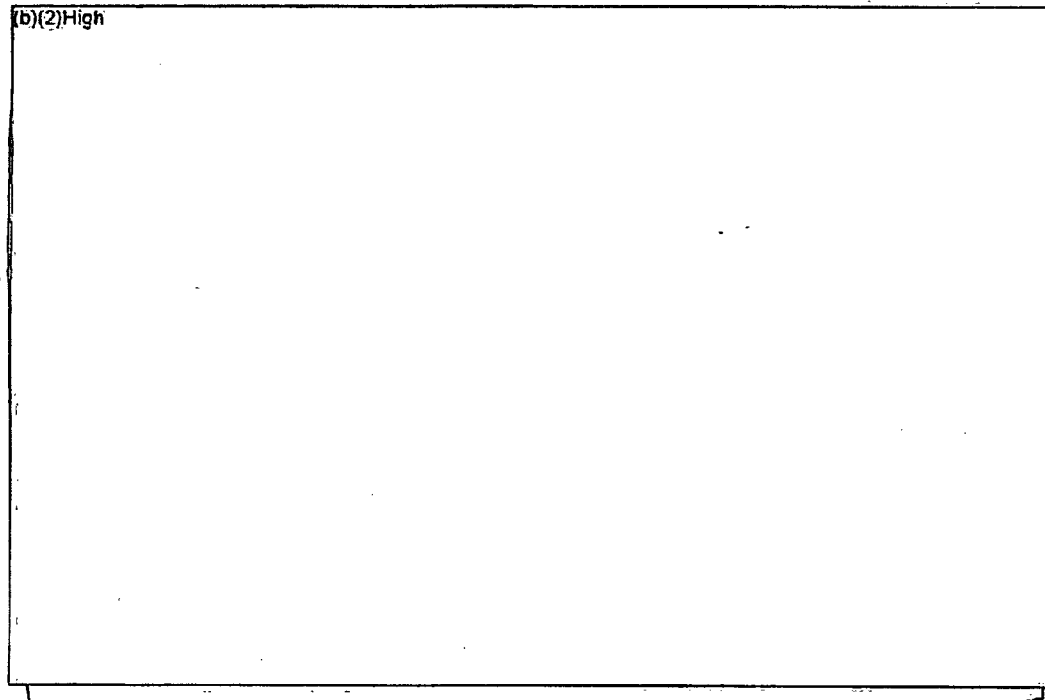


Figure 3-58 Hand Calculation of Ventilation Requirements for the Reference PWR SFP (British Units).

3.5 Pool Configuration

Supporting computational fluid dynamic (CFD) calculations were performed to study the air flow patterns in the reference BWR and PWR spent fuel storage buildings during a complete loss-of-coolant inventory accident. The CFD calculations showed the importance of an open 'downcomer' region to permit air flow to under the racks. In the reference plants, there was a large open region in the SFP for the dry storage cask. In a complete loss-of-coolant inventory accident, the air preferentially flowed into the cask region, under the racks, and upward through the assemblies. The large, open cask space region in one corner of the SFP allowed the downward flow of cool air to reach the bottom of the racks with minimal thermal mixing with the hot plume leaving the assemblies. Parametric calculations were performed, which showed substantially decreasing or eliminating an open downcomer region as an inlet path to under the racks inhibited the natural circulation flow through the racks. Both the reference plants had a large cask region and concentrations of empty cells, which permitted a robust, natural circulation flow pattern with minimal thermal mixing with the exiting hot plume. (b)(2)High

Ex. 2

(b)(2)High

The previous insights were developed primarily from a three-dimensional computational fluid dynamics (CFD) study that examined the flow patterns above, through, and around the spent fuel racks during accident conditions [Wagner, 2005a]. The study examined the response of the spent fuel pool and surrounding refueling room in the reactor building of the reference BWR to a complete loss-of-coolant inventory accident. All the water from the spent fuel pool is assumed to be lost, thereby leaving only air cooling of the fuel assemblies. The purpose of the study was to evaluate the role of the open regions in the SFP to promote better circulation and therefore better cooling. (b)(2)High

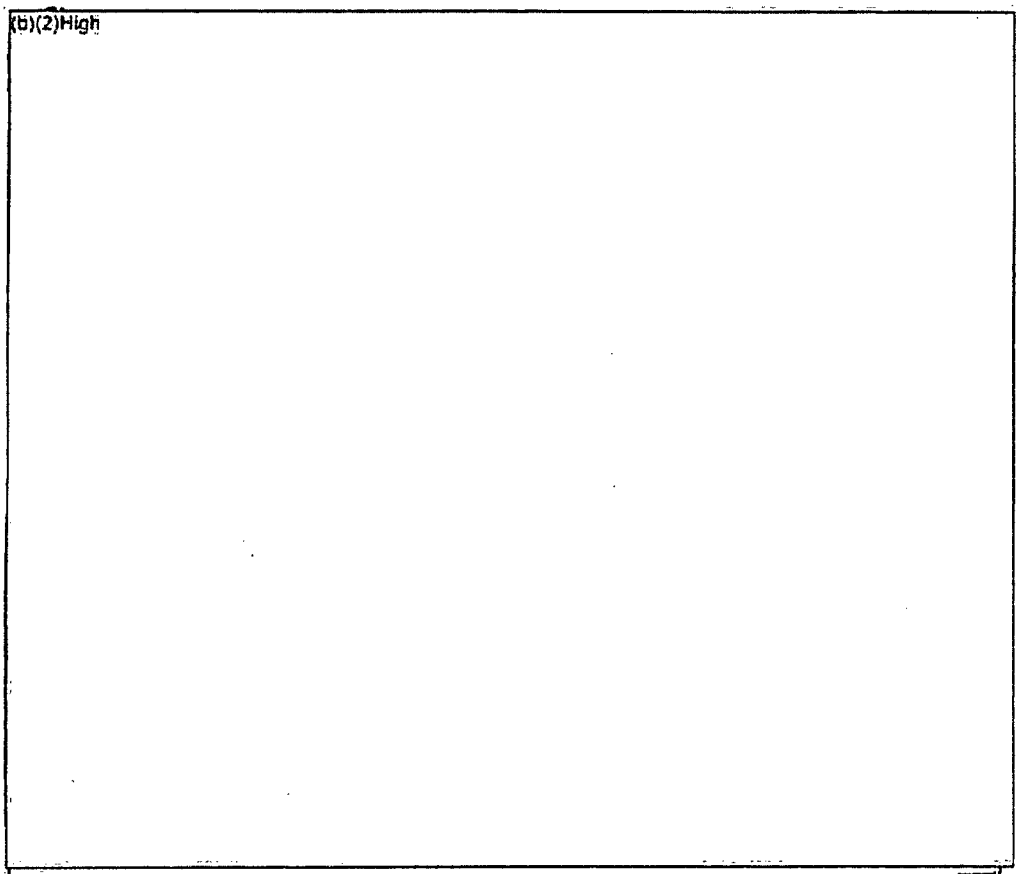
Ex. 2

(b)(2)High

The specifications and results for a few of the cases performed are summarized in Table 17. The base case used the reference BWR fuel distribution in the SFP racks. The reference BWR SFP has relatively large 12" gaps between the racks and the SFP wall on three sides (see Figure 2-1). The remaining side had variable spacing but includes regions with 30" to 80" gaps between the racks and the walls. In addition to the gaps between the racks and the SFP walls, there is a 120" x 120" cask region. The cask region does not contain racks and is periodically used by the reference plant to load older fuel into dry storage casks. The cask area and open spaces within or around the racks were previously judged important to promote natural circulation during a complete loss-of-water inventory accident [Chiffelle, 2003]. As shown Table 17, the newer CFD calculations varied the sizes of the open regions to see their impact on the natural circulation cooling effectiveness.

Ex. 2
Ex. 2

²³ The open areas permitted a natural circulation flow pattern. In the calculations, cool air flow (b)(2)High (b)(2)High across the refueling room floor, and down into the SFP. The hot gases from the SFP rose into the refueling room and exited (b)(2)High



Ex.
2

Figure 3-59 Schematic of the Reference BWR Reactor Building Showing the CFD Model Mesh.

The temperature responses for the cases summarized in Table 17 are shown in Figure 3-61 and Figure 3-62. The various supplemental air flow cases showed the sensitivity of the temperature response in the racks to reductions in open flow area relative to the reference BWR SFP configuration (i.e., Case 1). The layout of the reference plant left large areas for downflow around the racks on all four sides. The peak temperature rise in the racks was (b)(2)High

Ex. 2

for the reference plant configuration and assumed ventilation boundary conditions. The various sensitivity cases decreased the amount of open areas around the racks and filled the open rack cells with additional assemblies. In Cases 6 and 10, the total number of open rack cells from the base case was preserved as well as the layout of the assemblies. At the reference BWR plant, these open rack cells were spread out in a few large contiguous patterns. Additional fuel assemblies and flow restrictions were added to limit the flow area through open gaps around the racks. In Case 10, all open gaps around the racks were eliminated. However, the flow area of the open cells was still significant and represented the equivalent of 200% of the nominal cask area. The average temperature response in Cases 6 and 10 was essentially the same as the base case (Case 1). Consequently, it was concluded that the pattern of open cells in the reference plant SFP provided adequate cooling without the requirement for gaps around the racks or an open cask area.

Due to the effective cooling in cases with open rack cells, a number of other configurations were examined where there were no open cells, the gaps adjacent to the walls were removed, and the size of downcomer was parametrically reduced. Two geometry shapes were considered in the sensitivity cases (i.e., square and L-shaped), which gave generally confirming results (see Figure 3-62 for L-shaped area results). (b)(2)High

Ex 2

(b)(2)High
(b)(2)High The natural circulation flow pattern was effective and steady, which resulted in relatively lower peak temperatures. (b)(2)High

Ex 2

(b)(2)High

Ex 2

The smaller open cask area flow cases (b)(2)High were most susceptible to entraining hot gas under the racks which resulted in non-steady cooling patterns and higher peak temperatures. The results from these calculations showed that a single, small open flow area could have unsteady threshold behavior that results in temperature increases.

Ex 2

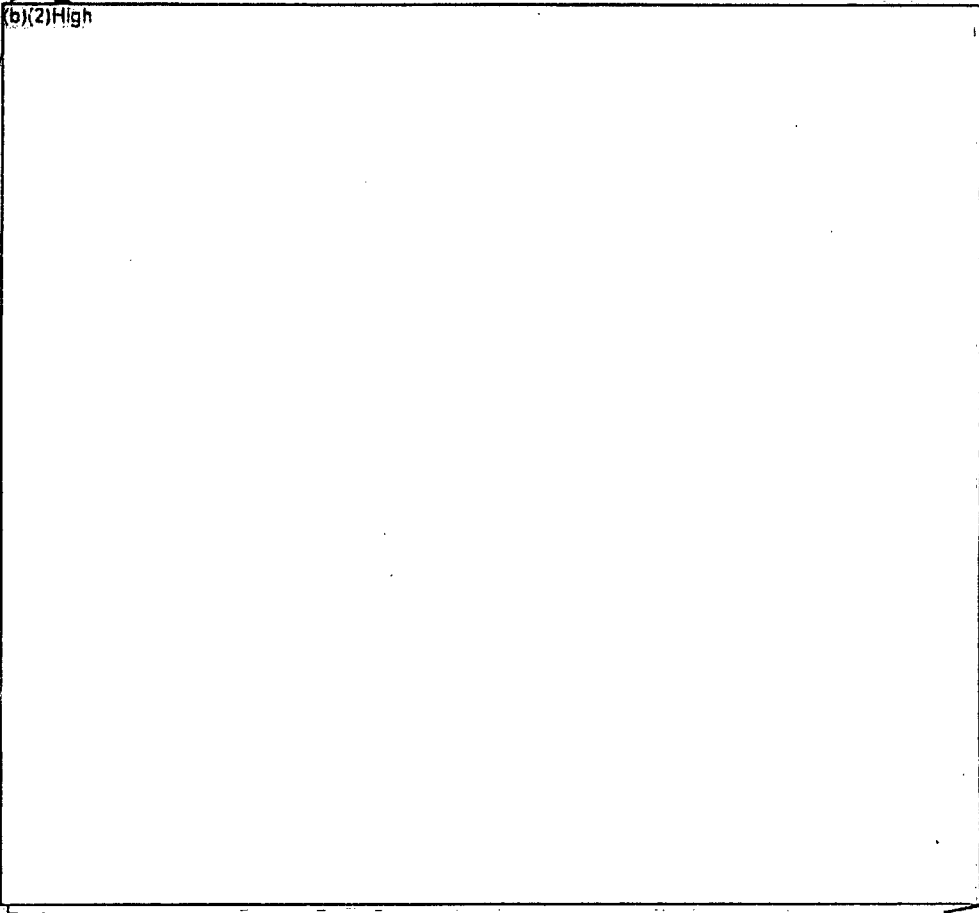
(b)(2)High
(b)(2)High The lack of an open area meant all airflow to under the racks went downward through the low-powered assemblies in the peripheral of the SFP. Consequently, the air flow was heated by the low-powered assemblies and also had a higher flow resistance than an open region or an empty cell.

Finally, some plants may use a weir wall to isolate the cask region from the SFP. The weir wall would effectively isolate the cask region from the rest of the SFP. The results from Cases 6 and 10 show that a weir wall would not effect the cooling of the reference BWR SFP if there are sufficient open regions. The empty rack cells provided an effective open flow area for air downflow. Hence, empty cells or some other open area is needed if there is a weir wall.

Table 17 Summary of BWR CFD Cases with Variable SFP Open Flow Area Configurations.

(b)(2)High

Ex.
2



Ex.
2

Figure 3-60 CFD Model Cross-Section of the SFP Racks for the Reference BWR SFP.

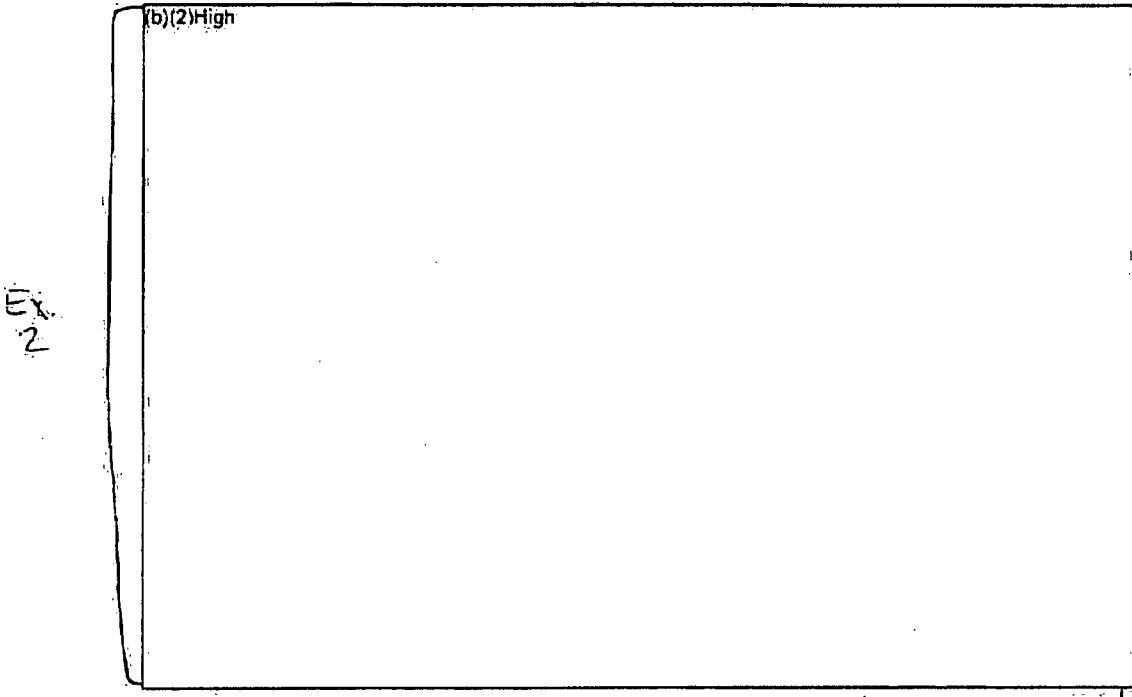


Figure 3-61 Peak Assembly Gas Temperatures for the Various Shaped Open Area Configurations.

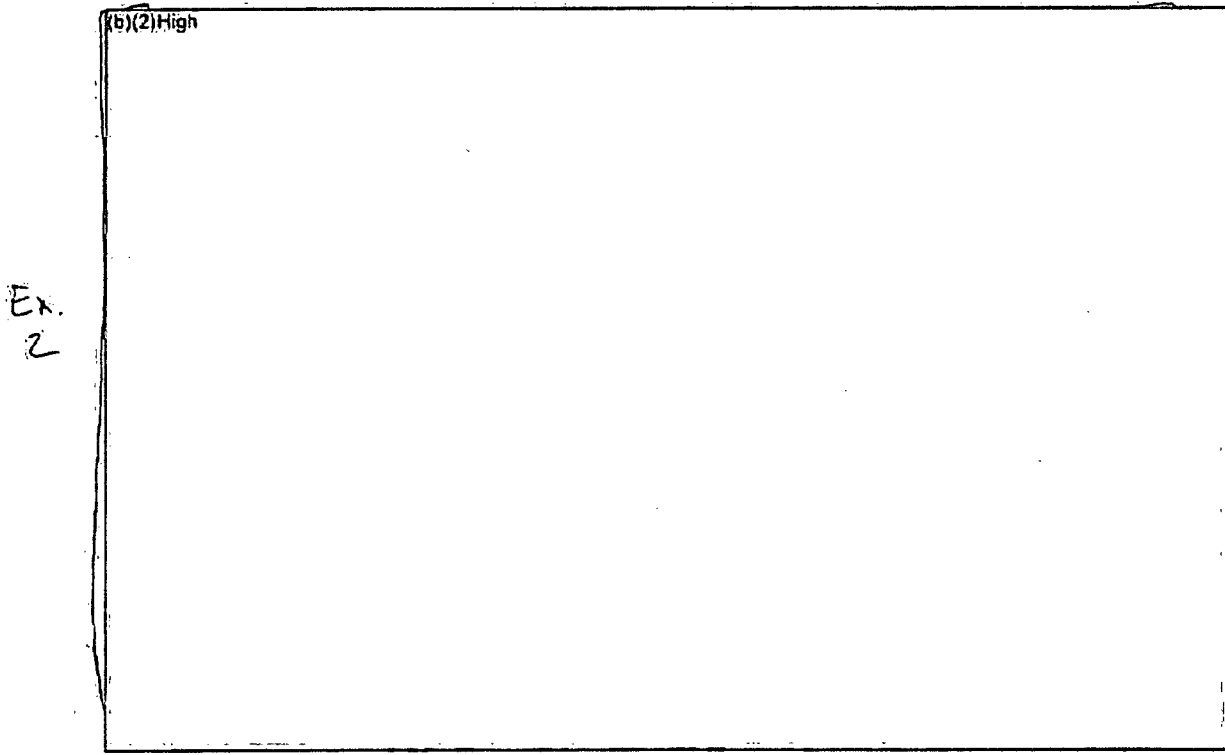


Figure 3-62 Peak Assembly Gas Temperatures for the Shaped Cask Area Configurations.

3.5.1 Summary of Pool Configuration Findings and Extension to Other Sites

In summary, parametric CFD calculations were used to assess the requirements for open area for the reference BWR plant. The reference BWR SFP had a relatively large number of open spaces that allowed cool air flow to under the racks in a complete loss-of-coolant inventory accident. The gaps between the racks and the SFP walls varied from 12" on 3 sides to 30" to 80" on the remaining side. In addition, there was a large 120" x 120" cask area and (b)(2)High rack cells were empty. Only 58% of the cross-sectional flow area of the SFP was filled with rack cells with spent fuel assemblies. Consequently, the reference plant may have more open area than other SFPs. The following insights were gained from the CFD sensitivity studies that were identified to improve spent fuel coolability.

Ex. 2

- SFPs with a large gap between the racks and the SFP walls allow room for downflow under the racks. In the reference BWR SFP, the gap was ~12", or approximately the dimension of two SFP rack cells. CFD Case 6 showed this configuration provided sufficient downflow area alone without a cask region. A uniform gap around the SFP provided redundant downflow regions for cool air. Plants with an open cask area already benefit from a large open space in one corner of the SFP. Figure 3-36 and Figure 3-37 illustrate examples of well-configured SFP with open regions around the periphery of the SFP.
- The reference plants had maintained sufficient extra space for a complete offload of the reactor core into the SFP. The results from CFD Case 10 showed the empty rack cells act as an open area for downflow under the racks. The greatest benefit occurs if the empty cells are placed in a coherent pattern on the periphery of the SFP (i.e., like a gap between the racks and the SFP wall). Case 10 is equivalent to 19% of the available modified cross-sectional area of the SFP open to downflow (i.e., through open, empty cell locations).

Ex. 2

- A modified configuration of the reference BWR SFP with only a small region for downflow (b)(2)High showed a higher susceptibility to overheating. The flow was restricted and oscillating thermal patterns developed that intermittently drew hot air under the racks. Furthermore, very high speed flows (~3-4 m/s) developed near the small open downcomer, which caused a Bernoulli Effect that further decreased the assembly coolability near the open downflow location.
- At the limit of no open flow area, the air was drawn under the racks through the low-powered assembly cells and much higher assembly temperature resulted.

Ex. 2

- Some plants use a weir wall to isolate the cask region from the SFP. The weir wall would effectively isolate the cask region from the rest of the SFP. The results from CFD Cases 6 and 10 show that a weir wall would not affect the cooling of the reference BWR SFP if there are sufficient open regions (b)(2)High.
- (b)(2)High The empty rack cells and spaces between the racks and walls can act as an effective open flow area for air downflow.
- Some multi-unit plants have a gate between the spent fuel pools. If the gate remained closed, then a loss-of-coolant accident would not spread to the adjacent pool. If applicable and

possible, strategies could be employed using the two pools to distribute the fuel assemblies. For example, if the outages are sufficiently staggered (e.g., ≥ 6 months), the last offload could be distributed across both pools. Similarly, the assemblies could be balanced between the two pools to provide equal, open downcomers.

- As a common sense recommendation, the storage of other materials (failed fuel, control rod blades) should be performed in a manner that promotes a coherent downcomer.
- The reference PWR SFP had several racks with open flux traps adjacent to each rack cell for criticality control. The benefit of the open flux traps contributing to down flow was not quantified. Since the flux traps are dispersed throughout the rack cells, they would not provide a contiguous flow path near the SFP wall. Consequently, their benefit is expected to be less beneficial than the aforementioned configuration. Nevertheless, the assemblies adjacent to open flux channels were quantified to enhance the coolability of the reference PWR assemblies relative to a uniform configuration but not as advantageous as a checkerboard configuration.

3.6 Miscellaneous Other Factors

The following factors were identified as affecting the assembly coolability.

- Most rack designs allow assemblies to be placed over rack feet. The rack foot is hollow and has holes on the sides to permit flow. Particularly in the reference PWR rack design, the additional resistance through the flow holes increased the aging time for coolability. Since the BWR assemblies are already restricted at the assembly nose-piece, the impact was not as substantial.
- The PWR reference SFP had 3 racks with an open flux channel design to store low or un-irradiated fuel. The flux channel enhanced heat removal by providing an empty flow channel for additional convective heat removal (see Figure 3-63). (b)(2)High
EX. 2. (b)(2)High While not as good as a 1x4 configuration (b)(2)High or the checkerboard configuration (b)(2)High it was much better than a uniform configuration in the rack design without flux traps (b)(2)High.
- Neither of the reference plant rack designs had drain holes in the sides of the rack cells. However, the SNL SFP experimental program rack design had two 1" drain holes near the bottom of the racks. The drain holes enhanced flow into the annulus between the BWR canister and the rack wall, which enhanced the assembly cooling.
- The CFD analyses showed a high speed air flow adjacent to the cask region as air flowed under the racks. Since the air flow is tangential to the rack inlet holes, it creates a low pressure region or Bernoulli Effect, which retards air flow into the racks. Regions of empty rack cells can be used to form a buffer zone adjacent to the cask region and provide alternate downflow regions along the walls. For example, see the open rack cell patterns used in the "improved" BWR and PWR SFP configurations (see Figure 3-36 and Figure 3-37, respectively).
- The reference PWR plant stored assemblies with different control materials in the guide tube locations. If the control materials and the end plugs could be removed, the additional flow through the guide tubes was shown to be beneficial (see case with flow through open guide tubes in Figure 3-65). Similarly, removing the BWR canister enhanced the coolability of the assemblies. It is recognized that these suggestions may not be practical.
- The reference PWR uses Zirlo cladding and the reference BWR uses Zr-2 cladding. Most modern BWR fuel assemblies use Zr-2 cladding whereas PWR assemblies use Zirlo, M5, and Zr-4 cladding. ANL characterized the oxidation kinetics for a variety of Zr-based alloys, which were used in the MELCOR SFP analyses [Natesan]. The various oxidation correlations showed some small differences between the various alloys. However, all alloys had large differences between the pre-breakaway rate versus the post-breakaway rate. Consequently, the inclusion of breakaway kinetics was the most significant aspect that should be considered (and was in the NRC SFP analyses).

Within the correlations for pre-breakaway or post-breakaway, Zirlo alloy was most reactive followed by Zr-4. Hence, the oxidation rate in the reference PWR SFP calculations will bound the other PWR assemblies using M5 and Zr-4. ANL did not test Zr-2 but it is expected that Zr-2 will react similarly to Zr-4 (i.e., ANL used Zr-4 as a surrogate for Zr-2). Hence, the BWR SFP calculations are expected to be prototypical of BWR fuel.

- The reference PWR used Westinghouse 15x15 fuel. However, the assembly types range from 14x14 to 17x17 and two vendors, Areva and Westinghouse, supply PWR fuel to United States plants. The number of rods and the grid spacer design is expected to affect the hydrodynamics. In particular, the laminar hydraulic characteristics of 17x17 fuel are expected to be slightly more resistive than the 15x15 based on insights from the BWR assembly pressure drop experiments in the SNL SFP experimental program. However, the scope of the test program only examined 9x9 BWR fuel. Similarly, the BWR plants are moving to 10x10 fuel from Areva or Global Nuclear Fuels (GNF) whereas all the MELCOR calculations were based on 9x9 fuel.

A key finding of the hydraulic testing in a low flow laminar regime were (a) higher viscous flow losses than traditional laminar textbook correlations (e.g., see [Todreas]) and (b) significant and measurable viscous, rather than inertia, flow losses through the grid spacers. The extension of the BWR data to 15x15 PWR fuel was estimated using hydraulic diameter squared scaling based on a review of the governing equations. The flow resistance in the experimental BWR was characterized in both the fully and partially populated rod regions of a BWR 9x9 assembly. Hence, there were two data points to permit extension to other hydraulic configurations.

Sensitivity calculations were performed that attempted to apply the scaled BWR assembly laminar hydraulic flow results from the SNL SFP experimental program to PWR fuel. The estimated hydraulic results for 15x15 fuel yielded a lower coolability than the base calculations using a bundle correlation from [Todreas] (b)(2)High

Ex. 2

(b)(2)High. It is believed that PWR hydraulic testing would reveal a lower overall hydraulic resistance when the multi-dimensional velocity profile between inside the assembly versus the gap between the assembly and the rack wall is considered.

Finally, most of the BWRs are now using 10x10 fuel designs (i.e., either the GNF design or the Areva design). There is no impact to the qualitative findings cited in this report. The 10x10 fuel design has a slightly smaller fluid hydraulic diameter in the fully populated region of the assembly but very similar hydraulic characteristics in the partially populated rod region. The 10x10 fuel will have slightly more cladding surface area, which can enhance the amount of oxidation. However, it was judged that the quantitative impact of these differences is expected to be small.

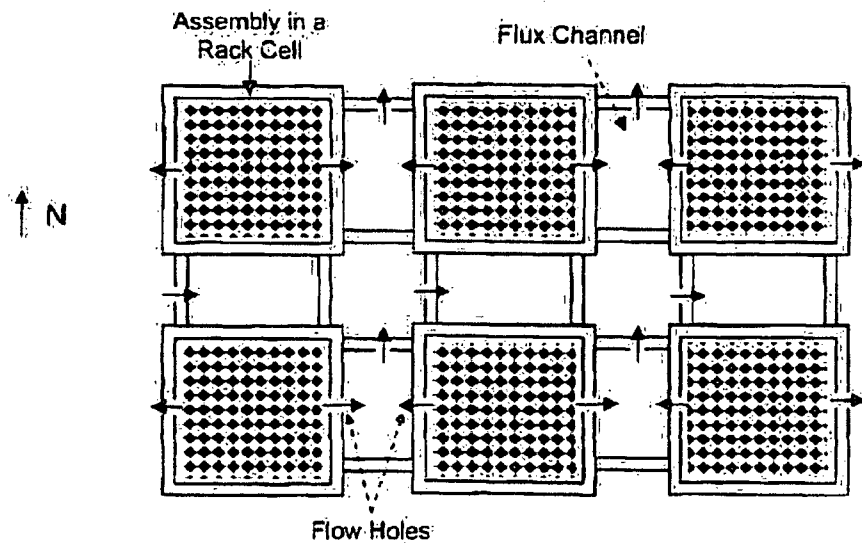


Figure 3-63 Illustration of the Reference PWR Plant Region I Racks with Flux Traps.

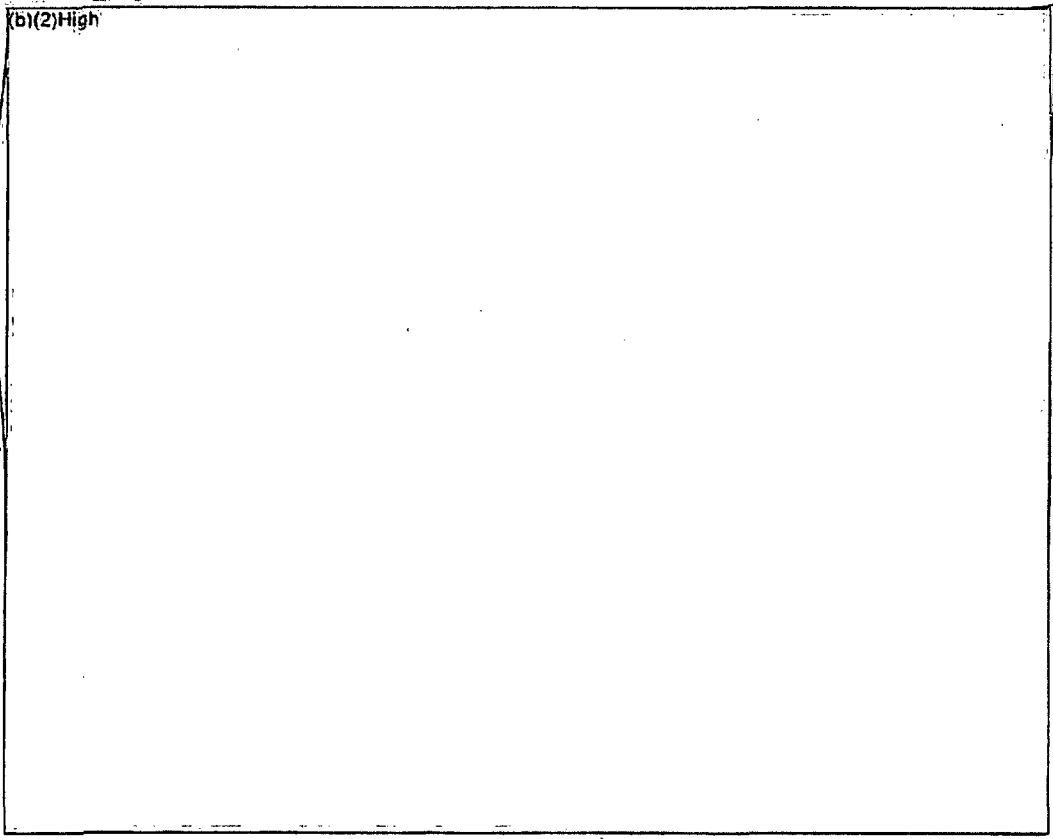


Figure 3-64 Gas Velocity Vectors Below the Racks in a Fluent CFD Calculation of a Complete Loss-of-Coolant Inventory Accident.

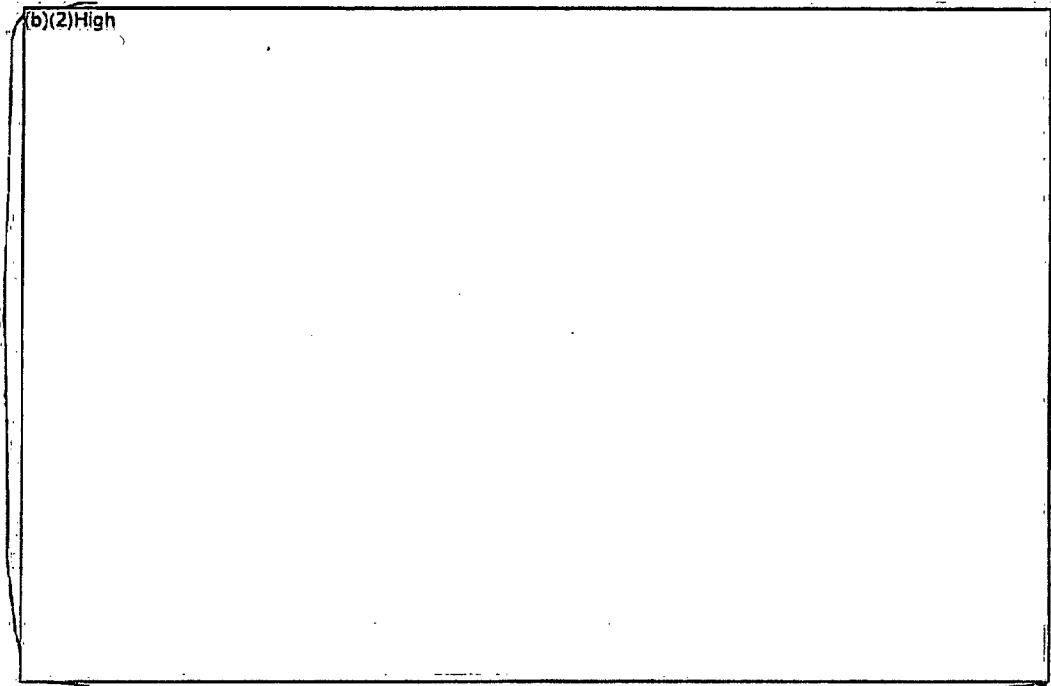


Figure 3-65 Comparison of the PCT versus the Range of Assembly Configurations in the Reference PWR SEP.

4. SUMMARY OF MITIGATION OPTIONS

Table 18 summarizes the various mitigation options cited in Section 3. The impact of each mitigation option is qualitatively ranked. As noted in the comments, some options are only effective for complete loss-of-coolant inventory accidents where a natural convection air flow can be established. Depending on the available instrumentation and an ability to diagnose the accident, it may be difficult to know where the leak is located and whether the accident will progress like a complete or partial loss-of-coolant inventory accident. Nevertheless, the first three options are ranked as having very high to high impact on the assembly coolability, regardless of the accident type. Preparation and application of multiple mitigation options can provide a compounding beneficial effect. (b)(2)High

Ex.
2

(b)(2)High

(b)(2)High Selected measures are being incorporated in to the procedures of NRC licensee's as a part of the NRC and industry's SFP mitigative strategies study.

Table 18 **Impact of Mitigation Options on Assembly Coolability.**

(b)(2)High

Ex.
2

Ex.
2

5. REFERENCES

- Chiffelle, R., et al., "Analysis of Spent Fuel Pool Flow Patterns Using Computational Fluid Dynamics: Part 1 - Air Cases," Sandia National Laboratories, Informal Report, June 2003.
- Collins, T. E., and Hubbard, G., "Technical Study of Spent Fuel Pool Accident Risk at Decommissioning Nuclear Power Plants," NUREG-1738, February, 2001.
- Gauntt, R. O. et al, "MELCOR Computer Code Manuals, Reference Manual, Version 1.8.5, Vol. 2, Rev. 2", Sandia National Laboratories, NUREG/CR-6119, SAND2000-2417/1.
- Khalil, I., and Webb, S., "Simulations of Natural Convection Airflow in a Completely Drained Pressurized Water Reactor Spent Fuel Pool using FLUENT," Sandia National Laboratories, Letter Report, Revision 1, October 2005.
- Lanning, D. D., Beyer, C. E., Geelhood, and K.J., FRAPCON-3 Updates, Including Mixed-Oxide Fuel Properties," NUREG/CR-6534, Vol. 4, PNNL-11513, Pacific Northwest National Laboratory, May 2005.
- Natesan, K., and Sopper, W.K. "Air Oxidation Kinetics for Zr-Based Alloys," NUREG/CR-6846, Argonne National Laboratories, June 2004.
- O'Donnell, G. M., Scott, H. H., and Meyer, R. O., "A New Comparative Analysis of LWR Fuel Designs," United States Nuclear Regulatory Commission, NUREG-1754, December 2001.
- Persily, A., National Institute of Standards, "Airtightness of Commercial and Institutional Buildings: Blowing Holes in the Myth of Tight Buildings", Airtightness and Airflow in Buildings: Principles, Thermal Envelopes VII Conference, Proceedings, December 6-10, 1998, Clearwater, FL, pp. 829-837.
- Ross, K. W., Wagner, K.C. and Gauntt, R. O., "Analysis of Spent Fuel Pool Flow Patterns Using Computational Fluid Dynamics: Part 2 - Partial Water Cases," Sandia National Laboratories, Letter Report to NRC, April 2003.
- Todreas, N. E., and Kazimi, M. S., "Nuclear Systems II - Elements of Thermal Hydraulic Design," Taylor and Francis, 2001.
- Wagner, K. C., and Gauntt, R. O., "MELCOR 1.8.5 Separate Effect Analyses of Spent Fuel Pool Assembly Accident Response," Sandia National Laboratories, Letter Report to NRC, Revision 0, June 2003.
- Wagner, K. C., and Gauntt, R. O., "Evaluation of a BWR Spent Fuel Pool Accident Response to Loss-of-Coolant Inventory Scenarios Using MELCOR 1.8.5," Sandia National Laboratories, Letter Report to NRC, Revision 2, December 2004.

- Wagner, K. C., and Gauntt, R. O., "Analysis of BWR Spent Fuel Pool Flow Patterns Using Computation Fluid Dynamics: Supplemental Air Cases," Sandia National Laboratories, Letter Report to NRC, Revision 2, October 2005a.
- Wagner, K. C., and Gauntt, R. O., "MELCOR 1.8.5 Separate Effects Analyses of PWR Spent Fuel Pool Assembly Accident Response," Sandia National Laboratories, Letter Report to NRC, Revision 2, October 2005b.
- Wagner, K. C., and Gauntt, R. O., "Analysis of Emergency Spray Mitigation of Spent Fuel Pool Loss-of-Coolant Inventory Accidents," Sandia National Laboratories, Letter Report to NRC, Revision 1, May 2006a.
- Wagner, K. C., and Gauntt, R. O., "Additional MELCOR Analyses of BWR Spent Fuel Pool Assembly Accident Response," Sandia National Laboratories, Letter Report to NRC, Revision 1, July 2006b.
- Wagner, K. C., and Gauntt, R. O., "Evaluation of a PWR Spent Fuel Pool Accident Response to Loss-of-Coolant Inventory Scenarios Using MELCOR 1.8.5," Sandia National Laboratories, Letter Report to NRC, Revision 3, July 2006c.
- Wagner, K. C., Dallman, R. J., and Annon, M.C., "Best-Estimate Evaluation Of Loss-Of-Coolant Inventory In A Nuclear Power Plant Spent Fuel Pool," *International Meeting on Best-Estimate Methods in Nuclear Installation Safety Analysis (BE-2000)*, Washington, DC, November, 2000.